UNIVERSITAT POLITÈCNICA DE VALÈNCIA

PRINCIPE FELIPE
CENTRO DE INVESTIGACION

Departamento de Biotecnología

Study of the SAGA deubiquitination module: Identification of new modulators and its implication on Spinocerebellar Ataxia Type 7.

Presentada por:

PAULA OLIETE CALVO

Para optar al grado de:

DOCTOR EN BIOTECNOLOGÍA

Dirigida por:

Dra. SUSANA RODRÍGUEZ NAVARRO

Tutelada por:

Dra. LYNNE PAULA YENUSH

Abril, 2017

La Dra. Susana Rodríguez Navarro, investigadora jefe del centro de Investigación Príncipe Felipe (CIPF) en Valencia (como directora de la tesis) y la Dra. Lynne Paula Yenush profesora del Dpto. de Biotecnología de la Escuela Técnica Superior de Ingenieros Agrónomos de la Universidad Politécnica de Valencia (UPV) (como tutor de Tesis de la UPV).

CERTIFICAN que la licenciada en Biotecnología PAULA OLIETE CALVO ha realizado bajo su dirección en el CIPF y bajo su tutela en la UPV respectivamente, el trabajo que lleva por título "Study of the SAGA deubiquitination module: Identification of new modulators and its implication on Spinocerebellar Ataxia Type 7", y autorizan su presentación para optar al grado de Doctor en Biotecnología.

Y para que así conste, expiden y firman el presente certificado en Valencia, Abril de 2017.

Dra. Susana Rodríguez Navarro
(Directora)

Dra. Lynne Paula Yenush
(Tutora)

Esta Tesis se ha realizado gracias a una beca pre-doctoral para la Formación de Personal Investigador (FPI (BES-2012058587)) asociada a proyecto (BFU-2011-23418) en el Centro de Investigación Príncipe Felipe de Valencia.

Agradecimientos

Ha llegado el momento de poder agradecer a todas aquellas personas que han hecho posible la finalización de esta tesis.

Quisiera dar las gracias especialmente a mi directora de tesis, la Dra. Susana Rodríguez Navarro por confiar en mí y haberme dado la oportunidad de formar parte de su equipo. Gracias por guiarme durante estos años y por compartir conmigo tu forma de ver la ciencia y la vida. Muchas gracias Susana.

También quisiera agradecer al Dr. José Enrique Pérez Ortín de la Universidad de Valencia, a toda la gente de su laboratorio y en especial a María por haber tenido la paciencia de enseñarme a hacer "GROs".

Gracias al Dr. Albert La Spada de la Universidad de San Diego por abrirme las puertas de su laboratorio y hacerme sentir como en casa aunque estuviera a miles de km. Muchas gracias a todos los miembros de su laboratorio, especialmente a Colleen con quién compartí bancada y muchas risas durante mi estancia. No quiero olvidarme de buenos amigos que conocí allí como son los miembros de "La familia"; a Berta, Aída, Stefano, Fernando, Julián y Jahir.

Quiero agradecer enormemente a los miembros de mi laboratorio, a mis amigos del I-25, por ser excelentes compañeros y por apoyarme durante todo el largo trayecto de esta tesis. A Ali, Lolo y Joan, a Meg por ayudarme a dar la vuelta a las ideas y tener la paciencia de escuchar todas mis dudas. A Elo y Carme por su apoyo incondicional, su gran amistad y por hacerme un hueco en sus vidas. No quiero olvidarme de antiguos compañeros de laboratorio: Encar, Ana y muy especialmente a mi amiga Vari con quién hice mis primeros pinitos en el laboratorio, por ser un referente durante estos años y por haber compartido grandes conversaciones contigo. A Amparo por escucharme, ayudarme, por tus buenas sugerencias y sobre todo por ser mi amiga. Gracias a mis compañeros del CIPF y en especial a

Martina con quién tuve la suerte de colaborar y de conocer de forma mucho más cercana.

Quiero dar las gracias a todos mis buenos amigos y amigas que tengo en diferentes lugares y que han vivido mis bajones y mis alegrías, gracias por vuestra comprensión y paciencia, por dedicar vuestro tiempo intentando entenderme y por hacer que sea mucho más amena la escritura de esta tesis. Mil gracias a mis compañeras de carrera con quienes empecé en este mundo; a Espe, Barbara, Lucía, Marta y a Pilar quién aun estando en la otra punta del mundo me manda mensajes de ánimo y apoyo. Agradecer a Rosalyne por ayudarme a ser consciente de lo que me rodea, a Gen por revisar toda la escritura y a Rocío, muchas gracias por cuidarnos.

Quiero agradecer con todo mi corazón a toda mi familia porque sin vuestra ayuda no hubiese podido llegar hasta el final. Muchas gracias por vuestro incansable apoyo, por animarme y por ayudarme a sacar fuerzas de donde hiciera falta. A Ana y Mercedes por ayudarme con la parte artística y por compartir tan buenos momentos juntas. Mención muy especial a mis queridos padres, por todas esas cosas que no acabaría nunca de enumerar, por confiar plenamente en mí, por ayudarme a seguir adelante y por tener la suerte de teneros a mi lado.

Por último, no puedo dejar de dar las gracias a mi compañero de aventuras, mi amigo, mi confidente, a Dani, por ver siempre el lado positivo de las cosas y por no cansarte de repetir que todo esto merece la pena. Y con mucho cariño termino agradeciendo a mi pequeño hijo Pablo por sacar siempre mi mejor sonrisa.

Acknowledgments

It is time to thank all those who have made possible the completion of this thesis.

I would especially like to thank my thesis director, Dr. Susana Rodríguez-Navarro for trusting me and giving me the opportunity to be part of her team. Thank you for guiding me during these years and for sharing with me your way of seeing science and life. Thank you very much Susana.

I would also like to thank Dr. José Enrique Pérez-Ortín of the University of Valencia, all the people in his laboratory and especially Maria for having the patience to teach me how to make "GROs".

Thanks to Dr. Albert La Spada of the University of San Diego for opening me the doors of his laboratory and making me feel at home even though I was thousands of miles away. Thanks to all members of his lab, especially Colleen who I shared bench and many laughs during my stay with. I do not want to forget good friends that I met there as members of "La familia"; To Berta, Aida, Stefano, Fernando, Julián and Jahir.

I want to thank the members of my laboratory, my I-25 friends, for being excellent colleagues and for supporting me during this last stage of the thesis. Thanks to Ali, Lolo and Joan, to Meg for helping me to turn the ideas around and have the patience to listen to all my doubts. Thanks to Elo and Carme for their unconditional support, their great friendship and for making a gap in their lives. I do not want to forget past members: Encar, Ana and especially my friend Vari who I did my first steps in the laboratory with, for being a reference during these years and for sharing great conversations with you. To Amparo for listening, helping me, for your good suggestions and above all for being my friend. Thanks to my

colleagues from the CIPF and especially Martina who I had the luck to collaborate and get closer.

I want to thank all my good friends that I have in different places who have suffered my downturns and my joys, thank you for your understanding and patience, to dedicate your time trying to understand me and for making this thesis much more enjoyable to write. A thousand thanks to my career partners I started in this world; To Espe, Barbara, Lucía, Marta and Pilar, who, while still on the other side of the world, sends me messages of encouragement and support. Thanks to Rosalyne for helping me to be aware of what surrounds me, to Gen to review all the writing and to Rocío for taking care of us.

I want to thank with all my heart to all my family because without your help I could not have reached the end. Thank you very much for your tireless support, for encouraging me and for helping me to draw strength wherever I needed it. To Ana and Mercedes for helping me with the artistic part and for sharing such good moments together. Special mention to my dear parents, for all those things that I would never finish listing, for trusting me fully, for helping me to go ahead and for having the good fortune to have you by my side.

Finally, I cannot fail to thank my adventure partner, my friend, and my confidant, Dani, for always seeing the positive side of things and for not getting tired of repeating that all this is worth it. And with much affection, I ended up thanking my little son Pablo for always getting my best smile.

ABSTRACT

Regulation of chromatin by epigenetic modifications is a fundamental step during the control of gene expression in eukaryotic cells. The participation of different factors including histone chaperones, chromatin remodeling complexes and histone-modifying complexes regulate chromatin dynamics and ensure the correct metabolism of transcripts that need to be exported to the cytoplasm. In these lines, post-translational modifications including monoubiquitination of histone H2B ($H2Bub^1$) and methylation of histone H3 represent a well-studied histone cross-talk which is required for chromatin integrity and transcription. Additionally, the transition from $H2Bub^1$ to its deubiquitinated form by Ubp8, the DUB enzyme from SAGA (Spt-Ada-Gcn5-acetyltranferase) co-activator complex, is fundamental to obtain a correct gene expression. In this work, we demonstrate that the histone chaperone Asf1 and the Ran-binding protein Mog1, participate in maintaining correct levels of $H2Bub^1$. We show that Mog1 is required for the trimethylation of histone H3 at lysine 4 ($H3K4me^3$), hence, acting as a modulator of histone cross-talk. Mog1 role into gene expression is also demonstrated by its physical and genetically interaction with transcription factors including SAGA and COMPASS complexes. Indeed, we demonstrate that Mog1 interacts genetically with TREX-2 subunits and affects mRNA export. During this work, we have also focused in understanding the molecular mechanisms surrounding Spinocerebellar Ataxia Type 7 (SCA7) which is a rare disease caused by amino acid glutamine (Q) repeats within the DUBm component, ATXN7. Therefore, our interest has been directed towards the study of new mechanisms that trigger SCA7 such as the DUB activity from SAGA complex, protein-protein interaction networks and metabolic profiles.

RESUMEN

La regulación de la cromatina a través de modificaciones epigenéticas es un paso fundamental durante el control de la expresión génica en células eucariotas. La participación de diferentes factores tales como chaperonas de histonas, complejos de remodelación de la cromatina y complejos modificadores de histonas, regulan la dinámica de la cromatina y garantizan el correcto metabolismo de los transcritos que necesitan ser exportados al citoplasma. De esta forma, las modificaciones postraduccionales que incluyen la monoubicuitinación de la histona H2B ($H2Bub^1$) y la metilación de la histona H3 representan un "cross-talk" de histonas la cual es requerida para la integridad de la cromatina y la transcripción. Además, la transición de $H2Bub^1$ a su forma desubicuitinada por Ubp8, la enzima DUB del complejo co-activador SAGA (Spt-Ada-Gcn5-acetiltranferasa), es necesaria para obtener una expresión génica correcta. En este trabajo, se demuestra que la chaperona de histona Asf1 y la proteína de unión a Ran, Mog1, participan en el mantenimiento de los niveles de $H2Bub^1$. Se demuestra que Mog1 es necesaria para la trimetilación de la histona H3 en la lisina 4 ($H3K4me^3$), actuando como un modulador del "cross-talk" de histonas. El papel de Mog1 en la expresión génica también se demuestra por sus interacciones físicas y genéticas con factores de transcripción, incluyendo los complejos SAGA y COMPASS. Además, demostramos que Mog1 interactúa genéticamente con subunidades de TREX-2 y afecta a la exportación de mRNAs. Durante este trabajo, también nos hemos centrado en la comprensión de los mecanismos moleculares que envuelven a la Ataxia Espinocerebelosa Tipo 7 (SCA7), que es una enfermedad rara causada por una repetición de aminoácidos glutamina (Q) dentro del componente del DUBm, ATXN7. Por lo tanto, nuestro interés se ha dirigido hacia el estudio de nuevos mecanismos que desencadenan SCA7, como la actividad DUB del complejo SAGA, las interacciones proteína-proteína y los perfiles metabólicos.

RESUM

La regulació de la cromatina a través de modificacions epigenètiques és un pas fonamental durant el control de l'expressió gènica en cèl·lules eucariotes. La participació de diferents factors tals com chaperones d'histones, complexos de remodelació de la cromatina i complexos modificadors d'histones, regulen la dinàmica de la cromatina i garanteixen el correcte metabolisme dels transcrits que necessiten ser exportats al citoplasma. D'aquesta forma, les modificacions postraduccionals que inclouen la monoubicuitinació de la histona H2B ($H2Bub^1$) i la metilació de la histona H3 representen un "cross-talk" d'histones la qual és requerida per a la integritat de la cromatina i la transcripció. A més, la transició d'$H2Bub^1$ a la seua forma desubicuitinada per Ubp8, l'enzim DUB del complex co-activador SAGA (Spt-Ada-Gcn5-acetiltranferasa), és necessària per a obtenir una expressió gènica correcta. En aquest treball, es demostra que la chaperona de histona Asf1 i la proteïna d'unió a Ran, Mog1, participen en el manteniment dels nivells d'$H2Bub^1$. Es demostra que Mog1 és necessària per a la trimetilació de la histona H3 en la lisina 4 ($H3K4me^3$), actuant com un modulador del "cross-talk" d'histones. El paper de Mog1 en l'expressió gènica també es demostra per les seues interaccions físiques i genètiques amb factors de transcripció, incloent els complexos SAGA i COMPASS. A més, vam demostrar que Mog1 interactua genèticament amb subunitats de TREX-2 i afecta a l'exportació de mRNA. Durant aquest treball, també ens hem centrat en la comprensió dels mecanismes moleculars que envolten a l'Atàxia Espinocerebelosa Tipus 7 (SCA7), que és una malaltia rara causada per una repetició d'aminoàcids glutamina (Q) dins del component del DUBm, ATXN7. Per tant, el nostre interès s'ha dirigit cap a l'estudi de nous mecanismes que desencadenen SCA7, com l'activitat DUB del complex SAGA, les interacciones proteïna-proteïna i els perfils metabòlics.

INDEX

ABBREVIATIONS 25

INTRODUCTION 29

SACCHAROMYCES *CEREVISIAE* AS A MODEL ORGANISM **31**

GENOME ORGANIZATION IN *S. CEREVISIAE* **32**

CHROMATIN ORGANIZATION **33**

POST-TRANSLATIONAL MODIFICATIONS 36

HISTONE ACETYLATION 38

HISTONE METHYLATION 39

HISTONE UBIQUITINATION AND HISTONE "CROSS-TALK" 41

HISTONES CHAPERONES 46

THE REGULATION OF GENE EXPRESSION BY RNA POL II IN *S. CEREVISIAE* **48**

TRANSCRIPTION INITIATION 48

SAGA CO-ACTIVATOR COMPLEX AS A MODULATOR OF TRANSCRIPTION REGULATION 52

DUBM FUNCTION AND STRUCTURE 55

TRANSCRIPTION ELONGATION 59

COUPLING TRANSCRIPTION TO MRNA EXPORT 61

THE TREX-2 COMPLEX 64

SAGA ACTIVITY IS LINKED TO TREX-2 COMPLEX 66

SAGA AND TREX COMPLEXES IN NUCLEAR PERIPHERY-GENE TETHERING 68

PROTEIN TRAFFICKING; MOG1 PROTEIN AND ITS ROLE IN RAN GTP/GDP CYCLE **70**

SPINOCEREBELLAR ATAXIA TYPE 7 (SCA7) DISEASE **74**

MATERIALS AND METHODS **79**

MATERIALS **81**

YEAST STRAINS 81

PRIMERS 85

COMMERCIAL KITS 88

ANTIBODIES 88

PRIMARY ANTIBODIES 89

SECONDARY ANTIBODIES 89

PLASMIDS 90

HUMAN CELL LINES 91

MICE 91

RADIOACTIVITY 92

METHODS **92**

SACCHAROMYCES CEREVISIAE **92**

YEAST CULTURES AND CELL GROWTH ASSAY 92

GENE DELETION AND PROTEIN TAGGING 93

GENOMIC DNA ISOLATION 94

PLASMID DNA ISOLATION FROM E. *COLI* 94

RNA ISOLATION 95

REVERSE TRANSCRIPTION OR CDNA SYNTHESIS 96

TRANSFORMATION OF YEAST CELLS 97

PCR (POLYMERASE CHAIN REACTION) 98

QUANTITATIVE-PCR 99

NUCLEIC ACIDS SEPARATION BY ELECTROPHORESIS 100

PROTEIN EXTRACTS FOR WESTERN BLOT 100

PROTEIN SEPARATION BY ELECTROPHORESIS 101

PROTEIN TRANSFER AND IMMUNODETECTION 102
PROTEIN PURIFICATION: THE TAP TECHNIQUE 103
PROTEIN IDENTIFICATION BY MASS SPECTROMETRY 105
COLLOIDAL COOMASSIE BLUE STAINING 105
TOTAL HISTONE EXTRACTION 106
PROTEIN IMMUNOPRECIPITATION (IP) 106
CHROMATIN IMMUNOPRECIPITATION (CHIP) 107
METABOLITE EXTRACTION AND ANALYSIS 109
MICROSCOPIC TECHNIQUES 112
In vivo protein localization 112
In Situ Hybridization (FISH) 112
IMAGE ANALYSIS 113
GENOMIC RUN-ON (GRO) AND MEASUREMENT OF MRNA LEVELS 113
HUMAN CELLS LINES 293T (HEK293T) 120
HEK293T GROW CONDITIONS 120
IN VITRO DUB ASSAY USING HEK293T CELLS 120
COLUMN FRACTIONATION AND ANALYSIS 121
MICE MODEL 123
MOUSE CEREBELLUM EXTRACTION AND RNA ISOLATION 123

OBJECTIVES 125

RESULTS AND DISCUSSION 129

CHAPTER 1 131
FUNCTIONAL CHARACTERIZATION OF THE NOVEL FACTORS ASF1 AND MOG1 INVOLVED IN THE UBIQUITINATION/DEUBIQUITINATION OF HISTONE H2B 131

1. DECIPHERING THE ROLE OF ASF1 IN TRANSCRIPTION **131**

ASF1 IS DISPENSABLE FOR SUS1 RECRUITMENT TO *GAL1* GENE, ITS INDUCTION AND MRNA EXPORT 131

ABSENCE OF *ASF1* REDUCES GLOBAL LEVELS OF H2B UBIQUITINATION AND COUNTERACTS THE EFFECTS OF *SUS1* DELETION 135

2. ROLE OF MOG1P IN THE CONTROL OF GENE EXPRESSION **137**

SUS1 INTERACTS GENETICALLY WITH MOG1 137

MOG1 INTERACTS GENETICALLY WITH FACTORS INVOLVED IN HISTONE H2B UBI/DEUBIQUITINATION 139

ABSENCE OF *MOG1* REDUCES GLOBAL LEVELS OF H2BUB^{1} *IN VIVO* 142

UBP8 PRESERVES THE ASSOCIATION WITH ITS PROTEIN PARTNERS IN *MOG1Δ* CELLS 144

MOG1 DOES NOT AFFECT THE LOCALIZATION OF THE DUB MODULE AND UBP8 RECRUITMENT TO ACTIVELY TRANSCRIBED GENES 146

CHROMATIN RECRUITMENT OF RAD6 IS DECREASED IN *MOG1Δ* CELLS 149

MOG1 INTERACTS GENETICALLY WITH THE METHYLTRANSFERASES AND AFFECTS H3K4ME^{3} LEVELS 151

SET1 RECRUITMENT TO CHROMATIN IS DECREASED IN ABSENCE OF *MOG1* 154

MOG1 ASSOCIATES WITH ACTIVE GENES 156

GENOME-WIDE ANALYSIS LINKS *MOG1* ABSENCE WITH DECREASED LEVELS OF TRANSCRIPTION AND MRNA CONCENTRATION. 157

MOG1 INTERACTS GENETICALLY WITH TREX-2 COMPONENTS AND IT IS INVOLVED IN MRNA EXPORT 167

LEVELS OF SWD2 ARE REDUCED IN ABSENCE OF *MOG1* 171

MOG1 CO-PURIFIES WITH COMPONENTS OF THE TRANSCRIPTION MACHINERY 172

DISCUSSION **177**

CHAPTER 2 **187**

MOLECULAR MECHANISMS OF THE DUBM RELATED DISEASE SPINOCEREBELLAR ATAXIA TYPE 7 (SCA7) **187**

METABOLIC PROFILE OF WT AND POLYQ-ATXN7 187

EXPRESSION LEVELS OF MITOCHONDRIAL AND RIBOSOMAL GENES ARE NOT AFFECTED IN SCA7 MICE CEREBELLUM 190

POLYQ REPETITIONS IN ATXN7 PROTEIN PRESERVES DUB ACTIVITY OF SAGA COMPLEX IN HUMAN CELL LINES 193

POLYQ-ATXN7 SEEM TO AFFECT THE ASSOCIATION BETWEEN ENY2 AND TREX-2 COMPLEX 196

DISCUSSION **198**

FUTURE PERSPECTIVES **207**

CONCLUSIONS **213**

ANNEXES **217**

BIBLIOGRAPHY **221**

ABBREVIATIONS

BMRB	Biological Magnetic Resonance Bank
BRE	TFIIB recognition element
BSA	Bovine serum albumin
CBP	Creb-binding domain
cDNA	Complementary DNA
ChIP	Chromatin Immunoprecipitation
COMPASS	Complex proteins associated with Set1
C-terminal	Carboxy-terminal
DAPI	4',6-diamidino-2-phenylindole
DMEM	Dulbecco's modified Eagle's medium
DNA	Deoxyribonucleic acid
dNTP	Deoxyribonucleotide triphosphate
DPE	Downstream promoter element
DPM	Desintegrations per minute
DRLPA	Dentatorubral-pallidoluysian atrophy
DRYGIN	Data repository of yeast genetic interactions
DTT	1,4-ditiotreitol
DUB	Deubiquitination
EDTA	Etilendiaminotetraacetic acid
EGTA	Ethylene glycol-bis(β-aminoethyl ether)-N,N,N',N'-tetraacetic acid
FACT	Facilitates chromatin transcription
FID	Free induction decays
FISH	Fluorescence in situ hybridization
GEF	Nuclear guanine nuclear exchange factor
GFP	Green fluorescent protein
GRO	Genomic Run-on
GTF	General transcription factor
HATs	Histone acetyltransferases
HC	Histone Chaperone

HDAC	Histone deacetylases
HEK	Human embryonic kidney
HEPES	Hydroxyethyl piperazineethanesulfonic acid
HMBD	Human betabolome database
Inr	Initiator element
IP	Immunoprecipitated
Kb	Kilobase
KDa	Kilodalton
LB	Luria-Bertani medium
LC-MS/MS	Liquid chromatography tandem-mass spectrometry
m/v	Mass/volume
MDa	Megadalton
Mog1	Multicopy suppressor of Gsp1
MOPS	(3-(N-morpholino)propanesulfonic acid)
mRNA	Messenger ribonucleic acid
mRNP	Messenger ribonucleoprotein particle
ncRNAs	Non-coding RNAs
NE	Nuclear envelope
NP-40	Nonidet P40
NPC	Nuclear pore complex
N-terminal	Amino-terminal
nTR	Nascent transcription rate
OD_{600}	Optical density 600nm
Oligo(dT)	Oligonucleotides deoxythymine
ORF	Open reading frame
PA	Protein A
PAF	RNA Pol II-associated factor complex
P-body	Processing body
PBS	Phosphate-buffer saline
PCR	Polymerase chain reaction
PEG	Polyethylene glycol
PEST	Penicillin/streptomycin

PIC	Pre-initiation complex
PMSF	Phenylmethanesulfonylfluoride
PNK	Polynucleotide kinase
Poly (A)$^+$	Polyadenylated
polyQ	Polyglutamine
PTMs	Post-translational modifications
qPCR	Quantitative PCR
RA	mRNA amount
RIPA	Radioimmunoprecipitation assay
RNA	Ribonucleic acid
RNA Pol II	RNA polymerase II
RP	Ribosomal protein
Rpm	Revolutions per minute
RS	mRNA stability
RSC	Chromatin structure remodeling complex
RT-PCR	Reverse transcription PCR
SAGA	Spt/Ada/Gcn5 acetyltransferase complex
SBMA	Spinal and bulbar muscular atrophy
SCA	Spinocerebellar ataxia type
SD	Standard deviation
SDS	Sodium dodecyl sulfate
SDS-PAGE	SDS polyacrylamide gel electrophoresis
SGD	Saccharomyces genome database
SIR	Silent information regulator
SLIK	SAGA-like
SPTm	SuPpressors of Ty module
SR	mRNA synthesis rate
SWI/SNF	SWItch/Sucrose Non Fermentable
TAF	TBP-associated factors
TAP	Tandem affinity purification
TBE	Tris-borate EDTA
TBP	TATA-binding protein
TBS	Tris-buffered saline
TCA	Trichloroacetic acid

TE	Tris-EDTA
TEV	Tobacco etch virus
TIV	*in vitro* transcripts
TR	Transcription rate
TREX	Transcription and export complex
TREX-2	Transcription export complex 2
TRIS	Tris(hydroxymethyl)aminomethane
TSS	Transcription start site
UAS	Upstream-activation sequence
USP	Ubiquitin specific protease
v/v	Volume/volume
WB	Western-blot
WT	Wild-type
YNB	Yeast nitrogen base
YPD	Yeast extract-peptone-dextrose
YPGal	Yeast extract-peptone-galactose
YPRaf	Yeast extract-peptone-raffinose

Introduction

Saccharomyces *cerevisiae* as a model organism

The majority of the experiments in this thesis have been conducted using the fungus Saccharomyces *cerevisiae (S. cerevisiae)* as a model organism. Yeast *S. cerevisiae* is a single-celled eukaryote with a 5 µm diameter and a replication time of 80-90 minutes under optimal laboratory conditions. It is considered as an ideal organism in the laboratory mostly due to its simplicity and easy growth requirements. Moreover, the ease of its genetic manipulation represents an excellent tool for researchers as different molecular strategies can be performed on it such as polymerase chain reaction (PCR) due to its efficiency of homologous recombination, cloning and transformation which offers scientists flexibility and advantages for experimentation (Duina et al., 2014).

During the last decades yeast has gained popularity at the scientific community. Back in the 1930´s, researchers started to use yeast as an experimental organism (reviewed in Mortimer, 2000; Mortimer and Johnston, 1986) and two decades ago, it became the first eukaryotic organism with its entire sequenced genome (Dujon, 1996; Goffeau et al., 1996). This fact represented a useful reference for higher organisms. Thus, the availability of powerful genetic and biochemical tools allows scientists to use yeast *S. cerevisiae* as a model organism permitting the understanding of equivalent processes in complex organisms.

Genome organization in *S. cerevisiae*

The genetic information contained within the cell is located in the nucleus and separated from the cytoplasm by the nuclear membrane. The nuclear pore complex (NPC) allows the interconnection between the cytoplasm and the nucleus. The organization of the genome in the nucleus is essential for regulation of gene expression. An example of nuclear organization is the differentiation between condensed and generally inactive heterochromatin and decondensed, transcriptionally active euchromatin (Elgin and Grewal, 2003; Grewal and Moazed, 2003). Several studies have postulated that chromosomes are compartmentalized into distinct positions in the nucleus known as chromosomal territories, thus having an impact in specific nuclear functions such as transcription and splicing (Cremer and Cremer, 2001). Chromosomes are arranged in a non-random manner within the nuclear space and are mostly localized at the center of the nucleus and relative to each other (Misteli, 2004). Moreover, several studies have demonstrated that although these chromosomes are organized into territories, chromosomes are dynamic structures and individual chromosomal regions can be repositioned, thus playing an important role in the regulation of gene expression (Gasser, 2002; Lanctôt et al., 2007).

The organization of the genome inside the nucleus defines its transcriptional activity. For instance, its organization in chromosomal territories originates interchromosomal spaces related with higher

transcriptional activity (Lanctôt et al., 2007; Meaburn and Misteli, 2007), while heterochromatin regions such as telomeres and silenced domains seem to move away from such spaces by anchoring them to the nuclear periphery (Capelson and Corces, 2004; Taddei et al., 2004, 2009). However, some genes such as *GAL1*, *INO1* and *HSP104* seem to be relocated at the nuclear envelope (NE) upon transcriptional activation (Cabal et al., 2006; Casolari et al., 2004).

Overall, genome organization in the nucleus might be considered as a hallmark for gene regulation and for other biological processes including cellular division and chromatin silencing.

Chromatin organization

Haploid cells of *S. cerevisiae* contains 12.000 Kb of genomic DNA and approximately 6200 genes which are subdivided into 16 chromosomes ranging in size between 250 kb and >2500 kb. The density of protein-encoding genes is quite high, approximately one gene every 2 Kb (50-fold higher than in the human genome). This is partly due to its low number of introns which represents approximately 4% of all genes (Goffeau et al., 1996; Spingola et al., 1999). In order to store vast amounts of genetic information within the cell nucleus, the DNA adopts a packaged state known as chromatin.

Chromatin is a dynamic structure that controls the access of factors that regulate the state of the genome. The basic structural unit of chromatin is the nucleosome (Kornberg, 1974). It consists of a histone octamer formed

by one H3/H4 tetramer and two H2A/H2B dimers around which 146 base-pairs (bp) of DNA are wrapped (Luger et al., 1997). Each nucleosome is separated by 10-60 bp of "linker" DNA. The incorporation of histone linker H1 promotes the stabilization of nucleosomes and wraps 20 bp of DNA resulting in the two full turns around the octamer (**Figure 1**).

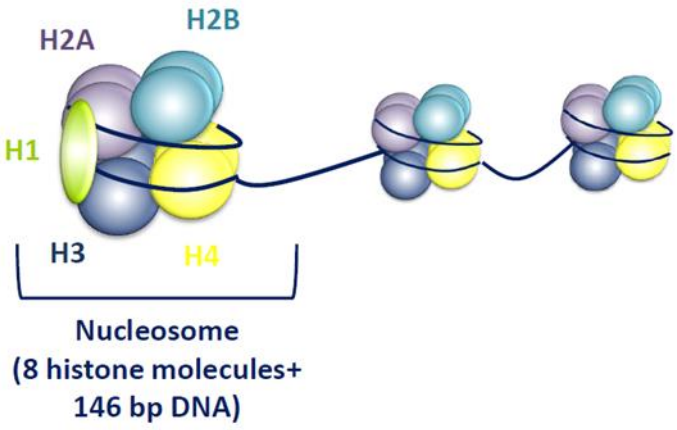

Figure 1. The basic unit of chromatin: the nucleosome. Nucleosome is the basic repeating structural and functional unit of chromatin which is composed of eight histone proteins: two of the histones H2A, H2B, H3 and H4 form a histone octamer which wraps around 146 base pairs. Histone H1 protein wraps an additional 20 base pairs of DNA resulting in the two full turns around the octamer. Nucleosomes are joined together by the linker DNA.

Each of the core histones contains an amino-terminal (N-terminal) tail domain of 20-35 residue segment rich in basic amino acids and a carboxyl-terminal (C-terminal) tail formed by a globular domain with its characteristic histone fold domain. For instance, histone tails do not significantly contribute to the structure or stability of chromatin but play

widespread roles in the folding of nucleosomal arrays into higher order structures (Hansen, 2002; Peterson and Laniel, 2004).

Histone exchange is initially facilitated by the disruption of histone-DNA contacts. Different factors are implicated in the process of histone exchange by diminishing the interaction among histone octamer-DNA and histone-histone interactions by different mechanisms including DNA methylation, non-coding RNAs (ncRNAs) post-translational modifications (PTMs) on histones, ATP-dependent chromatin remodellers or by changing nucleosomal composition carried by histone chaperones (HC).

Several biological processes are linked to chromatin configuration such as chromosome stability, gene expression and segregation. Regulatory factors access to chromatin during DNA replication, transcription and DNA repair leading to changes in chromatin status. For instance, the coordination and organization of the different events along chromatin is essential in order to maintain a correct spatial and temporal epigenetic code (Ehrenhofer-Murray, 2004). Thereby, the interconnection of chromatin-changing functions generates an epigenetic regulatory circuit that is still a subject of debate (Bönisch et al., 2008; Lawrence et al., 2016).

In the next sections, some PTMs and HC will be further described due to their connection to this thesis.

Post-translational modifications

Chromatin can be regulated by histone modifications playing an important role in transcription regulation. One of the first evidence supporting the role of histones in chromatin modification came from the work by Allfrey and colleagues where they postulated that changes in histones, nowadays known as post-translational modifications, had an effect on nuclear RNA metabolism permitting the inhibition and reactivation of RNA production along the chromosomes (Allfrey and Mirsky, 1964). High-resolution X-ray crystallography studies had lately revealed the structure of the nucleosome gaining insight into histone modifications and their effect on chromatin structure (Luger et al., 1997). Histones are highly basic proteins, positively charged, with high affinity for DNA that is negatively charged. The N-terminal tail of histones, as well as some positions in the C-terminal tail, can carry post-translational modifications including acetylation (Ac), phosphorylation (P), methylation (Me), ubiquitination (Ub), sumoylation (S) and ADP ribosylation (**Figure 2**).

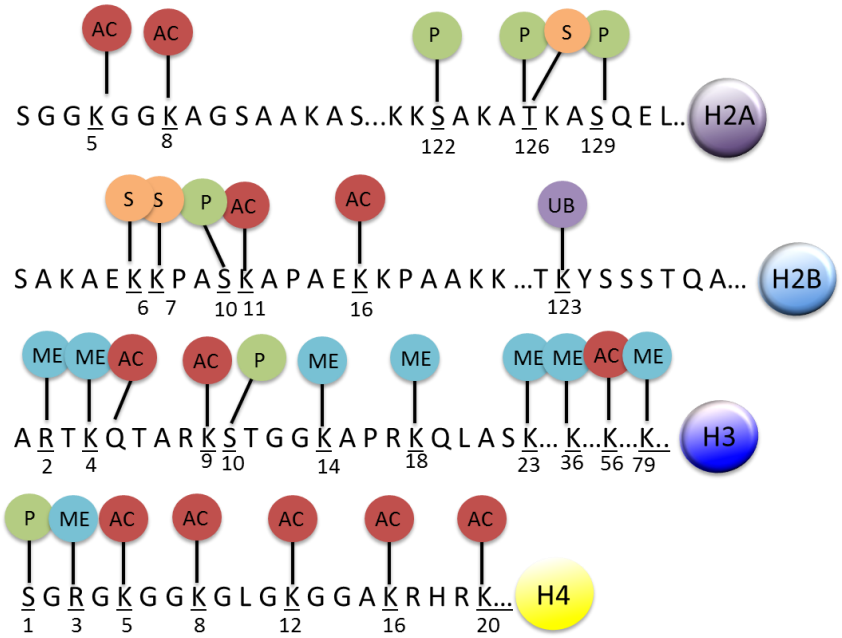

Figure 2. Overview of different classes of post-translational modification of the core histones. The colored shapes represent the histone tail modification at different residues. P: phosphorylation; Me: methylation; Ac: acetylation ; Ub: ubiquitination.; S: sumoylation. Information of this figure came from (Rando and Winston, 2012) and (Bhaumik et al., 2007).

These PTMs can be located within the upstream region, the core promoter and the 5´and 3´ends of the open reading frame (ORF). Depending on the type of histone modification it can have different effects on transcription. On the one hand, several modifications are associated with active transcription including acetylation of histone H3 and H4 or di- or trimethylation of H3K4 ($H3K4me^2$, $H3K4me^3$) which are known as euchromatin modifications. On the other hand, marks such as H3K9me and H3K27me, referred to as heterochromatin modifications are mainly

located at inactive genes and are attributed to transcription repression (Li et al., 2007). These marks can affect several biological processes without altering the DNA sequence and are known as epigenetic changes (Venkatesh and Workman, 2015). Processes such as DNA repair, cell cycle progression, transcription and replication are regulated by PTMs. Indeed, most PTMs are reversible since different enzymes are able to add or remove these epigenetic marks (Ehrenhofer-Murray, 2004; Henry et al., 2003; Kouzarides, 2007). In this section, PTMs with higher impact on transcription activity will be further analysed.

Histone Acetylation

Histone acetylation is catalysed by enzymes named histone acetyltranferases (HATs) that transfer the acetyl moiety from acetyl-coenzime A to the ε-amine of specific lysines. This epigenetic mark neutralizes the positive charge of lysines found in all four core histones H2B, H2A, H3 and H4 altering histone-DNA interaction and leading to open chromatin architecture (Bhaumik et al., 2007). HATs are related to decompaction of chromatin, promoting the accessibility of transcription factors (Shogren-Knaak et al., 2006; Sterner and Berger, 2000). Some studies have demonstrated that activating transcription factors recruit HATs to specific promoters (Brown et al., 2000), linking histone acetylation with active transcription.

The transcriptional adaptor Gcn5 was identified in yeast as the first histone acetyltranferase (Brownell et al., 1996) which had previously been

linked with transcription activation (Georgakopoulos et al., 1995). Later on, Gcn5 was identified in two protein complexes that contained HAT activity, the SAGA (Spt-Ada-Gcn5-Acetyltransferase) complex and Ada complex (Grant et al., 1997). This study revealed that recombinant Gcn5 was only able to acetylate free histones, whereas the SAGA and Ada2 complexes containing Gcn5 could acetylate nucleosomes; indeed, it also demonstrated that Gcn5 was able to acetylate on histones H3 and H2B.

Other HATs have also been identified in *S. cerevisiae* including Sas2, Sas3 and Esa1 (Rando and Winston, 2012). Sas2 contributes to the inactivation of gene expression in telomeres (Kimura et al., 2002). Esa1 acetylates histone H2A and H4 and belongs to NuA4 complex while Sas3 belongs to Nua3 complex (Allard et al., 1999; Grant et al., 1997).

Histones deacetylases (HDAC) enzymes are also related to transcription initiation by removing the acetyl moiety on specific histones. Contrary to HATs, HDACs enzymes are predominantly attributed to transcription repression, thus stabilizing the nucleosomes and preventing the entry of chromatin remodeling complexes. However, in some cases HDACs have been associated as activators of gene expression (De Nadal et al., 2004).

Histone Methylation

Histone methylation can occur at lysines, arginines or both. Lysines can be mono- di- or trimethylated, however, arginines in histones proteins can only be mono- or dimethylated (Shilatifard, 2006). Contrary to histone acetyltranferases which are able to modify several residues within the

same or different histones, histone methyltranferases are generally more specific about their histone targets (Bhaumik et al., 2007). The majority of histone methylases contain a SET domain which was named after D. *melanogaster* Su (var) 3-9, Enhancer of zeste (E(z)), and trithorax (trx) (Dillon et al., 2005). In *S. cerevisiae* three methyltranferases named as Set1, Set2 and Dot1 methlylate histone H3 at lysines 4, 36 and 79, respectively (Krogan et al., 2003a; Miller et al., 2001; Ng et al., 2002, 2003).

Histone H3K4 methylation is performed by SET1C/COMPASS (complex of proteins associated with Set1) complex which comprises Set1, Shg1, Sdc1, Swd1, Swd2, Swd3, Spp1 and Bre2 subunits and it is capable of catalyzing the mono-, di- and trimethylation of H3K4 (Shilatifard, 2012). The distribution of H3K4 along the gene depends on the number of methyl groups; for instance, monomethylation is enriched at the 3´end, demethylation peaks in the core gene while trimethylation occurs at the transcription start site and the 5´end of actively transcribed genes (Pokholok et al., 2005).

On the other hand, Set2 associates with serine 2-phosphorylated RNA Pol II (the elongating form of RNA Pol II), suggesting that Set2 plays an important role in transcription elongation (Li et al., 2002; Xiao et al., 2003). Di- and trimethylation are enriched at the 3´end of active genes, but only H3K36 trimethylation ($H3K36me^3$) has been correlated with transcription rates (Krogan et al., 2002; Pokholok et al., 2005; Rao et al., 2005). H3K36 methylation is necessary for the activation of Rpd3 deacetylase complex

which is required for deacetylation of nucleosomes in coding regions (Carrozza et al., 2005; Govind et al., 2010).

Finally, Dot1 (disruptor of telomeric silencing) is able to mono-, di-, and trimethylate H3K79. Dot1 methylates 90 % of histone H3 in the chromatin and it is required for establishment of telomeric-associated gene silencing (van Leeuwen et al., 2002; Ng et al., 2002; Shilatifard, 2006). This epigenetic mark is located at the promoters and ORFs of active genes, however, its contribution to transcription is not well established (Nguyen and Zhang, 2011). As in the case of H3K4, H2B ubiquitination is also required for H3K79 methylation (Vlaming et al., 2014; Wood et al., 2003a), however, contrary to H3K4 and H3K36, H3K79 methylation levels show little correlation with transcription levels (Rando and Winston, 2012).

Histone methylation is regulated by enzymes with opposite effects. For instance, in higher eukaryotes, deamination by the peptidyl arginine deiminase 4 (PADI4) deaminates arginines residues in the H3 tail (Cuthbert et al., 2004) while lysine (K)-specific demethylase 1A (LSD1) acts as a histone demethylase and transcriptional corepressor since demethylates histone H3 at lysine 4, a mark linked to active transcription (Shi et al., 2004). In yeast, Kdm5 demethylates di- and trimethylated H3K4 (Liang et al., 2007).

Histone Ubiquitination and histone "cross-talk"

Ubiquitination of histones involves the addition of 76-amino acid moiety on the C-terminal helix of histone H2B. Proteins can be polyubiquitinated

or monoubiquitinated. Polyubiquitination of histones regulate different cellular processes including protein degradation, DNA damage tolerance and apoptosis (Yang et al., 2014). On the contrary, lysine monoubiquitination is linked to the regulation of protein activity. A well characterized mechanism underlying the addition of ubiquitin is the monoubiquitination of histone H2B on lysine 123 in yeast (K123) or lysine 120 in mammals (K120) and on histone H2A, a PTM that is not detected in *S. cerevisiae* (Osley, 2006). Histone H2B monoubiquitination is implicated in a variety of biological processes such as cellular growth, transcription initiation and elongation and gene silencing (Pavri et al., 2006).

In *S. cerevisiae*, Rad6 catalyses the monoubiquitination of H2B ($H2Bub^1$) in conjunction with the E3 ubiquitin ligase Bre1 (Wood et al., 2003b). Furthermore, these two proteins act in association with Lge1 which is also required for $H2Bub^1$ (Hwang et al., 2003; Song and Ahn, 2010).

$H2Bub^1$ is related to active transcription since Rad6 and Bre1 associate to promoters by the interaction with activators and with RNA Pol II (Weake and Workman, 2008). Therefore, H2B is ubiquitinated co-transcriptionally and its levels correlate with RNA Pol II elongation rates (Fuchs et al., 2014). $H2Bub^1$ requires the presence of PAF complex which comprises Paf1, Rtf1, Ctr9, Leo1, and Cdc73 subunits and has also been associated with initiating and elongating forms of RNA Pol II. In addition, PAF complex affects H3K4 and H3K79 methylation through its effect on H2B ubiquitination (Shilatifard, 2006; Wood et al., 2003a; Xiao et al., 2005). Recent research has hypothesized that Rtf1 subunit of PAF complex acts as a cofactor in

H2Bub^1 by promoting the ability of Bre1 to direct Rad6 to lysines on H2B or by stimulating Rad6 catalytic activity in the presence of Bre1 (Van Oss et al., 2016).

Importantly, some researchers have shown that monoubiquitination of H2BK123 promotes nucleosome assembly across yeast genome (Fleming et al., 2008). For instance, mutations in *RAD6* and *LGE1* genes lead to lower levels of nucleosomes genome-wide (Batta et al., 2011).

Some other studies have proved that H2Bub^1 cooperates with FACT to regulate transcription elongation (Pavri et al., 2006). Additionally, the Bur1/Bur2 cyclin-dependent proteinase kinase complex (Bur complex) is also required for H2Bub^1 since deletion of these components reduce H2Bub^1 levels (Wood et al., 2005).

As previously mentioned, H2Bub^1 mediated by Rad6/Bre1/Lge1 complex is a prerequisite for H3K4 and H3K79 methylation in yeast and higher eukaryotes, this fact is a clear example of histone cross-talk (Osley, 2006; Shilatifard, 2006, 2012) (**Figure 3**). Mutations affecting H2Bub^1 reduce H3K4 and H3K79 methylation levels, although mutation of the H3 methylation lysines does not show an effect on H2Bub^1, suggesting that this histone cross-talk appears to function unidirectionally (Sun and Allis, 2002).

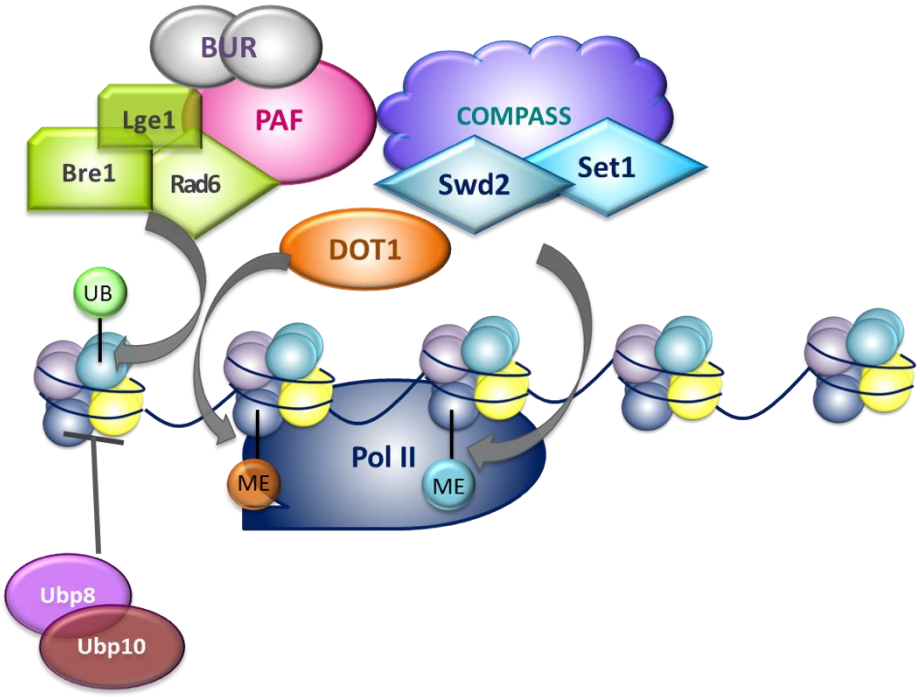

Figure 3. Schematic representation of histone cross-talk. Rad6/Bre1/Lge1 monoubiquitinate histone H2B on lysine 123 which requires interactions with the PAF and the BUR complexes. H2Bub^{1} signal for the activation of histone H3 methylation on Lys 79 and Lys 4 by Dot1 and COMPASS, respectively. H2Bub^{1} promotes the association of Swd2 with chromatin which in turn facilitates the interaction between COMPASS and Swd2, resulting in H3K4me^{2} and H3K4me^{3} by Set1. The removal of the ubiquitin moiety is conducted by deubiquitination enzymes such as Ubp8 and Ubp10.

Moreover, H2Bub^{1} specifically affects to di-and trimethylation of H3K4 and H3K79 while it is dispensable for monomethylation of H3 (Dehé et al., 2005; Shahbazian et al., 2005a). Another research observed that H2Bub^{1} stabilizes the methyltransferase COMPASS complex promoting the recruitment to chromatin of Cps35/Swd2 COMPASS subunit, essential for methyltransferase activity *in vivo* (Lee et al., 2007). In addition, Vitaliano-Prunier et al., demonstrated that monoubiquitination of H2B by

Rad6/Bre1 promotes ubiquitination of Swd2 resulting in the control of Spp1 recruitment, a COMPASS subunit necessary for trimethylation of H3K4 (Vitaliano-Prunier et al., 2008). Overall, these studies suggest that Swd2 is a key factor for histone cross-talk.

Both the addition and the removal of the ubiquitin moiety are required for optimal transcription. H2B is deubiquitinated by two ubiquitin-specific proteases in *S. cerevisiae;* Ubp8 and Ubp10. Ubp8 is a member of the SAGA complex and it is able to remove ubiquitin both *in vivo* and *in vitro* (Daniel et al., 2004; Henry et al., 2003). SAGA integrity is required for a correct Ubp8 deubiquitinase activity, as deletion of SAGA components such as Spt20 increases H2Bub^{1} levels (Daniel et al., 2004; Henry et al., 2003; Ingvarsdottir et al., 2005; Lee et al., 2005). Furthermore, the correct assembly of the DUBm is also necessary for H2Bub^{1} deubiquitination (Köhler et al., 2010; Samara et al., 2010). Another mechanism that relates Ubp8 to transcription elongation is the fact that Ubp8 is required for Ctk1 recruitment resulting in phosphorylation of the RNA Pol II C-terminal domain (CTD), and for Set2 recruitment to the 5´end of the ORF (Wyce et al., 2007).

Ubp10 also acts on H2Bub^{1} deubiquitination but acts on different pools of H2Bub^{1} on the cell, as deletion of both Ubp8 and Ubp10 leads to increased levels of H2Bub^{1} more than either of single deletions. Contrary to Ubp8 which is related to active transcription, Ubp10 function is associated to silenced regions (Gardner et al., 2005).

Histones Chaperones

Histone chaperones (HC) are proteins that act directly on nucleosomes as they are able to control the removal and replacement of histones from promoters and transcribed regions, thus, HC participate in the assembly and disassembly of nucleosomes (Avvakumov et al., 2011; Das et al., 2010). The interaction between chaperones and histones is not limited, in fact, a given histone can be bound by different chaperones (Mattiroli et al., 2015). HC can be classified depending on the histone substrate to which they bind, the majority of chaperones bind to H2A-H2B or H3-H4 oligomers, however, some chaperones can bind through its different domains to both hetero-oligomers (Venkatesh and Workman, 2015). Cycles of nucleosome assembly and disassembly coordinate different cellular events such as DNA repair, transcription and replication. Once histones are synthesized in the cytoplasm and shuttle into the nucleus they associate with chaperones that assist their assembly and disassembly. The interaction among H3/H4 complex with Asf1 chaperone is of particular interest in terms of nucleosome assembly and disassembly (Mousson et al., 2007). Histone chaperone anti-silencing function 1 (Asf1) was identified as a gene whose overexpression inhibits the silencing of chromatin in *S. cerevisiae* (Le et al., 1997) and it is conserved across eukaryotic species as a H3/H4 chaperone (Munakata et al., 2000). Deletion of *ASF1* in *S. cerevisiae* leads to defects in DNA repair and replication, histone modification and transcription (Adkins et al., 2004; Ramey et al., 2004; Recht et al., 2006; Sutton et al., 2001a). Asf1 has been suggested to

function as a mediator of active transcription since it has been associated with promoters and coding regions of actively transcribed genes, hence, it functions as an elongation factor capable of dissemble and reassemble histones during transcription elongation (Schwabish and Struhl, 2006). Indeed, Asf1 facilitates H3 eviction and deposition during RNA Pol II elongation during transcription activation.

In line with this, Asf1 plays a range of functions in chromatin metabolism; first, it stimulates the activity of acetyltransferases in charge of modifying H3 at lysine 9 and 56. Studies have shown that overexpression of Asf1 promotes the acetylation of lysine 9 and Gcn5- dependent acetylation activity on lysine 56 of newly synthesized histone H3 (Adkins et al., 2007). In addition, later studies showed that the interaction among creb-binding domain (CBP) and Asf1 is necessary for Asf1 to promote acetylation of H3K56 by CBP (Das et al., 2014). Secondly, Asf1 functions in coordination with the DNA damage checkpoint control Rad53 since both proteins interact physically and functionally and coexist in the same complex. However, in response to DNA damage Asf1 is dissociated from Rad53 suggesting that Asf1 functions as an effector of Rad53-dependent repair and recovery from DNA damage and block DNA replication (Emili et al., 2001; Hu et al., 2001). Furthermore, Asf1 also associates with Rtt109, a histone acetyltranferase for H3K56. Cells lacking *ASF1* exhibit absence of H3K56, proposing that Asf1 contribute to the maintenance of H3K56 thus playing a role in transcription control (Recht et al., 2006; Schneider et al., 2006).

The regulation of gene expression by RNA Pol II in *S. cerevisiae*

Transcription initiation

The synthesis of RNA from a DNA template requires the control of numerous steps. Transcription initiation is mediated by RNA Pol II and it requires the assembly and coordination of the transcription preinitiation complex (PIC) into the core promoter which is formed by the general transcription factors (GTFs) which includes TFIIA, TFIIB, TFIID (and or SAGA), TFIIE, TFIIF and TFIIH (Shandilya and Roberts, 2012) (**Figure 4**).

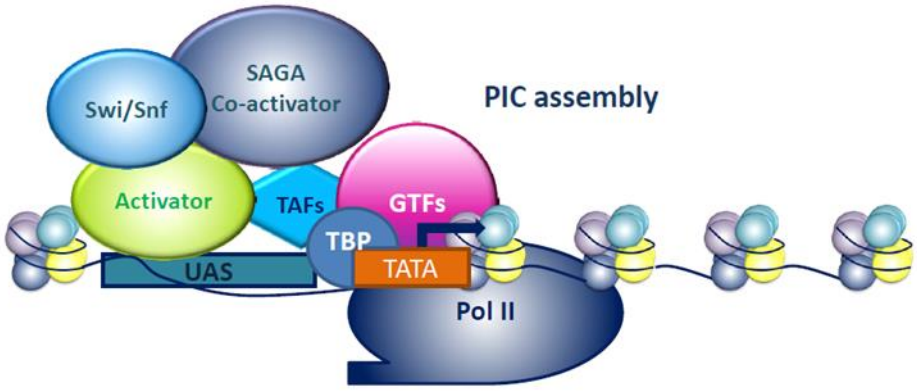

Figure 4. Schematic representation of PIC assembly and transcription initiation. Transcription initiation starts upon interaction of one or more activators to the upstream-activation sequence (UAS) which recruits various co-activators such as SAGA complex and chromatin-remodeling complexes (Swi/Snf) facilitating the binding of GTFs. TATA sequence is recognized by TATA binding protein (TBP) and TBP-associated factors (TAFs) which bind to the promoter DNA, subsequently, TBP alters the TATA sequence facilitating the assemble of other GTFs. Together, co-activators and nucleosome remodelers facilitate the recruitment of RNA Pol II and the GTFs to form the PIC on the promoter thus promoting transcription initiation.

Introduction

Transcription factors recognize the promoter sequence in response to regulatory factors which leads to conformational changes on RNA Pol II required for transcription initiation. Once activators bind to the upstream-activation sequence (UAS), several co-activator complexes such as chromatin-remodeling complexes, histone-modification enzymes and mediator are recruited into the core promoter which makes nucleosomal DNA elements more accessible to GTFs. Additionally, promoter elements serve as binding sites for subunits of the transcription machinery to direct transcription. These elements include the TATA-box (TBP binding site), Inr (initiator element), DPE (downstream promoter element) and BRE (TFIIB recognition element) (Hahn, 2004). DNA elements at the core promoter can extend 35 bp upstream and/or downstream of the transcription start site (TSS) (Smale and Kadonaga, 2003; Thomas and Chiang, 2006). Genes can be classified depending on the presence of a TATA box (TATA-containing) or absence (TATA-less) promoters. The TATA box has a consensus sequence and is located around 30-120 bp upstream of the TSS in *S. cerevisiae*. TATA sequence is recognized by TATA binding protein (TBP) and TBP-associated factors (TAFs) which bind to the promoter DNA. Following this binding, TBP alters the TATA sequence facilitating the assemble of other GTFs (Shandilya and Roberts, 2012). TBP recruitment can be stimulated by activators which act during transcription activation, hence transcriptional activity has been correlated with the degree of TBP occupancy (Kuras and Struhl, 1999).

Two major pathways of transciption activation are found in yeast including the TFIID transcription factor and SAGA complex (Grant et al., 1997; Mizzen et al., 1996). TFIID regulates 90 % of the yeast genes which correspond to housekeeping genes. On the contrary, SAGA regulates the remaining 10 % of the genes which mainly correspond to stress genes which contain promoters characterized by having a TATA box, while those genes regulated by TFIID present promoters with similar sequences known as TATA-like (Huisinga and Pugh, 2004).

As seen in previous sections, there exists a wide range of factors capable of altering chromatin structure at the core promoter, hence contributing to transcription regulation. Some of these elements involve the participation of HC, PTMs and chromatin-remodeling factors. According to this, changes in transcription are correlated with changes in chromatin structure. Several chromatin-remodeling factors have been described to influence on chromatin dynamics. These factors use the energy of ATP hydrolysis to change the structure of nucleosomes by disrupting histone-DNA interactions (Clapier and Cairns, 2009; Rando and Winston, 2012). Some of the yeast chromatin-remodeling factors include the SWI/SNF (Switch sucrose non fermentable) and RSC (remodeling the structure of chromatin) and the ISW (imitation switch) family (ISW1 and ISW2) which are all implicated in nucleosome remodeling. For instance, SWI/SNF remodeler slides and ejects nucleosomes at diverse loci but lacks a role in chromatin assemble. Moreover, the ISW family optimize nucleosome

spacing promoting chromatin assembly and are implicated in both transcription activation and repression (Clapier and Cairns, 2009).

An active transcription starts after conformational changes at the TSS occur and the template strand of the promoter is positioned within the active side of RNA Pol II. Then, transcription initiation begins with the synthesis of the first phosphodiester bond of RNA. After the synthesis of about 30 bases of RNA, RNA Pol II is released from the core promoter together with the transcription factors to enter into the elongation stage.

The carboxyl-terminal domain (CTD) of the largest subunit of RNA Pol II, Rpb1, plays a critical role in transcription regulation since it is dynamically modified by PTMs hence facilitating or impeding recruitment of regulator factors of RNA Pol II. During transcription initiation CTD remains unmodified when recruited to promoter regions; however, the transition from initiation to elongation is partly regulated by phosphorylation of this domain. Cyclin-dependent kinase 28 (Kin28) from TFIIH phosphorylates Ser5 from CTD facilitating the escape of RNA Pol II from promoter. Furthermore, DNA helicase Rad25 remodels the PIC and promotes the dissociation of 11-15 bases of DNA at the TSS facilitating the introduction of a single-stranded DNA template into the active site of RNA Pol II and hence, promoting the transition from initiation into an early transcription elongation (Saunders et al., 2006; Weake and Workman, 2010). Therefore, changes in the CTD phosphorylation state of RNA Pol II are coupled with transcription stage (Harlen and Churchman, 2017).

SAGA co-activator complex as a modulator of transcription regulation

SAGA (Spt-Ada-Gcn5-Acetyltransferase) is a well-characterized co-activator complex that is conserved from yeast to humans. SAGA from *S. cerevisiae* is a 1.8 MDa protein complex that is composed of at least 20 subunits which are organized into 4 modules; HATm (Histone acetyltranferase), DUBm (Histone deubiquitination), SPTm (Suppressor of Ty) and TAFm (TBP-associated factor) (**Figure 5**) (Baker and Grant, 2007; Lee et al., 2011; Rodríguez-Navarro, 2009; Weake and Workman, 2008).

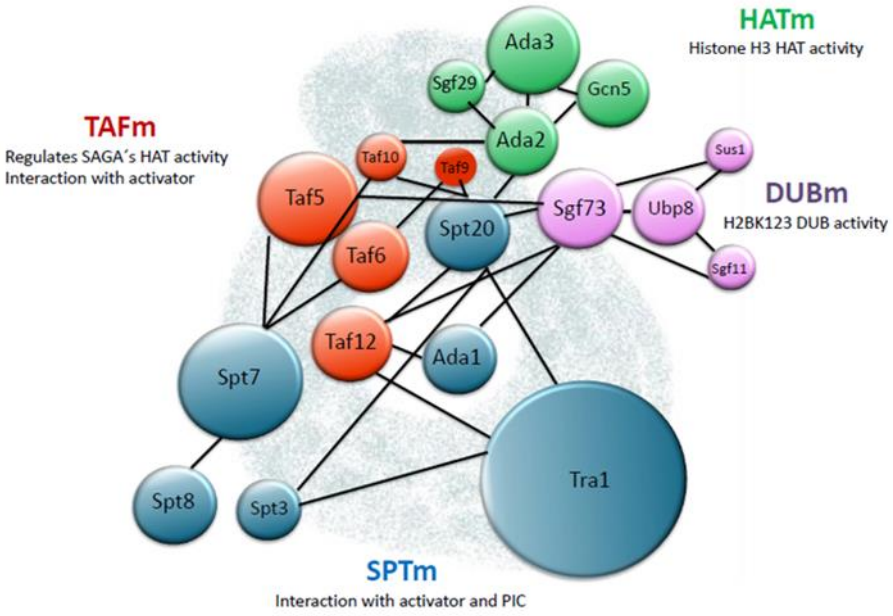

Figure 5. Schematic representation of the localization SAGA´s subunits. SAGA contains 4 distinct modules which are represented in blue (SPTm); red (TAFm); purple (DUBm) and green (HATm). The area of the circle represents the relative molecular weight of SAGA´s subunits. Lines represent the probable physical interaction between subunits. This figure is adapted by the work from different groups (Han et al., 2014; Setiaputra et al., 2015; Weake and Workman, 2012).

The HATm has histone H3 K9/14 HAT activity and consists of Gcn5, Ada2, Sgf29 and Ada3 (Grant et al., 1997). The DUBm is composed of Sgf73, Ubp8, Sus1 and Sgf11 and posseses H2B lysine 123 (K123) deubiquitination activity (Ingvarsdottir et al., 2005; Köhler et al., 2006; Lee et al., 2005, 2009; Pascual-García et al., 2008; Rodríguez-Navarro et al., 2004). Several TAFs including Taf5, Taf6, Taf9 Taf10 and Taf12 constitute the TAFm and are implicated in both regulating SAGA´s HAT activity and interaction with activators (Durairaj et al., 2014). The SPTm is composed of Tra1, Spt3, Spt7, Spt8, Ada1 and Spt20 which are involved in transcription regulation by interacting with activator and PIC and are also involved in recruiting the HATm (Brown et al., 2001). Null mutations in *ADA1*, *SPT20* and *SPT7* disrupt SAGA complex and cause severe phenotypes, these members are considered as SAGA core components (Sterner and Berger, 2000).

As we have seen, SAGA harbors two enzymatic activities which are tightly associated with gene expression; histone H3 acetyltransferase by Gcn5 (Grant et al., 1997) and histone H2B deubiquitination (DUB) activity by Ubp8 (Daniel et al., 2004; Henry et al., 2003). These activities are necessary for the regulation of histones post-translational modifications of histones H2B and H3 altering the genome-wide chromatin status. The diverse activities related to SAGA complex allow this complex to modulate transcription at many promoters by regulating chromatin modifications by its enzymatic activities, stimulating PIC assembly and modulating several steps in early transcription elongation. For instance, Spt3 and Spt8 subunits from SPTm were shown to interact with TBP, modulating TBP

interaction with certain promoters (Warfield et al., 2004). The SPTm contacts with activator and PIC and it is implicated in regulating transcription initiation in addition to maintaining SAGA´s structural integrity (Durairaj et al., 2014). Tra1 subunit is also part of NuA4 complex and it has been reported that it interacts with several activators including Gcn4 and Gal4 (Brown et al., 2001). The TAFm is shared with TFIID complex and it appears to form a structural core on which SPTm, DUBm and HATm are assembled (Han et al., 2014).

The coordination of the subunits within each of the four modules is necessary for its correct function. For example, Gcn5 activity is modulated by Ada2 and Ada3 subunits (Grant et al., 1997) and it contains a bromodomain that directly binds to acetylated lysines in histone tails, indeed, Sgf29 subunit contains a Tudor domain capable of binding H3K4me^2 and H3K4me^3 which are marks related to active transcription (Hassan et al., 2002; Vermeulen et al., 2010). Furthermore, Ubp8 catalytic subunit from the DUBm becomes active when it forms a complex with Sgf11, N-terminus of Sgf73 and Sus1 (Köhler et al., 2008; Lang et al., 2011; Lee et al., 2009). In line with this, the full assembly of SAGA modules is essential to increase the substrate recognition and specificity of Gcn5 and enhance Ubp8 catalytic activity on nucleosomes (Bian et al., 2011; Lang et al., 2011; Samara et al., 2010). In addition, recent research of DUBm architecture has revealed that the DUB module is positioned close to Gcn5, which could explain the reported cross-talks between histone H2B deubiquitination and histone H3 acetylation (Durand et al., 2014).

SAGA recruitment and histone acetylation occur prior to PIC formation at the *GAL1* promoter (Bhaumik and Green, 2001). Interestingly, in addition to its role in H2B deubiquitination activity, Sus1 has been shown to promote PIC formation thus participating in transcription initiation at the SAGA-regulated genes independently of its H2B DUB function (Durairaj et al., 2014). Alternatively, SLIK (SAGA-like) complex is related in composition and substrate specificity to SAGA complex, however it lacks the Spt8 protein and contains a truncated form of Spt7 (Pray-Grant et al., 2002; Sterner et al., 2002). SLIK function within the cell remains unsolved, remarkably, it uniquely contains the protein Rtg2 which is linked to the retrograde response pathway (Pray-Grant et al., 2002).

DUBm function and structure

As previously introduced, the DUBm is composed of 4 proteins which are conserved from yeast to humans. The DUBm contains yUbp8/hUSP22, ySus1/hENY2, ySgf73/hATXN7 and ySgf11/hATXN7L3 and is responsible for the deubiquitination of histone H2B (Atanassov et al., 2016; Galán and Rodríguez-Navarro, 2012; Helmlinger et al., 2004).

As cited earlier, monoubiquitination of H2B ($H2Bub^1$) at yeast K123 and human K120 is a transient modification catalysed by Rad6/Bre1/Lge1 complex and a common feature of active transcription (Bonnet et al., 2014; Robzyk et al., 2000; Song and Ahn, 2010; Wood et al., 2003b). In addition to its contribution on transcription activation, it is also involved in transcription elongation, mRNA splicing, DNA replication and repair and

mRNA export (Fuchs and Oren, 2014; Fuchs et al., 2014). H2B-ub[1] is also a mark for di- and trimethytlation of histone H3 at lysines 4 and 79 which is associated with transcription elongation (Dover et al., 2002; Kim et al., 2009; Laribee et al., 2005; Lee et al., 2007; Sun and Allis, 2002; Vlaming et al., 2014; Wood et al., 2005).

Although the DUB activity is borne by Ubp8 subunit, the correct assemble of the 4 DUBm proteins is essential for the activation of the enzyme Ubp8 (Ingvarsdottir et al., 2005; Köhler et al., 2008; Lee et al., 2005, 2009). Several studies have provided insights into the crystal structure of the DUBm showing that the four components are remarkably intertwined (Köhler et al., 2010; Morgan et al., 2016; Samara et al., 2010). According to these studies, the DUBm contains the full Ubp8, Sgf11, Sus1 and an Sgf73 N-terminal fragment extending to either residue 96 (Köhler et al., 2010) or 104 (Samara et al., 2010). Ubp8 contains two globular domains: the ubiquitin specific protease (USP) or catalytic lobe which contains the C-terminal USP domain and the ZnF-UBP or assembly lobe that contains the N-terminal Zinc Finger-Ubiquitin Binding Protein (ZnF-UBP) domain. Thus, the DUBm is organized into two lobes: in the assembly lobe Sgf11 N-terminal helix binds to the Ubp8 ZnF-UBP domain by Sus1 whereas in the catalytic lobe Sgf11 C-terminal zinc finger domain binds to the Ubp8 catalytic domain. Between the lobes lies Sgf73 which is responsible for the binding of the two globular domains of Ubp8 allowing the DUBm to act together as one structurally integrated module. Additionally, deletion of *SGF11* or *SUS1* results in the dissociation of Ubp8 from Sgf73 which

confirms the structural integrity of the DUBm (Ingvarsdottir et al., 2005; Köhler et al., 2006; Lee et al., 2005) (**Figure 6**).

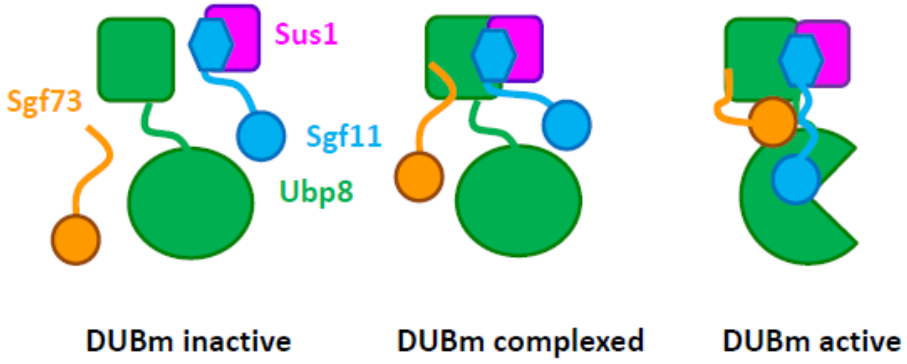

Figure 6. Ubp8 catalytic activity requires the assembly of the SAGA DUBm. Free Ubp8 presents a ZnF-UBP domain (green square) and an inactive catalytic domain (green full circle). Sus1 forms a complex with Sgf11 by wrapping around its N-terminal helix (hexagon). Full activated Ubp8 (sharp teeth) requires the correct position of ZnF domains of Sgf11 (blue circle) and Sgf73 (orange circle). Figure adapted from the work by Köhler and colleagues (Köhler et al., 2010).

Mutations in *SGF73* and *SGF11* lead to a significant impairment of DUB activity (Köhler et al., 2006, 2008, 2010; Lee et al., 2009). Deletion of Sgf11-ZnF results in almost loss of Ubp8 catalytic activity since it destabilizes the compact folding of the DUBm (Samara et al., 2010, 2012). Further studies also demonstrated that Sgf73 point mutations affect on the structure of DUBm disrupting the enzymatic activity of Ubp8 by impacting Ubp8 ubiquitin-binding fingers region suggesting that Sgf73 contributes to Ubp8 structure and to the stability and folding of the DUBm

(Yan and Wolberger, 2015). Furthermore, NMR studies have also provided new contributions to the understanding of DUBm organization into nucleosomes, arginine residues at the ZnF helix of Sgf11 are key to Sgf11 interaction with nucleosomal DNA and this is important for the optimal position of the DUBm on the nucleosome particle and DUBm activity (Koehler et al., 2014). Recent research has proposed that the DUBm principally contacts H2A/H2B by the basic Sgf11-ZnF domain. In addition, these researchers also found that the DUBm deubiquitinates from either intact or disassembled nucleosomes suggesting that it is able to act at diverse points as RNA Pol II transcribes through chromatin (Morgan et al., 2016). In addition to the organization of the DUBm components for Ubp8 activation, some studies have reported that DUBm needs to be assembled into SAGA complex for its correct function. However, some researchers have suggested that Sgf73 interaction with the proteasomal ATPase Rpt2p leads to the dissociation of the DUBm from SAGA complex which is functionally active, raising the possibility that a separated DUBm may function independently of SAGA complex (Lim et al., 2013). Indeed, unpublished data from our lab has also demonstrated the existence of an independent and functional DUBm from SAGA complex upon deletion of Spt7 subunit (García- Molinero et al*.,* in revision).

Similarly to the yeast complex, human USP22 (hUSP22) also deubiquitinates histones H2A and H2B (Zhang et al., 2008a, 2008b; Zhao et al., 2008). Interactions of hUSP22 with hATXN7, hENY2 and hATXN7L3 are required for Ubp8 incorporation in the human SAGA complex (STAGA) and

for hUSP22 activation (Lang et al., 2011). Several research have related these proteins with human malignancies, for instance, polyglutamine expansion at the N-terminal region of hATXN7 causes Spinocerebellar Ataxia type 7 (SCA7) disease (information regarding to SCA7 disease can be found at the end of this section).

Transcription elongation

Transcription elongation occurs when RNA Pol II releases from GTFs and enters into the coding region of a given gene, signaling the recruitment of the elongation machinery including factors involved in mRNA processing, mRNA export and chromatin function (Li et al., 2007).

The C-terminal domain of Rpb1, RNA Pol II largest subunit, undergoes dynamic phosphorylation during transcription which affects the recruitment of mRNA processing and histone modifying complexes such as PAF, FACT and COMPASS among others (Buratowski, 2009). Two major phosphorylation events appear to control transcription elongation; Ser5 phosphorylation mediated by the TFIIH-associated kinase 28 (Kin28) (Buratowski, 2003; Komarnitsky et al., 2000) and Ser2 phosphorylation by cyclin-dependent kinase Ctk1 (Cho et al., 2001; Komarnitsky et al., 2000).

During transcription elongation, the PAF complex facilitates the binding of COMPASS, FACT and the ubiquitin ligases Rad6/Bre1/Lge1 to the Ser5-phosphorylated CTD resulting in H2B monoubiquitination and accumulation of H3K4me^3 at the 5´-end of the coding gene. In addition, Ubp8 deubiquitination activity on histone H2B mediates the recruitment

of kinase Ctk1 which phosphorylates RNA Pol II at Ser2, and subsequently regulates the recruitment of Set2 methyltransferase (Wyce et al., 2007). Set2 interacts with Rpb1 which depends on the phosphorylation of CTD at Ser2 (Krogan et al., 2003a; Xiao et al., 2003). Thus, H3K36me^3 mediated by Set2 is associated with the elongating RNA Pol II and occur during the later stages of transcription elongation (Krogan et al., 2003a; Shilatifard, 2006) (**Figure 7**) .

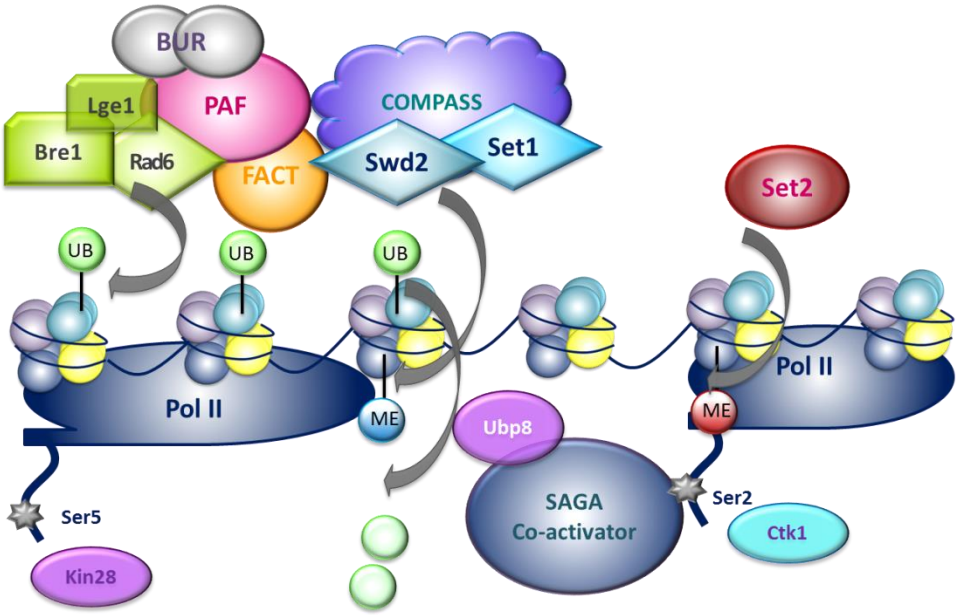

Figure 7. Schematic model for transcription elongation. PAF facilitates the binding of FACT, COMPASS and Rad6/Bre1/Lge1 to the Ser5-phosphorylated CTD mediated by Kin28 which results in H2Bub^1 and subsequent accumulation of H3K4me^3 by COMPASS complex. The removal of ubiquitin on H2B by the DUB enzyme Ubp8 facilitates the recruitment of Ctk1 kinase which phosphorylates RNA Pol II at Ser2. Ser2-phosphorylated CTD regulates the recruitment of Set2 methyltransferase promoting H3K36me^3 during later stages of transcription elongation.

Methylation of H3K36 recruits the Rpd3 deacetylase complex which removes the acetyl marks and leaves the nucleosome in a stable state (Carrozza et al., 2005). Overall, subsequent cycles of H2B ubiquitination/deubiquitination are essential for transcription activation and for establishing correct histone methylation patterns at the gene body.

SAGA contribution in transcription elongation is also linked to Sus1 protein from SAGA DUBm. In our lab we have shown that Sus1 subunit co-purifies with RNA Pol II and mRNA export factors which are co-transcriptionally recruited to coding regions (Pascual-García et al., 2008). Additionally, Gcn5 subunit from the HAT complex stimulates modification and eviction of nucleosomes in transcribed coding regions such as at the *GAL1* gene thus promoting RNA Pol II elongation (Govind et al., 2007).

Coupling transcription to mRNA export

Messenger RNA (mRNA) export depends on the coordination and participation of several complexes and export factors that modulate the different steps for the transport of mRNA transcripts from the nucleus to the cytoplasm towards the nuclear pore complex (NPC). Before mRNA is exported to the cytoplasm, mRNA transcripts must firstly be processed which includes the addition of a 5´-cap, splicing out of introns and 3´-end cleavage and polyadenylation (Kelly and Corbett, 2009). A large subset of studies have pointed out that transcription is coupled with mRNA export suggesting that mRNA processing is a dynamic process and intimately

interconnected with upstream processes (Rodríguez-Navarro and Hurt, 2011). In these lines, mRNAs are exported from the nucleus as messanger ribonucleoproteins (mRNPs) complexes that start to be assembled during transcription.

Yeast NPCs are large assemblies of 60 MDa that are located within the nuclear envelope. NPCs have an eightfold symmetrical core structure (called the spoke complex) that is inserted between a cytoplasmic and a nuclear ring. The NPC contains approximately 30 different nuclear pore proteins (nucleoporins) that exist in 8 to 32 copies in each NPC. The majority of nucleoporins are located symmetrically on both sides of the NPC, however, several NPC are located either on the cytoplasmic or nuclear side of the NPC. For instance, Nup1, Nup2, Nup60 and Mlp1-Mlp2 are found at the nuclear side of the NPC (Beck and Hurt, 2017; Schwartz, 2016).

Fully mature mRNPs complexes are later recognized by the essential conserved export receptor, the Mex67-Mtr2 heterodimer in *S. cerevisiae* (Segref et al., 1997) which mediates the interaction among the mRNPs and the NPC, in fact, most export factors are recruited cotranscriptionally suggesting that export factors are recruited to the sites of transcription to promote correct mRNA export (Lei et al., 2001; MacKellar and Greenleaf, 2011). Mex67 recruitment to mRNA transcripts is enhanced by the participation of adaptor proteins which are deposited along nascent transcripts. Transcription and export (TREX) complex participates in this process, thus determining the efficiency of mRNA export. TREX is

composed of mRNA export adaptor proteins, Sub2 and Yra1, and components of the THO complex (Hpr1, Mft1, Thp2 and Tho2) (Abruzzi et al., 2004; Chávez et al., 2000; Reed and Cheng, 2005; Strässer et al., 2002). Yra1 is recruited to the transcription machinery and subsequently transferred to the nascent mRNA, it directly interacts with the TREX subunit Sub2 which is recruited in the early stages of transcription (Abruzzi et al., 2004; Strässer and Hurt, 2001). Yra1 was the first RNA-binding protein characterized which directly binds to Mex67/Mtr2 and bridges the shuttling Mex67/Mtr2 exporter to the NPC (Sträßer and Hurt, 2000). Sub2 and Mex67 compete for the binding of Yra1 since both proteins bind to the same domains of Yra1, thus Sub2 is displaced from Yra1 by the binding of Mex67 (Strässer and Hurt, 2001). Once the mRNP enters into the NPC cytoplasmic face, Gle1 and inositol hexaphosphate (IP6) activate the DEAD-box helicase Dbp5 which remodels mRNPs by removing Mex67 thus preventing mRNPs from returning to the nucleus (Ling and Song, 2010).

Additionally, TREX complex is co-transcriptionally recruited (Abruzzi et al., 2004; Strässer et al., 2002) and several labs have shown that TREX mutants induce a defect in RNA Pol II elongation close to the 3´end preventing mRNP rearrangement and polyadenylation resulting in the release of mRNA from the transcription site (Rougemaille et al., 2008; Saguez et al., 2008).

The TREX-2 complex

TREX-2 complex is a conserved multiprotein complex in yeast composed of Sus1, Sac3, Thp1, Sem1 and Cdc31 which is located at the NPC at least at the steady state and it is required for efficient poly $(A)^+$ mRNA export and gene tethering to the nuclear periphery (**Figure 8**) (Faza et al., 2009; Fischer et al., 2002, 2004; González-Aguilera et al., 2008; Rodríguez-Navarro et al., 2004).

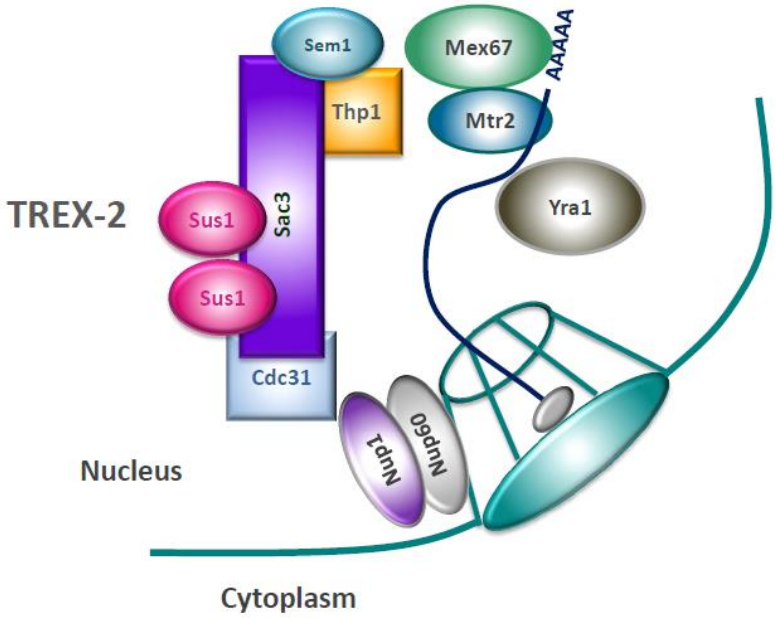

Figure 8. Schematic illustration of the TREX-2 complex. TREX-2 is composed by Sac3-Thp1-Sem1-Sus1-Cdc31 proteins and interacts with nucleoporines Nup1 and Nup60 at the NPC. The binding of TREX-2 to export factors Mex67/Mtr2 heterodimers together with Yra1 promotes the export of mRNA molecules to the NPC.

Jani and colleagues revealed the crystal structure of TREX-2 complex and showed that Sus1 and Cdc31 bound to a central region of Sac3 (the CID domain) that adopts a long α-helix conformation, around which one Cdc31 and two Sus1 molecules are wrapped (Jani et al., 2009). Hence, Sac3 acts as a scaffold coordinating the interactions among the transcription and mRNA export machineries.

At steady state, Sac3 is stably associated with the NPC through interactions between its CID region and nucleoporins Nup1 and Nup60 (Fischer et al., 2002, 2004). On the other hand, Sus1 and Cdc31 stabilize the NPC-TREX-2 complex whereas Thp1 and Sem1 bind to a central region of Sac3 generating two juxtaposed winged-helix domains which bind nucleic acid (Ellisdon et al., 2012). Thp1 and Sac3 subunits interact with the export factor Mex67-Mtr2 (Fischer et al., 2002). Mutations that impair the binding of Sus1, Thp1 or Cdc31 to Sac3 generate defects in mRNA export and cell growth (Ellisdon et al., 2012; Jani et al., 2009).

Several results correlate TREX-2 components with transcription, for instance, TREX-2 interacts with the Mediator complex regulating mRNA export suggesting a mechanism for coupling transcription with mRNA processing (Schneider et al., 2015). During gene gating, TREX-2 also mediates the relocation of active genes to the nuclear periphery (Cabal et al., 2006). TREX-2 also promotes the transcriptional memory seen with several yeast genes (Chekanova et al., 2008).

SAGA activity is linked to TREX-2 complex

Over the past years some studies have described several mechanisms which connect transcription with mRNA export. A clear example of this interconnection resides in protein Sus1 which is a component of both SAGA and TREX-2 complexes and plays a key role in coupling transcription activation and mRNA export (Rodríguez-Navarro et al., 2004). Indeed, the interconnection between SAGA and TREX-2 regulates different steps of gene expression. Sus1 participates in both transcription initiation and elongation as it is recruited to the UAS upon gene activation and to coding regions (Köhler et al., 2006; Pascual-García et al., 2008). Its role in transcription elongation was demonstrated by studies from our lab showing that it purifies with the elongating form of RNA Pol II. Sus1 binding to the UAS and ORF of *ARG1* is partially mediated by the TREX-2 component Sac3 (Pascual-García et al., 2008). Indeed, Sus1 associates with the mRNA adaptor Yra1 and the export factor Mex67 co-transcriptionally ensuring the coupling between transcription elongation and mRNA export (Pascual-García et al., 2008; Rodríguez-Navarro, 2009). Moreover, Sus1 is responsible for TREX-2 targeting to the NPC since cells lacking *SUS1* lead to a mislocalization of TREX-2 complex (Köhler et al., 2008) (**Figure 9**). Some other studies link Sus1 with chromatin positioning and it has been demonstrated that it is responsible for *GAL1* tethering to the nuclear periphery (Cabal et al., 2006). Additionally, other SAGA subunits are also involved in mRNA export; the loss of the DUBm component Sgf73 partly disrupts Sus1 association to TREX-2 complex and

leads to a mislocalization of Sus1 to the cytoplasm (Köhler et al., 2008; Pascual-García and Rodríguez-Navarro, 2009a; Pascual-García et al., 2008). Furthermore, Sgf11 subunit also participates in mRNA export since deletion of *SGF11* enhances the mRNA export defect observed in *sus1Δ* cells (Köhler et al., 2006).

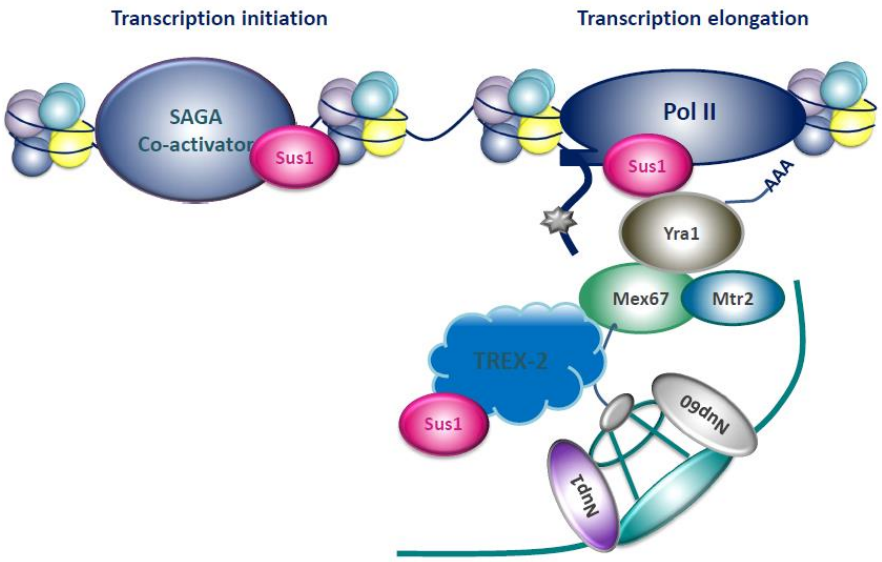

Figure 9. SAGA and TREX-2 interplay. Sus1 belongs to both SAGA and TREX-2 complexes and participates in both transcription initiation, elongation and mRNA export. Thus, Sus1 is recruited to the UAS region via SAGA upon gene activation and it is also recruited to transcribed chromatin by phosphorylation of RNA Pol II. Sus1 as part of TREX-2 complex participates in the export of mRNA towards the NPC by its interaction with Yra1 and Mex67/Mtr2 and nucleoporines.

Work from our lab contributed to the understanding of TREX-2 complex and its role in histone H2B deubiquitination. With this work, we demonstrated that Sem1 component from TREX-2 complex also facilitates the linkage between SAGA and TREX-2 since Sem1 is required for the

induction of SAGA regulated genes *GAL1* and *ARG1* and it also takes part in SAGA-dependent deubiquitination activity (García-Oliver et al., 2013).

SAGA and TREX complexes in nuclear periphery-gene tethering

Previous research have proposed that in *S. cerevisiae* part of the transcription process occurs in the region next to the NPC enabling the interaction among the gene locus and the NPC and thus, stabilizing and activating the chromatin region to be transcribed ensuring the correct posterior mRNA export. These studies suggest that nuclear position plays an active role in determining optimal gene expression levels (Brickner et al., 2007; Cabal et al., 2006; Casolari et al., 2004; Taddei et al., 2006). A subset of genes including *INO1*, *HXK1*, *GAL1*, *GAL2*, *GAL7*, *GAL10*, *HIS4*, *HSP104*, *PRM1* and *STL1* have been shown to relocalize to the nuclear periphery after transcription activation (Raices and D'Angelo, 2017).

Several components of SAGA complex including Gcn5, Ada2 and Spt7 interact with the inner nuclear basket protein Mlp1 and it has been shown that they associate with the same region of the *GAL* promoters supporting previous results that relied upon visualization of *GAL* loci at the NPC (Luthra et al., 2007). Additionally, deletions of *SUS1*, *NUP1* and *SAC3* impairs the relocalization of *GAL1* to the nuclear periphery following its activation (Cabal et al., 2006; Green et al., 2012). The binding of TREX-2 complex to the NPC has been proposed to function by integrating mRNA export with earlier steps in gene expression which promote gene stability by the inhibition of R-loop formation (reviewed in García-Oliver et al.,

2012; Rodríguez-Navarro and Hurt, 2011). R-loops seem to occur in mutants affecting mRNP formation and processing as has been shown in mutants of the THO/TREX complex (Huertas and Aguilera, 2003). Indeed, transcription elongation is impaired by R-loops (Tous and Aguilera, 2007).

Further work on TREX-2 by Schneider and coworkers showed that Mediator complex participates in connecting RNA Pol II to TREX-2 and NPCs, furthermore the interaction between TREX-2 and mediator is required for the targeting of *GAL1* and *HXK1* genes to the nuclear periphery (Schneider et al., 2015). Other advances have also contributed to the understanding of the molecular mechanisms that mediate nuclear periphery-gene tethering. For example, targeting of *INO1* to the nuclear periphery is mediated by GRS1 and GRS2 (Gene recruitment sequences) which present binding sites for transcription factors that mediate gene-relocation (Ahmed et al., 2010). Controversy exists among the studies since some researchers have hypothesized that NPC interact with transcribable regions of the genome and that serves as a platform for gene-gating (Ptak et al., 2014). However, some other researchers have demonstrated that active genes are rarely co-localize with the nuclear envelope and that the distance between active site loci and the nuclear periphery is not suitable for the tethering of active genes to the NPC (Guet et al., 2015).

Interestingly, some studies have also suggested that upon gene repression, genes are maintained at the nuclear periphery for future generations where they are poised for transcription and are reactivated faster in

response to a future induction, a mechanism known as transcription memory (D'Urso and Brickner, 2014). One well-established example for this phenomenon is the inducible *INO1* gene. Once the gene is repressed, *INO1* remains associated with the nuclear periphery for some generations exhibiting faster rate of transcriptional reactivation (Brickner et al., 2007). Therein, the association of genes to the nuclear periphery promotes a more efficient gene expression and enhances transcriptional memory (Taddei et al., 2006; Texari et al., 2013).

Protein trafficking; Mog1 protein and its role in Ran GTP/GDP cycle

Ran is an evolutionary conserved member of the Ras superfamily of small GTPases which plays critical roles in nucleocytoplasmic transport of macromolecules through the NPC (Görlich and Kutay, 1999). Additionally, Ran is implicated in cell cycle regulation and microtubule assembly dynamics (Desai and Hyman, 1999). Ran mediates the Ran GTPase cycle which is involved in nuclear import and export pathways, hence, proteins destined to the nucleus contain nuclear localization signals (NLS) while proteins destined for the cytoplasm present a nuclear export signal (NES). The directionality of transport is based on nuclear Ran GTP-bound and cytoplasmic Ran GDP-bound (Görlich and Kutay, 1999).

The GTPase activity of Ran (Gsp1 in *S. cerevisiae*) is mediated by tightly controlled cycles of GTP binding and hydrolysis, producing GTP-and GDP-

bound forms that interact with several regulators and effectors. Thus, the nuclear guanine nuclear exchange factor (GEF) named as Rcc1 in vertebrates (Prp20 in *S. cerevisiae)* catalyses GDP release and GTP-binding (Bischoff and Ponstingl, 1991). In contrast, the conversion of RanGTP to RanGDP occurs in the cytoplasm and it is mediated by a Ran GTPase-activating protein (Ran GAP) known as Rna1 in *S. cerevisiae* and its co-activators Ran binding proteins such as Yrb1 which shuttles rapidly between the nucleus and cytoplasm although at steady-state it is localized in the cytoplasm (Künzler and Hurt, 2001; Plafker and Macara, 2000). The transport of RanGDP to the nucleus is mediated by the transport factor NTF2 (Steggerda et al., 2000). Therefore, Ran regulators are responsible for maintaining Ran in a predominantly GDP-bound state in the cytoplasm and in a GTP-bound state in the nucleus (Görlich and Kutay, 1999).

Mog1 (multicopy suppressor of Gsp1) also participates in the Ran GTPase pathway and it was first identified in yeast (Oki and Nishimoto, 1998) and subsequently in vertebrates (Steggerda and Paschal, 2000). Researchers have shown that Mog1 has a functional interaction with Ntf2 and it is required for nuclear-protein import that binds to Ran (yeast Gsp1) (Baker et al., 2001; Oki and Nishimoto, 1998). Additionally, it is able to rescue the temperature sensitive growth defect phenotype associated with yeast Gsp1 (Tatebayashi et al., 2001) (**Figure 10**).

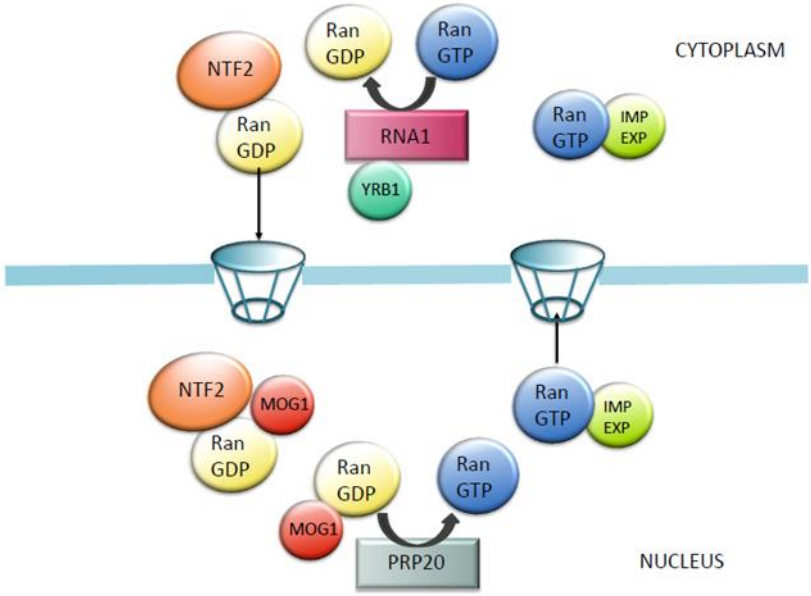

Figure 10. Simplified scheme of the Ran GTP/GDP cycle. The activity of Ran is mediated by cycles of GTP/GDP-bound forms. Ran-specific regulatory proteins catalyse the interchange between Ran-GTP and Ran-GDP. The nuclear guanine nucleotide exchange factor Prp20 catalyses the exchange of GDP for GTP in the nucleus, along with Mog1 which binds to Ran-GDP and Ntf2 promoting nuclear import. The Ran-GDP is exported to the cytoplasm where two cytoplasmic regulatory proteins for Ran; The Ran GTPase activating protein (Rna1) and the Ran-binding protein 1 (Yrb1) catalyse GTP hydrolysis on Ran. The nuclear transport factor 2 (Ntf2) mediates the transport of Ran-GDP to the nucleus to complete the cycle.

In addition to its role in nuclear-protein import, it has been established that Mog1 in higher eukaryotes interacts with cardiac sodium channel Nav1.5 and regulates cell surface trafficking of Nav1.5 (Wu et al., 2008). The Nav1.5 is encoded by the *SCN5A* gene and it is required for generation and maintenance of the cardiac potential (Tian et al., 2004; Yong et al., 2007). Some studies have suggested that overexpression of Mog1

enhances Nav1.5 trafficking which rescues the associated *SCN5A*/Nav1.5 mutations responsible for Brugada syndrome (BrS) and sick sinus syndrome (Chakrabarti et al., 2013). Furthermore, recent studies in zebrafish have shown that deletion of *MOG1* results in abnormal cardiac looping during embryogenesis, indeed, it decreases the expression of several genes involved in cardiac morphogenesis which suggests that Mog1 is implicated in cardiac physiology and development (Zhou et al., 2016).

Spinocerebellar ataxia type 7 (SCA7) disease

Spinocerebellar ataxia type 7 (SCA7) is an autosomal hereditary neurodegenerative disease included in the polyglutamine expansion disorders caused by a mutation in the ataxin-7 protein (ATXN7) (homologue of yeast Sgf73) (David et al., 1997; Garden and La Spada, 2008). Cloning of the gene responsible for SCA7 showed an unstable expansion of a CAG repeat (polyQ) close to the N-terminal region of ATXN7 on SCA7 patients (David et al., 1997; Garden and La Spada, 2008; Lindblad et al., 1996). Patients with this disease present a highly variable number of repetitions ranging from 38 to 130; however, unaffected population usually contained 7-17 repeats. Indeed, there is a negative correlation between the CAG repeat size and the age of onset (David et al., 1998).

Common features found in SCA7 patients are related to neuron degeneration in the retina, cerebellum and brainstem (McCullough and Grant, 2010). Cerebellar degeneration found in these patients leads to ataxia where a reduction of the ability to coordinate muscle movement is affected. Retinal degeneration characterized by cone-rod dystrophy retinal degeneration with a subsequent progressive blindness is a unique feature on SCA7 (Aleman et al., 2002). Other related clinical symptoms include muscle weakness, amyotrophy, dysarthria, dysphagia, hearing loss and intellectual impairment. The sites in the CNS most affected by the disease are mainly localized in cerebellar Purkinge cells, dentate nucleus, inferior olive, spinal cord, retina and brainstem (Hands and Wyttenbach, 2010).

At least nine heritable disorders containing a polyglutamine tract have been previously described including Huntington's disease (HD), dentatorubral pallidoluysian atrophy (DRPLA), spinal and bulbar muscular atrophy (SBMA), and the spinocerebellar ataxias SCA1,SCA2, SCA3, SCA6, SCA7, and SCA17 (Orr and Zoghbi, 2007) (**Table 1**) .

Disease	Gene product	Normal repeat length	Expanded repeat Length	Main Clinical features
HD	Huntingtin	6–34	36–121	Chorea, dystonia, cognitive deficits, psychiatric problems
SCA1	Ataxin1	6–44b	39–82	Ataxia, slurred speech, spasticity, cognitive impairment
SCA2	Ataxin2	15–24	32–200	Ataxia, polyneuropathy, decreased reflexes, infantile variant with retinopathy
SCA3	Ataxin3	13–36	61–84	Ataxia, parkinsonism, spasticity
SCA6	CACNA1A	4–19	10–33	Ataxia, dysarthria, nystagmus, tremors
SCA7	Ataxin7	4–35	37–306	Ataxia, blindness, cardiac failure in infantile form
SCA17	TBP	25–42	47–63	Ataxia, cognitive decline, seizures, and psychiatric problems
SBMA	Androgen receptor	9–36	38–62	Motor weakness, swallowing, gynecomastia,decreased fertility
DRPLA	Atrophin	7–34	49–88	Ataxia, seizures, choreoathetosis, dementia

Table 1. Polyglutamine disorders caused by a polyglutamine tract expansion. Table adapted by the work by Orr (Orr and Zoghbi, 2007).

All polyQ disorders are slowly progressive and similar aspects found in these diseases are the aggregation of polyQ proteins into nuclear inclusions (NIs) in the brain of patients (Garden and La Spada, 2008).

Some researchers have attempted to answer how polyglutamine expanded ATXN7 (referred as polyQ-ATXN7) alters SAGA activity. In light of this, some studies have suggested that polyQ-ATXN7 disrupts SAGA integrity and diminishes HAT activity (McMahon et al., 2005; Palhan et al., 2005). Indeed, another study reported that the reduction in Gcn5 expression accelerates cerebellar and retinal degeneration in a SCA7 mouse model (Chen et al., 2012). However, some others have shown that histone or nucleosomal acetylation activities are unaffected in SCA7, however, there exists transcriptional defects in SCA7 mouse model since polyQ-ATXN7 alters TFTC/STAGA recruitment and chromatin structure leading to photoreceptor dysfunction (Helmlinger et al., 2006).

Other studies have attempted to identify and characterize the molecular mechanisms involved in the disease thus enabling the understanding of tissue specificity of SCA7. McCullough and colleagues identified REELIN (factor involved in the maintenance and development of Purkinge cells an cerebellum) as an ATXN7 target gene and found that polyQ-ATXN7 decreased ATXN7 occupancy showing increased levels of H2B monoubiquitination at the REELIN promoter (McCullough et al., 2012).

Yvert and coworkers also expressed mutant ATXN7 under the control of retinal and cerebellar promoters and showed that polyQ-ATXN7

overexpression leads to deficiencies in motor coordination. Moreover, mutant ATXN7 accumulated into NIs sequestering several chaperone/proteasome subunits (Yvert et al., 2000). Later studies expressed mutant ATXN7 (92 polyQ) in all neurons from the central nervous system (CNS), except for Purkinge cells. Mice expressing this protein showed a typical SCA7 phenotype with motor dysfunction, however, degeneration on cerebellar Purkinge cells was also detected. This new approach suggested that the degeneration of Purkinge cells can occur in a non-cell-autonomous way which suggests that mutant ATXN7 protein might be expressed in other cells which could also be linked to disease development (Garden et al., 2002). Due to this finding, researchers considered the possibility that glial dysfunction could lead to Purkinge cell degeneration and demonstrated that expression of mutant ATXN7 in glial cells was sufficient to produce Purkinge cells degeneration thus implicating glial cells in SCA7 pathogenesis (Custer et al. 2006).

The cone-rod homeobox protein (CRX) is a photoreceptor-specific transcription activator which is mainly expressed in retinal photoreceptors cells and it is involved in controlling the expression of other genes related to photoreceptors such as rhodopsin. La Spada et al., produced transgenic mice expressing mutant ATXN7 (92 Q) through the retina by inserting the transgene into the murine prion protein promoter (MoPrP) construct. These mice developed a cone-rod dystrophy which was linked to retinal degeneration and lose of visual function. As mutations in CRX have been related to cone-rod dystrophy, researchers found that mutant ATXN7

interfered with the CRX transcription of photoreceptors genes and recruited CRX into NIs. This study suggests that one of the key hallmarks of this pathology might be linked to the suppression of CRX transactivation by the interaction with the transgene (La Spada et al., 2001). Indeed, later studies also confirmed CRX contribution into SCA7 pathogenesis (Chen et al., 2004). Although researchers are trying to understand the molecular basis of this disease, further studies are needed in order to find a tempting therapeutic approach.

Materials and Methods

Materials

Yeast strains

All yeast strains used in this thesis are described in the following table.

Name	Genotype	Origen
BY4741	Mat a, leu2-Δ0, his3-Δ1, met15-Δ0, ura3-Δ0	EUROSCARF
BY4742	Mat α, leu2-Δ0, his3-Δ1, met15-Δ0, ura3-Δ1	EUROSCARF
SUS1-TAP	Mat α, ade2, his3, leu2, trp1, ura3, SUS1-TAP::*URA3*	This laboratory
SUS1-GFP	Mat a, leu2-Δ0, his3-Δ1, met15-Δ0, ura3-Δ0, SUS1-GFP::*HIS3*	Rodriguez-Navarro et al., 2004
SUS1-TAP *asf1Δ*	Mat α, ade2, his3, leu2, trp1, ura3, SUS1-TAP::*URA3* asf1*::KanMX4*	Pamblanco et al., 2014
SUS1-GFP	Mat a, leu2-Δ0, his3-Δ1, met15-Δ0, ura3-Δ0 SUS1-GFP::*KanMX4*	This laboratory
SUS1-GFP *mog1Δ*	Mat a, leu2-Δ0, his3-Δ1, met15-Δ0, ura3-Δ0 SUS1-GFP::*KanMX4* mog1::*HIS3*	This Thesis
UBP-GFP	Mat a, leu2-Δ0, his3-Δ1, met15-Δ0, ura3-Δ0 UBP8-GFP::*HIS3*	This laboratory
SGF11-GFP	Mat a, leu2-Δ0, his3-Δ1, met15-Δ0, ura3-Δ0 SGF11-GFP::*HIS3*	This laboratory
SGF11-GFP *mog1Δ*	Mat a, leu2-Δ0, his3-Δ1, met15-Δ0, ura3-Δ0 SGF11-GFP::*HIS3* mog1*::KanMX4*	This Thesis

UBP8-GFP *mog1Δ*	Mat a, leu2-Δ0, his3-Δ1, met15-Δ0, ura3-Δ0 UBP8-GFP::*HIS3* mog1::*KanMX4*	This Thesis
UBP8-TAP	Mat a, leu2-Δ0, his3-Δ1, met15-Δ0, ura3-Δ0 UBP8-TAP::*HIS3*	This laboratory
UBP8-TAP *mog1Δ*	Mat a, leu2-Δ0, his3-Δ1, met15-Δ0, ura3-Δ0 UBP8-TAP::*HIS3* mog1::*KanMX4*	This Thesis
RAD6-TAP *mog1Δ*	Mat a, leu2-Δ0, his3-Δ1, met15-Δ0, ura3-Δ0 RAD6-TAP::*URA3* mog1::*HIS3*	This Thesis
RAD6-TAP	Mat a, leu2-Δ0, his3-Δ1, met15-Δ0, ura3-Δ0 RAD6-TAP::*URA3*	This Thesis
SWD2-TAP *mog1Δ*	Mat a, leu2-Δ0, his3-Δ1, met15-Δ0, ura3-Δ0 SWD2-TAP::*KanMX*4 mog1::*HIS3*	This Thesis
SET1-TAP *mog1Δ*	Mat a, leu2-Δ0, his3-Δ1, met15-Δ0, ura3-Δ0 SET1-TAP::*HIS3* mog1::*URA3*	This Thesis
SWD2-TAP	Mat a, leu2-Δ0, his3-Δ1, met15-Δ0, ura3-Δ0 SWD2-TAP::*KanMX4*	Dr. Buratowski
SET1-TAP	Mat a, leu2-Δ0, his3-Δ1, met15-Δ0, ura3-Δ0 SET1-TAP::*HIS3*	Dr. Buratowski
MOG1-TAP	Mat a, leu2-Δ0, his3-Δ1, met15-Δ0, ura3-Δ0 MOG1-TAP::*URA3*	This Thesis
MOG1-TAP ADA2-HA	Mat a, leu2-Δ0, his3-Δ1, met15-Δ0, ura3-Δ0 MOG1-TAP::*URA3* ADA2-HA::*KanMX4*	This Thesis

MOG1-TAP ADA2-HA UBP8-PK	Mat a, leu2-Δ0, his3-Δ1, met15-Δ0, ura3-Δ0 MOG1-TAP::*URA3* ADA2-HA::*KanMX4* UBP8-PK*::HIS3*	This Thesis
UBP8-PK ADA2-HA	Mat a, leu2-Δ0, his3-Δ1, met15-Δ0, ura3-Δ0 ADA2-HA::*KanMX4* UBP8-PK*::HIS3*	This Thesis
MOG1-TAP SGF73-HA UBP8-PK	Mat a, leu2-Δ0, his3-Δ1, met15-Δ0, ura3-Δ0 MOG1-TAP::*URA3* SGF73-HA::*LEU2* UBP8-PK::*HIS3*	This Thesis
SGF73-HA UBP8-PK	Mat a, leu2-Δ0, his3-Δ1, met15-Δ0, ura3-Δ0 SGF73-HA::*LEU2* UBP8-PK*::HIS3*	This Thesis
UBP8-PK	Mat a, leu2-Δ0, his3-Δ1, met15-Δ0, ura3-Δ0 UBP8-PK::*HIS3*	This Thesis
MOG1-HA	Mat a, leu2-Δ0, his3-Δ1, met15-Δ0, ura3-Δ0 MOG1-HA::*KanMX4*	This Thesis
sus1Δ	Mat a, leu2-Δ0, his3-Δ1, met15-Δ0, ura3-Δ0, sus1::*KANMX4*	This laboratory
asf1Δ	Mat a, leu2-Δ0, his3-Δ1, met15-Δ0, ura3-Δ0, asf1::*KanMX4*	EUROSCARF
asf1Δsus1Δ	Mat a, leu2-Δ0, his3-Δ1, met15-Δ0, ura3-Δ0, asf1::*KanMX4*, sus1::*HIS3*	Pamblanco et al., 2014
sgf73Δmog1Δ	Mat a, leu2-Δ0, his3-Δ1, met15-Δ0, ura3-Δ0 sgf73::*HIS3 mog1::KanMX4*	This Thesis
sgf73Δ	Mat a, leu2-Δ0, his3-Δ1, met15-Δ0, ura3-Δ0 sgf73::*HIS3*	This Thesis
ubp8Δ mog1Δ	Mat a, leu2-Δ0, his3-Δ1, met15-Δ0, ura3-Δ0 Ubp8::*KanMX4* mog1::*HIS3*	This Thesis

ubp8Δ	Mat a, leu2-Δ0, his3-Δ1, met15-Δ0, ura3-Δ0 Ubp8::*KanMX4*	This Laboratory
bre1Δ	Mat a, leu2-Δ0, his3-Δ1, met15-Δ0, ura3-Δ0 bre1::*KanMX4*	EUROSCARF
rad6Δ	Mat a, leu2-Δ0, his3-Δ1, met15-Δ0, ura3-Δ0 rad6::*KanMX4*	EUROSCARF
rad6Δmog1Δ	Mat a, leu2-Δ0, his3-Δ1, met15-Δ0, ura3-Δ0 rad6::*KanMX4* mog1::*HIS3*	This Thesis
set1Δ	Mat a, leu2-Δ0, his3-Δ1, met15-Δ0, ura3-Δ0 set1::*KanMX4*	EUROSCARF
set2Δ	Mat a, leu2-Δ0, his3-Δ1, met15-Δ0, ura3-Δ0 set2::*KanMX4*	EUROSCARF
sgf11Δmog1Δ	Mat a, leu2-Δ0, his3-Δ1, met15-Δ0, ura3-Δ0 sgf11::*KanMX4* mog1::*HIS3*	This Thesis
sgf11Δ	Mat a, leu2-Δ0, his3-Δ1, met15-Δ0, ura3-Δ0 sgf11::*KanMX4*	This Laboratory
sac3Δmog1Δ	Mat a, leu2-Δ0, his3-Δ1, met15-Δ0, ura3-Δ0 sac3::*KanMX4* mog1::*HIS3*	This Thesis
sac3Δ	Mat a, leu2-Δ0, his3-Δ1, met15-Δ0, ura3-Δ0 sac3::*KanMX4*	This Thesis
thp1Δ	Mat a, leu2-Δ0, his3-Δ1, met15-Δ0, ura3-Δ0 thp1::*LEU2*	This Thesis
thp1Δ mog1Δ	Mat a, leu2-Δ0, his3-Δ1, met15-Δ0, ura3-Δ0 thp1*::LEU2* mog1::*HIS3*	This Thesis

set1Δmog1Δ	Mat a, leu2-Δ0, his3-Δ1, met15-Δ0, ura3-Δ0 set1::*KanMX4* mog1::*URA3*	This Thesis
set2Δmog1Δ	Mat a, leu2-Δ0, his3-Δ1, met15-Δ0, ura3-Δ0 set2::*KanMX4* mog1::*URA3*	This Thesis
dot1Δmog1Δ	Mat a, leu2-Δ0, his3-Δ1, met15-Δ0, ura3-Δ0 dot1::*KanMX4* mog1::*LEU2*	This Thesis
dot1Δ	Mat a, leu2-Δ0, his3-Δ1, met15-Δ0, ura3-Δ0 dot1::*KanMX4*	Dr. San Segundo
mog1Δ	Mat α, leu2-Δ0, his3-Δ1, met15-Δ0, ura3-Δ0 mog1::*HIS3*	This Thesis
mog1Δ	Mat α, leu2-Δ0, his3-Δ1, met15-Δ0, ura3-Δ0 mog1::*KanMX4*	EUROSCARF

Primers

The selected primers for use in *S. cerevisiae* in quantitative PCR (qPCR) are described below. All of them were purchased from Sigma-Aldrich. Primers used in qPCR were designed following the recommendations given by Light Cycler 480 Real-Time PCR System with a Tm close to 60 °C and an amplicon size between 100-180 bp.

Gene	Region	5'-3' sequence
GAL1-FW	Promoter	AAAATTGGCAGTAACCTGGCC
GAL1-RV		CCCCAGAAATAAGGCTAAAAAACTAA
GAL1-FW	ORF	TTGCTAGATCGCCTGGTAGAGTC
GAL1-RV		GGCGCAAAGCATATCAAAATC
SCR1-FW RT	ORF SCR1	AACCGTCTTTCCTCCGTCGTAA
SCR1- RV RT		AGAACTACCTTGCCGCACCA
IntV-FW	Intergenic region Chromosome V	TGTTCCTTAAGAGGTGATGGTGA
IntV-RV		GTGCGCAGTACTTGTGAAAACC
ADH1-FW	Promoter	TCGTTGTTCCAGAGCTGATG
ADH1-RV		AACTGGAAGGAAGGCCGTAT
ADH1-FW	5´ORF	ACGAATCCCACGGTAAGTTG
ADH1-RV		AAGCGTGCAAGTCAGTGTGA
PMA1-FW	Promoter	AAAAGGCCAAATATTGTATTATTTTCA
PMA1-RV		TTCACTATTGGTGTTATAGGAAAGAAA
PMA1-FW	5´ORF	CAGCTCATCAGCCAACTCAA
PMA1-RV		TCGTCGACACCGTGATTAGA
YEF3-FW	Promoter	TTTTTCGCTTCCTCGAGTATAA
YEF3-RV		GAAAGAGAGCGTAAGAAAAAGAGA
YEF3-FW	5´ORF	CACTGCTGACAACAGACACG
YEF3-RV		TTGATACCCTTGGCCAATTC

The subsequent primers purchased from DTT were designed to study mRNA expression at the promoters of the selected primers in qPCR following the recommendations given by Light Cycler 480 Real-Time PCR System with a Tm close to 60 °C and an amplicon size between 100-150 bp.

GENE	5´-3´SEQUENCE
RPL10-FW	TCGGATCTTAGCATCAGGGA
RPL10-RV	GGAGCGTCTCTTTTCCTCTG
RPL19-FW	GATCCTCATCCTTCTCATCCAG
RPL19-RV	AAGCCTGTTACTGTCCAATTC
RPL18A-FW	AGATTCGCATACGGTACAGTG
RPL18A-RV	CTTTTGTGACTGGCGGTGA
RPL23-FW	TTAGCTCCTGTGTTGTCTGC
RPL23-RV	ACTTCTTTCTGACCCTTTCC
RPL37-FW	CTGATGGCAGACTTCACTGT
RPL37-RV	AGTACACTTGCTCCTTCTGTG
RPL8-FW	CTCCAAAGGGATGCTCCAC
RPL8-RV	TTGGTGTTGTGGCTGGT
RPL35-FW	GCTTGTATTTCTTGCCCTTGT
RPL35-RV	GTCCAAGCTCTCCAAGATACG
RPL6-FW	GGCAATGACAAACTTCTGGTG
RPL6-RV	CTGTCCTGATCATCCTCACTG
RPL27-FW	GGTGCCATCGTCAATGTTCT
RPL27-RV	CTGCCTGCTGTCGAGATG
RPS23-FW	GGCTTTCTTGTACTGTTTGTCAT
RPS23-RV	GCACCTCCTCTCTCTTTCTCT
MPC2-FW	CTAGTCCAGCACACACCAAT
MPC2-RV	CCGACTCATGGATAAAGTGAG
TMEM33-FW	CAAAGCACGCTGGTAAAAGC
TMEM33-RV	CGCTGTGCAATTCATGATGAC
SLco1c1-FW	CCAGGAAGACATAACCCACA
SLco1c1-RV	CCAATGTTACTCCCAGCATCT
SLc20a1-FW	AGCTCATAAGCCATTAGGAAC
SLc20a1-RV	GTGATGTCGTGGTTCGTCT
CP-FW	CTTGTCTCCAACATTTGCATGA
CP-RV	GAAGGTTGTGTATCGCCAGTT
HEPH-FW	ACACATGCTCAACTCTGGTAA

HEPH-RV	ATTGCTACTTACTGCTCAGACC
Idh3b-FW	AAGTGACTTCACGTGGACTAC
Idh3b-RV	AGGTGCTGAGTTCCATGAAG
Idh3g-FW	GCCACCATACTTAGCAGATG
Idh3g-RV	AATGCTCAAGCCAACTCTCC
GAPDH-FW	GTGACTCATACTGGAACATGTAG
GAPDH-RV	AATGGTGAAGGTCGGTGTG

Commercial Kits

Along this work the following commercials kits have been used following manufacturer´s instructions:

Name	Company
Wizard™ Plus SV Minipreps DNA Purification System™	Promega
Wizard™ SV Gel and PCR Clean-Up System™	Promega
Amersham Western Blotting Detection Kit™ (ECL Select)	GE Healthcare
Coomassie coloidal Novex Colloidal Blue Staining Kit™	Invitrogen
NUPAGE protein gels 4-12% Bis-Tris Gel™	Invitrogen
Maxima SYBR® Premix Ex Taq™	Takara
Histone extraction Kit	Abcam
DNA Kit Purification	Zymoresearch
Bradford Assay	Biorad

Antibodies

During this thesis the following antibodies have been used at the indicated concentrations for Western blot analysis (WB), chromatin immunoprecipitation (ChIP) or protein Immunoprecipitation (IP).

Primary Antibodies

Name	Host	Dilution and Application	Company
Anti-TAP	Rabbit	1:5000 (WB)	Thermo scientific (Pierce)
Anti-Flag	Rabbit	1:2000 (WB)	Sigma Scientific
Anti-HA	Rat	1:1000 (WB), 1:1000 (ChIP)	Roche
Anti-PK	Mouse	1:10000 (WB); 1:1000 (IP)	ABD Serotec
Anti-PGK	Mouse	1: 15000(WB)	Invitrogen
Anti-Myc	Mouse	1:5000 (WB)	Santa Cruz Biotechnology
Anti-H2B	Rabbit	1:10000	Active Motif
Anti-H2Bub[1]	Rabbit	1:5000 (WB)	Cell Signaling Technology
Anti-H3K4me[3]	Rabbit	1:5000 (WB)	Abcam
Anti-H3	Rabbit	1:10000 (WB)	Abcam

Secondary Antibodies

Name	Company
Anti-mouse-IgG-ECLTMHRP	GE Healthcare
Anti-Rabbit-IgG-ECLTMHRP	GE Healthcare
Anti-Rat-IgG-ECLTMHRP	DAKO

ECL Select developer from GE Healthcare was used for immunostaining detection and High performance chemiluminescence films (Amersham Hyperfilm ECL, GE Healthcare) for signal detection.

Plasmids

The following table contains the plasmids used to obtain the required cassettes for tagging or gene deletion (Lengronne et al., 2006; Longtine et al., 1998; Puig et al., 2001; Wach et al., 1994).

Name	Description	Origin
pFA6a-KanMX4	Integrate KanMX4 marker for gene deletion	Wach et al.,1994
pFA6a-HIS3	Integrate HIS3 marker for gene deletion	Longtine et al.,1998
pFA6a-URA3	Integrate URA3 marker for gene deletion	Longtine et al.,1998
pFA6a-GFP-HIS3	Integrate GFP tag with HIS3 marker	Longtine et al.,1998
pFA6a-HA-HIS3	Integrate HA epitope with HIS3 marker	Longtine et al.,1998
pBS2623	Integrate TAP epitope with KanMX4 marker	Puig et al., 2001
pBS1539	Integrate TAP epitope with URA3 marker	Puig et al., 2001
pUC19-6xPKHIS3	Integrate 6 copies of PK epitope with HIS3	Lengronne et al., 2006
pGADT7 AD ATXN7-10Q	Integrate ATXN7 protein with 10Q repetitions	Dr. La Spada
pGADT7 AD ATXN7-113Q	Integrate ATXN7 protein with 113Q repetitions	Dr. La Spada

The next table contains the plasmids used for the expression of human proteins in HEK293T cells:

Name	Description	Origin
pCMV myc-ATXN7-92Q	Expression of human ATXN7-92Q	Dr. La Spada
pCMV myc-ATXN7-10Q	Expression of human ATXN7-10Q	Dr. La Spada
pCMV HIS 6X-ATXN7L3	Expression of human ATXN7L3	Dr. La Spada
pCMV ENY2-3XFLAG	Expression of human ENY2	Dr. La Spada
pDEST-USP22-FLAG-HA	Expression of human USP22	Addgene

Human cell lines

Human embryonic kidney cells 293 (HEK293T) were purchased from ATCC (https://www.atcc.org/Products/All/CRL-3216.aspx).

Mice

Non-transgenic and PrP-floxed-SCA7-92Q BAC littermates were created at the University of San Diego (California) and University of Washington (Washington) (Furrer et al., 2011). All studies and procedures were approved by an Institutional Animal Care and Use Committee at the University of Washington or at the University of California, San Diego (U.S.A).

Radioactivity

UTP [alpha-33P] - 3000Ci/mmol, 10mCi/ml, PerkinElmer

dCTP [alpha-33P] - 3000Ci/mmol, 10mCi/mL, Hartmann Analytic

ATP, [γ-32P] - 3000Ci/mmol, 10mCi/ml, PerkinElmer

Methods

Saccharomyces cerevisiae

Yeast cultures and cell growth assay

Yeast cultures: Cells were cultured in the following media depending on the desired condition:

Rich media YPD (YPD): 1 % yeast extract (m/v), 2 % peptone (m/v) and 2 % glucose (m/v).

YPGal: YP plus 2 % galactose (m/v) as carbon source, 1 % yeast extract (m/v) and 2 % peptone (m/v).

YPRaf: YP plus 2 % rafinose (m/v) as carbon source, 1 % yeast extract (m/v) and 2 % peptone (m/v).

Synthetic complete (SC) medium: yeast nitrogen base (YNB) without amino acids, and 1.7 % ammonium sulphate (m/v) $(NH4)_2SO_4$ at 0.5 % (m/v) and 0.2 % Drop out Mix (m/v). The Drop out contains a mix of all aminoacids at 0.2 %.

Yeast were grown in either liquid medium (at 30 °C with 140 rpm agitation) or on the surface of a solid 2 % (m/v) agar plate. Auxotrophic yeast strains transformed with plasmids or integration cassettes were cultured in synthetic minimum medium (SC) lacking the amino acid corresponding to the auxotrophy. Yeast strains containing plasmids or integration cassette expressing the geneticine gene (*KanMX4*) were selected by the addition of geneticine 20 mg/ml to the selection plates.

Cell growth Assay

For the growth analysis, yeast cultures were diluted up to 0.5 OD_{600}, 4 serial dilutions were prepared (1:10; 1:100; 1:1000; 1:10000) and 5 µl of each dilution were spotted onto YP+glucose or YP+galactose plates and incubated at various temperatures, generally at 30 °C and 37 °C.

Gene deletion and protein tagging

Both gene deletion and epitope tagging (TAP, MYC, GFP, PK and HA) were performed through integration prior PCR amplification of the cassette (Baudin et al., 1993). Briefly, this strategy consists on the design of primers that contain two distinct regions, one that permits the homologous recombination to the target chromosomal sequence and the second part which allows the PCR amplification of a selectable marker. Following PCR amplification, the obtained cassette was used for yeast transformation. The selectable markers used in this work were *KanMX4* which confers resistance to the antibiotic geneticine or genes that complete the auxotrophy present in the yeast strains (*HIS3*, *URA3*, and *LEU2* etc.). To

confirm the deletion or the tagging of the gene, PCR or Western blot analysis was performed respectively. The methodology to obtain the desired PCR cassette is described below.

Genomic DNA isolation

To obtain genomic DNA, 5 ml of yeast culture were grown in YP+Glucose at 30 °C overnight. Cells were centrifuged at 2.500 rpm during 3 minutes and were washed twice with sterile deionized water. 200 µl of Lysis buffer (2 % Triton X-100 (v/v), 1 % SDS (m/v), 100 mM NaCl, 10 mM Tris-HCl pH 8.0 and 1 mM EDTA pH 8.0), 200 µl of phenol:chloroform:isoamyl alcohol (25:24:1) and 200 µl of glass beads were added to the cell pellet. Cell breakage was conducted in a vortex Genie-2 model (Scientific Instruments) at 4 °C for 15 minutes. Cells were centrifuged at 13.200 rpm for 10 minutes at 4 °C. The aqueous phase was collected and passed into a new 1.5 ml tube where 2 volumes of 96 % cold ethanol (v/v) and 60 µl of NaCl 5 M were added to precipitate the DNA during 1 hour at - 20 °C. To collect the DNA, the sample was centrifuged at 13.200 rpm for 15 minutes at 4 °C and cell pellet was washed with 70 % cold ethanol (v/v). Finally, supernatant was eliminated and once the pellet was air-dried, it was resuspended in 50 µl of sterile water and maintained at - 20 °C until use.

Plasmid DNA isolation from E. *coli*

To obtain plasmid DNA, *Wizard*™ Plus *SV* Minipreps *DNA Purification System™* (Promega) was used following the manufacturer's instructions.

RNA isolation

For total RNA extraction, 10 ml of yeast cells grown in YPD overnight at 30 °C were collected by centrifugation. Cells were washed twice with cold sterile water and the cell pellet was immediately frozen in liquid nitrogen and stored at - 80 °C until further processing. The cells were thawed on ice and resuspended in 0.5 ml of LETS buffer (0.1 M LiCl, 10 mM EDTA, 10 mM Tris-HCl, 0.2 % SDS (m/v)), additionally, 0.5 ml of phenol:choloroform:isoamyl alcohol (5:1 pH 4.3) and 0.3 ml of glass beads were added to the cells. Cells breakage was performed by vortexing the mixture during 6 rounds of 30 seconds on/off at 4 °C. Subsequently, samples were centrifuged for 5 minutes at 13.200 rpm at 4 °C. The supernatant was collected and passed into a new tube, and a second extraction with chloroform:isoamyl alcohol (24:1) was conducted. The RNA was precipitated by the addition of 500 µl 5M LiCl and left overnight at - 80 °C. Cell pellet was obtained by centrifugation for 20 minutes at 13.200 rpm at 4 °C and washed with 70 % ethanol (v/v) and resuspended in 500 µl sterile water. The RNA was again precipitated with 50 µl of 3 M NaAc and 2 volumes of 100 % EtOH (v/v) and left for at least 3 hours at - 80 °C. The RNA pellet was obtained by centrifuging for 20 minutes at 13.200 at 4 °C. The precipitate was washed with 70 % EtOH, the pellet was air-dried and resuspended in sterile water. The concentration of RNA was obtained by measuring the absorbance at 260 nm with the use of a spectrophotometer Nanodrop 2000 (Thermo Fisher)

Reverse Transcription or cDNA synthesis

From the RNA extraction, 2 µg of RNA was incubated with 1 unit of DNAse (Sigma 20 U/µl) at room temperature for 15 minutes in a final volume of 20 µl. The RNA was extracted twice with a mixture of 500 µl phenol:chloroform:isoamyl alcohol (25:24:1) and a third extraction was performed with chroloform:isoamyl alcohol (24:1). The RNA was precipitated overnight with 1 µl glycogen and two volumes of 100 % EtOH and subsequently centrifuged for 20 minutes at 13.200 rpm at 4 °C. The pellet was washed with 70 % ethanol (v/v) and resuspended in 20 µl of deionized water. Then, 1 µg of RNA treated with the DNAse was incubated with 1 µl of random primers (Invitrogen) and 1 µl of dNTP Mix (dATP, dCTP, dGTP and dTTP) at 4 mM concentration (Invitrogen) at 65 °C during 5 minutes followed by incubation on ice. To this mix, 4 µl of 5X first-strand buffer (Invitrogen), 2 µl 0.2 M DTT and 1 µl RNase OUT (40 U/µl) (Invitrogen) was added and incubated for 2 minutes at 37 °C. Half of the mixture was used as negative control of DNA presence and the rest was used for reverse transcription for which 1 µl of reverse transcriptase M-MLV (Invitrogen) was added to the mix. Samples were incubated first for 10 minutes at 25 °C and second, for 50 minutes at 37 °C. To stop the reaction, the samples were stored at -20 °C. For the amplification of reverse transcription product (cDNA), 3 µl of 1/20 dilution of the obtained cDNA was used as a template in the qPCR. The reaction volume for these studies was 10 µL.

Transformation of yeast cells

Yeast cells were transformed following the described lithium acetate protocol (Gietz et al., 1995). Yeast cells were grown in 50 ml YP+Glucose medium until an OD_{600} 0.6 was reached. Cells were collected by centrifugation at 1.800 rpm for 3 minutes and washed with sterile deionized water. Cells were resuspended in 0.5 ml 0.1M LiAc and incubated for 15 minutes at 30 °C. Then, 5 µl of salmon sperm DNA carrier dissolved in TE (1 M Tris-HCl pH 8.0, 0.5 M EDTA pH 8.0) at 2 mg/ml concentration, 1-5 µg of the integrative/deletion cassette obtained by PCR or 0.1-1 µg of plasmid DNA were added to the cells. To this mix, the following reagents were added; 240 µl of 50 % PEG (v/v), 30 µl sterile deionized water and 30 µl LiAc 1M.

The tube containing the mix was vigorously mixed and incubated first for 30 minutes at 30 °C and for 20 minutes at 42 °C in a thermomixer (Eppendorf). Cells were later centrifuged for 2 minutes at 1.800 rpm and cell pellet was resuspended in 200 µl sterile deionized water to be spread into agar plates.

Depending on the selective marker contained in the plasmid or integrative/deletion cassette, cells were spread on the corresponding minimum selective medium. In those transformations where geneticine antibiotic was used as selective marker, cells were recovered in YP+Glucose medium during 2-4 hours at continuous shaking at 30 °C. This

step is needed for the cells to express the necessary amount of antibiotic to allow them growing in plates containing 0.2 mg/ml geneticine.

PCR (Polymerase Chain Reaction)

The reactions were performed in reaction of final volumes of 50 µl (PCR for integration cassette) or 15 µl (PCR test). For the integration cassette the following reagents were used in a final 50 µl volume: 1 µl DNA template from 1:25 diluted commercially Miniprep (Promega), 36.3 µl of sterile deionized water, 0.3 µl Taq polymerase (Roche), 5 µl of 10X buffer Taq polymerase (Roche), which includes $MgCl_2$, 1.2 µl of each 10 mM primer (forward and reverse) and 5 µl of a mixture of the 4 mM dNTPs (dATP, dCTP, dGTP and dTTP). In this case, the following PCR program was used as indicated: 95 °C 3 minutes, 9 cycles (94 °C 15 seconds, 54 °C 30 seconds, 72 °C 2 minutes, 94 °C 15 seconds), 25 cycles (54 °C 30 seconds, 72 °C 2 minutes + 5 seconds per cycle), 72 °C 7 minutes and 4 °C.

For the PCRs test: 1 µl of DNA template, 9.55 µl of sterile deionized water, 0.15 µl of Taq polymerase (Roche), 1.5 µl of 10X buffer Taq polymerase (Roche) including $MgCl_2$, 0.45 µl of each primer 10 mM and 1.5 µl of a mixture of the dNTPs 4 mM . The following amplification protocol was used in general: 1 cycle of 3 minutes at 94 °C; 30 cycles composed of 30 seconds at 94 °C, 30 seconds at the optimal annealing temperature for each oligonucleotide pair and a time variable extension (1 minute per kb) to 72 °C; finally, 72 °C for 10 minutes and 4 °C.

Quantitative-PCR

The analysis of gene expression and the chromatin recruitment of the studied genes were performed by RT-PCR and quantitative PCR using the LightCycler ™ thermocycler 480 (Roche). 5 µl of SYBR Premix Ex Taq (Tli RNase H Plus (Takara)), 1.25 µl of each of the primers, 3 µl of DNA or cDNA template and 1.5 µl of sterile water were used in each replicate. All samples contained technical triplicates. The relative quantification of each PCR amplicon was obtained following the next calculations:

$$\boldsymbol{ChIP\ qPCR}: Primers\ efficiency\text{^}\ (CT\ positive\ control - CT\ IP\ sample) * 100/\ Primers\ efficiency\text{^}\ (CT\ positive\ control - CT\ INPUT\ sample) * 100$$

$$\boldsymbol{RT-qPCR}: Primers\ efficiency\text{^}\ (CT\ positive\ control - CT\ sample) * 100$$

Primer efficiency was determined for each protein and primer pair, at least 80 % primer efficiency was required to be used for each qPCR being calculated with the formula: (10-(1/slope obtained for each PCR reaction)).

Each calculation was normalized using different reference genes: *SCR1* for *GAL1* expression and for the ChIP an intergenic region from the chromosome V (ChrV: 9754-9837).

Nucleic acids separation by electrophoresis

Separation of DNA fragments was carried out in agarose gels of varying concentration (0.8 % - 2 % (m/v)) according to the sizes of the DNA fragments. Gels were prepared in 1X TAE buffer (40 mM Tris-acetate, 1 mM EDTA pH 8.0), which was also used as electrophoresis buffer. The gels were prepared by adding 3 µl of ethidium bromide 10 mg/ml per 50 ml of gel. The samples were mixed with loading buffer 6X (bromophenol blue 0.25 % (m/v) , Blue xylene cyanol 0.25 % (m/v) 30 % glycerol (v/v)) to a final concentration 1X and electrophoresis was performed at the constant voltage (6-10 V/cm) for a variable time depending on the required resolution .

Protein extracts for Western blot

To obtain protein extracts, two different protocols were used depending on the studied protein. In the case of protein extract with sodium hydroxide (NaOH), cell cultures were grown in YP+Glucose, centrifuged (3 minutes at 2.500 rpm) and washed with cold sterile distilled water. The cells were resuspended in 1.000 ml of water and 150 µl of 0.2 M NaOH were left for 10 minutes on ice and centrifuged for 1 minute at 13.200 rpm. The supernatant was aspirated and the pellet was resuspended in 50 µl of loading buffer proteins SDS-PAGE 2X (250 mm Tris-HCl pH 6.8, 140 mM SDS, 30 mM bromophenol blue, 27 mM glycerol) containing 0.1 mM DTT and samples were incubated at 95 °C for 5

minutes. Cells were centrifuged for 10 minutes at 13.200 rpm and the supernatant, which is the protein extract, was transferred to a new tube.
Protein extracts by trichloroacetic acid (TCA) were obtained by the following procedure: cell cultures were centrifuged for 3 minutes at 2.500 rpm and washed with cold sterile distilled water. The cell pellet was resuspended in 100 µl of cold deionized water, 20 µl 100 % TCA and 100 µl of glass beads. The mixture was vortexed for 15 minutes at 4 °C. Later, 1 ml of cold 5 % TCA (v/v) was added to the lysate and centrifuged for 20 minutes at 13.200 rpm at 4 °C. The supernatant was discarded along with the glass beads and the pellet was resuspended in 50 µl of loading buffer proteins SDS-PAGE 2X containing 4 % β-mercaptoethanol and 20 µl of Tris base 2 M to neutralize the pH. Samples were centrifuged for 5 minutes at 13.200 rpm to remove cell debris and beads. The extract was incubated for 5 minutes at 95 °C before being separated by electrophoresis in a polyacrylamide gel.

Protein separation by electrophoresis

Protein extracts were separated according to their size by electrophoresis in denaturing polyacrylamide gels which were prepared following the specifications detailed in Sambrook and Russell {Citation}Electrophoresis was developed in cuvettes Mini Protean II and III (BioRad) at 120 V constant voltages and the required time to separate the desired protein. The electrophoresis buffer was prepared with 25 mM Tris-base, 190 mM de glycine and SDS 0.01 % (m/v).

Denaturing gradient polyacrylamide gels 4-12 % NUPAGE Bis-Tris Gel™, were purchased from Invitrogen using the commercial buffer, MOPS (3-(N-morpholino) propanesulfonic acid).

Protein transfer and immunodetection

The separated proteins were transferred electrophoretically into a nitrocellulose membranes 0.45 µm (Hybond-ECL Amersham Biosciences) with a mini trans-blot cell Biorad following the procedure described in Sambrook and Russell (Sambrook & Russell, 2001). The transference buffer contained 25 mM Tris pH 8.3, 192 mM glycine, 0.1 % SDS (m/v) and 20 % methanol (v/v). Protein transference was conducted for 1 hour and 100 V, in case of histones, a 100 V voltage and 15 minutes followed by 30 minutes at 60 V was applied.

The transferred proteins were stained with Ponceau solution at 1 % (m/v) in 1 % acetic acid (v/v) for 3 minutes, washing the membrane with distilled water. The membrane was blocked with TBS (0.02 M Tris-HCl pH 7.6, 0.8 % NaCl (m/v)) and 0.01 % Tween-20 (v/v)) which was supplemented with 2 % blocking agent (m/v) of (ECL-Advance, GE Healthcare) for 40 minutes at room temperature. The primary antibody was diluted in TBS-Tween blocking agent with 2 % (m/v) and the membrane was incubated in this solution for one hour at room temperature or overnight at 4 °C depending on the antibody specifications. The membrane was washed three times for 15 minutes with TBS-Tween. The secondary antibody was also prepared in TBS-Tween blocking agent with 2 % (m/v) and the membrane was

incubated for 1 hour at 4 °C. The membrane was washed three times for 15 minutes with TBS-Tween and chemiluminescent detection was performed using ECL Advance (GE Healthcare) following the manufacturer's instructions.

Protein Purification: The TAP technique

Tandem Affinity Purification (TAP) technique allows the purification under native conditions of protein complexes (Puig et al., 2001). The TAP method requires fusion of the TAP tag, either N- or C-terminal to the protein of interest. The TAP tag consists on a protein A (PA), which binds tightly to IgG followed by tobacco etch virus protease (TEV) cleavage site and finally by a calmodulin binding peptide (CBP) (**Figure 11**). These experiments followed the previously described protocol with some modifications (Puig et al., 2001; Schmitt et al., 1999).

2 liters of cells in YP+Glucose were grown until an OD_{600} 2.5 was reached. This absorbance corresponds to approximately 12-15 grams of cell pellet. Cell culture was centrifuged for 3 min at 3.500 rpm and was immediately frozen with liquid nitrogen. Cells were resuspended in 25 ml lysis buffer (10 mM Tris-HCl pH 8.0, 150 mM NaCl, 20 % glycerol (v/v), Nonidet P-40 at 0.1 % (v/v), 1 mM PMSF, 1 mM DTT and Complete protease cocktail inhibitor (Roche)) and 25 ml glass beads which were broken in a BeadBeater (Fritsch-Pulverisette) at 4 °C under 3 rounds of 4 minutes at 490 rpm with a 1 minute pause between the rounds. Lysate was centrifuged for 1 hour at 4 °C at 14.000 rpm and the supernatant was

incubated with 400 µl of IgG-Sepharose 6 Fast Flow™ (Amersham Biosciences) for 1 hour at 4 °C in a turning wheel. The IgG- Sepharose beads were washed with 10 ml LB 1X buffer (10 mM Tris-HCl pH 8.0, 150 mM NaCl, 20 % glycerol (v/v) and Nonidet P-40 0.1 % (v/v)). Later, beads were incubated with 3-4 µg TEV protease during 2 hours at 16 °C in a turning wheel. This digestion allows the cleavage of the TEV protease site, thus releasing the calmodulin epitope and obtaining the TEV eluate from the protein of interest. Finally, the TEV eluate was purified using 400 µl of the Calmodulin Affinity Resin (Stratagene) with 4mM $CaCl_2$ and incubated for 1 hour at 4 °C in a turning wheel. Following the incubation, the resin was washed with 5 ml of the LB buffer supplemented with 2 mM $CaCl_2$ and 1 mM DTT. The final elution was conducted by incubating the resin with 350 µl elution buffer (5 mM EGTA, 10 mM Tris-HCl pH 8.0 and 50 mM NaCl) for 10 min at 37 °C. This step was performed 3 times. The eluate was precipitated with TCA in a 10 % final concentration (v/v). The eluate was resolved by SDS-PAGE. In some cases, following TCA precipitation, the protein pellet was analysed by mass spectrometry LC-MS/MS (Liquid chromatography tandem-mass spectrometry).

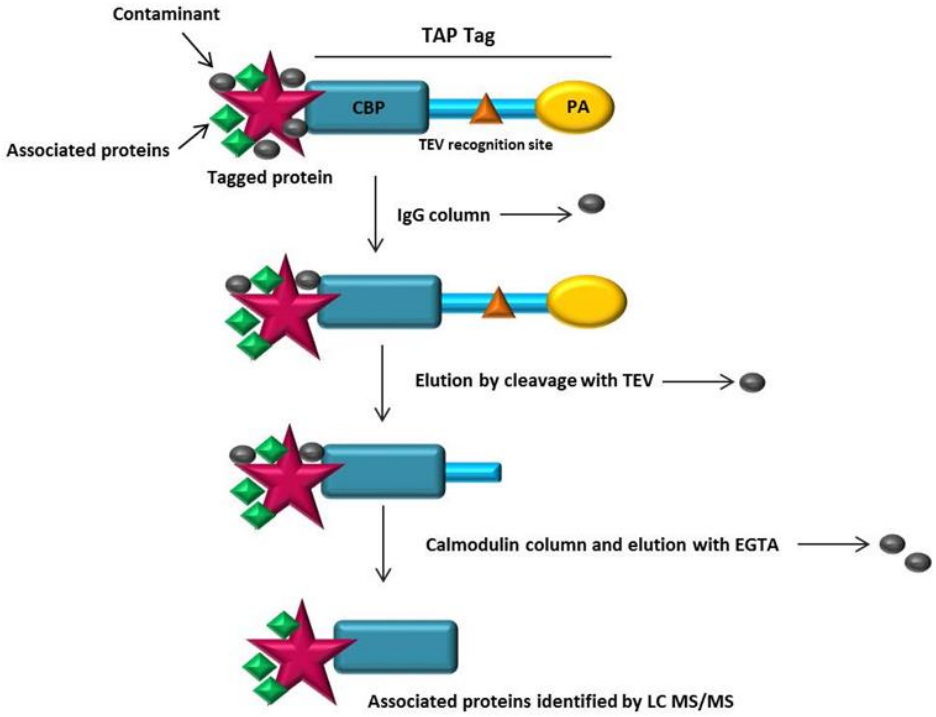

Figure 11. TAP purification schematic procedure

Protein identification by mass spectrometry

Protein identification by mass spectrometry was performed by LC-MS/MS by the mass spectrometry service (*Servei Central de Suport a la Investigació* (SCSIE)) at the University of Valencia (UV) following the standards of Proteored Spain (www.proteored.org) and the SCSIE at UV (www.scsie.uv.es)

Colloidal coomassie blue staining

Protein staining was performed with Colloidal Coomassie blue powder by immersing the gel in solution dye for at least 30 minutes, and then several

washings with destaining solution (30 % methanol (v/v), acid acetic 5 % (v/v)) to remove dye excess.

Total histone extraction

Cell cultures were harvested by centrifugation for 3 minutes at 3.000 rpm and washed with cold sterile water. Cell pellet was resuspended in 10 ml of 20 % TCA, centrifuged at 3.000 rpm for 3 minutes and cells were frozen in liquid nitrogen. After thawing the pellet, it was resuspended in 0.5 ml of 20 % TCA and 200 µl of glass beads were added for cell breakage. The mixture was vortexed applying 5 cycles of 1 minute on 1 minute off at 4 °C. The lysate was collected in a new tube and glass beads were washed twice with 0.2 ml 5 % TCA which was added to the previous lysate. The lysate was later centrifuged for 10 minutes at 3.000 rpm and the resulting pellet was resuspended in 0.2 ml of Laemmli buffer (0.06 M Tris pH 6.8; 10 % SDS; 0.0025 % blue bromophenol) with 5 % beta- mercaptoethanol and 50 µl of 2 M Tris-Base. Cell pellet was boiled for 3 minutes at 95 °C and centrifuged for 10 minutes at 3.000 rpm. The supernatant was transferred to a new tube and store until use.

Protein Immunoprecipitation (IP)

For protein immunoprecipitation, 50 ml yeast cultures grown in YP+Glucose were collected at 0.5 OD_{600}. Cells were washed once with 10 ml LB 1X buffer (10 mM Tris-HCl pH 8.0, 150 mM NaCl, 20 % glycerol (v/v) and Nonidet P-40 0.1 % (v/v) and resuspended in 200 µl lysis buffer (LB 1X, 0.5 mM DTT, 1 mM PMSF and 1X Complete protease cocktail

inhibitor (Roche)). Cell breakage was performed by vortexing at 4 °C by applying 4 rounds of 1 min on 1 min off with the addition of 200 µl glass beads to the resuspended cells. Following centrifugation of the broken cells, 30 µl of the extract was reserved (Input) and 30 µl of protein buffer 4X was added. The rest of the volume was incubated with beads (Dynabeads, Invitrogen) for 2 hours at 4 °C in a turning wheel. In this case, beads were not previously coated with an antibody since proteins were tagged with the TAP-tag which includes a protein A region that recognizes the IgG from the Dynabeads. The immunoprecipated samples (IP) were washed 3 times for 10 minutes with LB 1X and 0.5 mM DTT. To elute the samples, two rounds of 25 µl of loading buffer 4X were added to the beads and incubated for 3 min at 95 °C, supernatant was removed with the use of a magnetic strip and passed into a new tube and stored until use.

Chromatin Immunoprecipitation (ChIP)

Chromatin immunoprecipitation was performed by using 50 ml of 0.5 OD_{600} yeast cultures grown in YP+Glucose or YP+Rafinose in case the desired gene was *GAL1* which required a 2 % galactose or glucose induction for 25 minutes. Cultures were cross-linked for 20 minutes at room temperature with 1 % formaldehyde final concentration (Sigma) under continuous shaking at 140 rpm. Cells were later quenched with 125 mM glycine. Subsequently, cells were collected by centrifugation and washed 3 times with 25 ml cold Tris-saline buffer (150 mM NaCl, 20 mM Tris-HCl, pH 7.5). Cells were broken for 15 min at 4 °C by adding 300 µl of

lysis buffer (50 mM HEPES-KOH at pH 7.5, 140 mM NaCl, 1 mM EDTA, 10 % glycerol, 0.5 % NP-40, 1 mM PMSF and proteases inhibitors) and 200 µl glass beads. Cells extracts were sonicated in a Bioruptor sonicator (Diagenode) for 30 minutes in 30 seconds on and 30 sec off cycles and centrifuged for 15 minutes at 12.000 rpm. 10 µl of chromatin extract were saved as the Input. The rest of the lysate was used for immunoprecipitation with magnetic beads (Dynabeads, Invitrogen) for 2 hours at 4 °C in a turning wheel allowing the binding of the protein A from the TAP tag to the beads. Beads were later washed with the following buffers; twice with lysis buffer, twice with lysis buffer supplemented with 360 mM NaCl, twice with wash buffer (10 mM TRIS-HCl, pH 8.0, 250 mM LiCl, 0.5 % NP-40, 125 mM Nadeoxycholol, and 1 mM EDTA) and once with TE. For samples elution, 50 µl of elution buffer (50 mM TRIS-HCl, pH 8, 10 mM EDTA, 1 % SDS) were added to the beads for 10 min at 65 °C. This step was repeated twice. Input and immunoprecipitations (IP) samples were incubated overnight at 65 °C to reverse the crosslinking. 100 µg/250 µl Proteinase K (Ambion) was added to the IP and Input for 1.5 hours at 45 °C. DNA was extracted using the DNA purification Kit (Zymoresearch) following the manufacturer's instructions. DNA was used for the qPCR reaction by using the desired primers. In all cases, at least three biological replicates were performed to obtain the standard deviation.

Metabolite extraction and analysis

The metabolic profile of yeast cells was determined as previously described (Palomino-Schätzlein et al., 2013) following the subsequent procedure:

Yeast cultures

sgf73Δ cells expressing human ATXN7 containing the 10Q or the 113Q repetitions were grown in SC-LEU agar plate at 30 °C until yeast colonies were observed. One colony of each condition (10Q or 113Q) was inoculated in 10 ml SC-LEU and incubated at 30 °C in continuous shaking until an OD_{600} 0.4-0.5 was reached.

Cell collection

Cells were collected by centrifuging 10 ml culture at 2.000 rpm during 1 minute. Cell pellet was washed first with 1 ml phosphate buffer (Na_2HPO_4 100 mM, pH 7.4) and twice with 0.5 ml of the same buffer. Cells were quenched with 160 µl methanol at -20 °C. The resulting pellet was frozen in liquid nitrogen and stored at -80 °C. At least 3 different replicates were used for both conditions.

Metabolite extraction

For metabolites extraction, 80 µl of chloroform at 4 °C were added to the cell pellet and resuspended for 5 minutes in ice. To break the cells, cells were introduced in liquid nitrogen during 1 minute and subsequently left on ice for 2 minutes, this step was repeated 2 more times. Subsequently,

125 µl of MilliQ water and 125 µl of chloroform were added to each sample following vortex until a homogenous emulsion was observed. Samples were later centrifuged for 15 minutes at 13.000 rpm for phase separation. At this point, the upper part which corresponds to the aqueous phase was collected with a pipette and passed into a new tube, while the remaining chloroform and methanol in the lower phase (lipophilic phase) was collected and passed into a new tube. A new round of centrifugation of 13.000 rpm during 2 minutes was applied to each collected phase to check the lack of mixed phases. The aqueous phase was frozen into liquid nitrogen and introduced in a lyophilizer to eliminate the remaining water and methanol. Finally, samples were introduced in liquid nitrogen and preserved at -80 °C until its use.

NMR sample preparation

Cell extracts were defrosted at 4 °C on ice before NMR acquisition. For the aqueous phase, 0.55 ml of phosphate buffer (Na_2HPO_4 100 mM, pH 7.4) in D_2O with 0.2 mM TSP was added to the samples and passed into an NMR tube. Following the measurement, samples were stored at -20 °C.

NMR spectroscopy

NMR spectroscopy and spectra processing and metabolite quantification was performed by the NMR facility of the Centro de Investigación Príncipe Felipe (CIPF). NMR spectra were recorded at 27 °C on a Bruker AVI-600 using a 5 mm TCI cryoprobe and processed using Topspin3.2 software (Bruker Biospin). 1H 1D noesy NMR spectra were acquired with 128 free

induction decays (FIDs). 64k data points were digitalized over a spectral width of 30 ppm. A 4s relaxation delay was incorporated between FIDs and water presaturation was applied. The FID values were multiplied by an exponential function with a 0.5 Hz line broadening factor.

Metabolite quantification and statistical analysis

Signals in the ^{1}HNMR spectra were assigned to the corresponding metabolites with the help of spectral databases HMBD (Human Metabolome Database) and BMRB (the Biological Magnetic Resonance Bank) and previous results. Spectra were normalized to total intensity to minimize the differences in concentration and experimental error during the extraction process. Optimal integration regions were defined for each metabolite, an attempt being made to select the signals without overlapping. Integration was performed with MestreNova 8.1.

Principal component analysis (PCA) and projection on latent structure-discriminant analysis (PLS-DA) analysis was performed with SIMCA-P 13.0 (Umetrics, Sweden). For this analysis, the metabolite tables generated from spectra integration were univariate scaled (each value being divided by the standard deviation of each variable) and mean centered for an easier interpretation of the data and to take the variation of small signals into account. Univariate analysis and box plots were performed with unscaled, normalized concentration data in Excel.

Microscopic techniques

In vivo protein localization

Visualization of GFP-tagged proteins was performed directly in living cells grown in SC medium at OD_{600} 0.3-0.5. The cells were washed with PBS 1X (13.7 mM NaCl, 0.27 mM KCl, 0.43 mM de Na_2HPO_4 and 0.14 mM KH_2PO_4) and incubated in ice with 1 ml methanol for 10 minutes for its fixation. Cells were centrifuged for 3 minutes at 2.000 rpm and resuspended in 1X PBS. Living cells tagged with GFP were visualized using Leica TCS SP2 AOBS confocal microscope with the support of the confocal microscopy service at the Centro de Investigación Príncipe Felipe.

In Situ Hybridization (FISH)

Fluorescence in situ hybridization against poly $(A)^+$ RNA was done by growing yeast cells in 100 ml of YP+Glucose medium overnight at 30 °C to an 0.5 OD_{600} and shifted to 39 °C for 2 hours the following day. Subsequently, cells were fixed by adding 10 % formaldehyde and incubated for 60 min at room temperature. The fixative formaldehyde was removed by two rounds of centrifugation and washed with 0.1 M potassium phosphate (pH 6.4). Cells were resuspended in ice-cold washing buffer (1.2 M sorbitol and 0.1 M potassium phosphate, pH 6.4) digested with 0.5 mg/ml of Zymolyase 100T and applied on poly-l-lysine-coated slide wells. Cells not adhered to the slides were removed by aspiration. Cells were rehydrated with 2X SSC (0.15 M NaCl and 0.015 M sodium citrate) and were hybridized overnight at 37 °C in 20 µl of prehybridization

buffer with 0.8 pmol of Cy3-end-labeled oligo (dT) in a humid chamber. Following the hybridization, slides were washed with 2X SSC at room temperature for 5 minutes and 1X SSC, air-dried and mounted using 3.5 µl/well VECTASHIELD® Mounting Medium with DAPI. Detection Cy3-oligo (dT) was performed using Leica TCS SP2 AOBS confocal microscope with the support of the confocal microscopy service at the CIPF.

Image analysis

Bands obtained by Western Blot were analysed with the Image J program (Health National Institute (NIH), USA, http://imagej.nih.gov/ij/).

Genomic Run-On (GRO) and measurement of mRNA levels

The genomic run-on (GRO) protocol allows the genome-wide analysis of yeast nascent transcription which was performed following the experimental procedures (García-Martínez et al., 2004). This method combines *in vivo* labelled RNA and nylon macroarrays to calculate TR (Transcription Rate) for all yeast genes.

To perform the experiment, cells were grown overnight at 30 °C in YP+Glucose medium at 120 rpm up to an exponential phase (OD_{600}=0.5). Cells were measured with the use of a counter Coulter (Beckman Coulter) to estimate the number of cells in each of the samples with different cellular volumes. Cells were collected into two aliquots; the first aliquot was obtained for the GRO experiment to measure TR and the second for

RNA isolation followed by cDNA synthesis to obtain the mRNA amount (RA) (**Figure 12**).

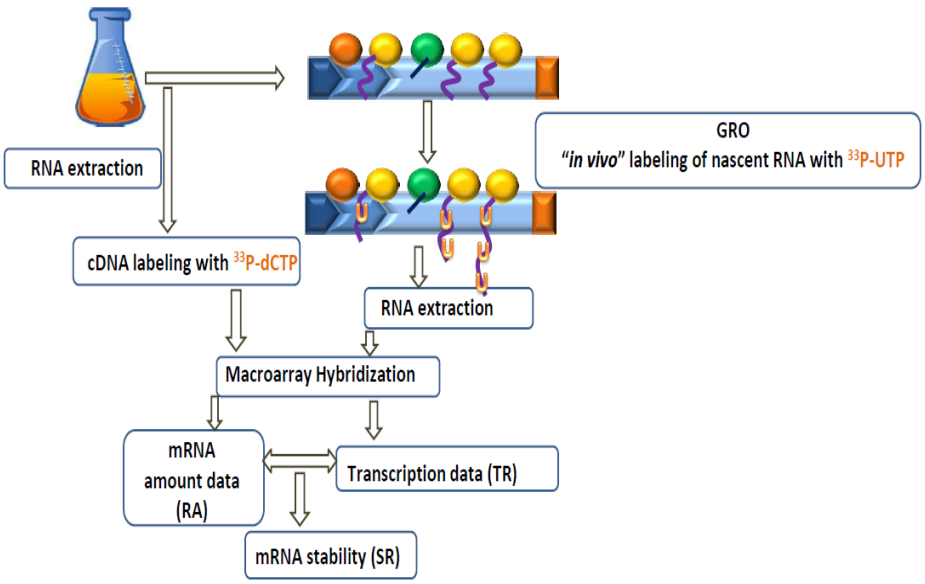

Figure 12. Experimental design of the genomic run-on protocol to determine Transcription rate (TR) and mRNA amount (RA). Cells were grown and collected into two different aliquots to obtain the TR and RA data. The first aliquot was used for the run-on analysis after normalization with the in vitro transcripts; the values obtained are proportional to the RNA pol II density on the probe region for each gene. The second aliquot was used to obtain the RNA and subsequently the labelled cDNA by RT, thus obtaining the mRNA amount (RA). The same membrane is used for both the GRO and mRNA samples after stripping. mRNA stability data is obtained by the division of RA by TR.

To obtain **the transcription rate (TR),** the experiment was divided into the following phases:

1. *in vivo* transcription

Cells were collected, washed with cold sterile water and resuspended in 120 µl cold sterile water. To permeabilize the cells, 20 ml of 0.5 % N-lauryl

sarcosine sodium sulfate (sarkosyl) were added to the cells and incubated for 20 minutes on ice. Cells were centrifuged for 2 minutes at 4.000 rpm and 1 ml sarkosyl was added to the pellet and transferred into 1.5 ml tubes. After spinning down the cells, *in vivo* transcription was performed by adding 162 µl of the transcription MIX; 120 µl of 2.5X transcription buffer (50 mM Tris-HCl [pH 7.7], 500 mM KCl, 80 mM MgCl), 16 µl of AGC mix (10 mM each of CTP, ATP, and GTP), 6 µl of DTT (0.1 M) and 20 µl of [α-^{33}P] rUTP (10 µCi/µl). The final volume was adjusted to 300 µl with distilled water and the mix was incubated for 5 minutes at 30 °C to allow transcription elongation. To stop the reaction, 1 ml of cold water was added and cells were centrifuged for 1 minute at 6.000 rpm (the upper part contains the non-incorporated radioactivity).

2. *In vitro* transcription

In order to obtain the *in vitro* transcripts for the GRO experiment, we adapted the protocol described in the literature (Huang and Yu, 2013). The main purpose of this step is to obtain *in vitro*-synthesized RNAs labeled with P^{33} with the use of DNA-dependent phage T7 RNA polymerases. We generated three different types of RNA transcripts using control probes from Bacillus (*pGIBs-Thr, pGIBs-Phe, pGIBs-Lys).* Each mix contained (in a total volume of 20 µl): 10X Transcription buffer (2 µl); 10 mM ACG mix (1 µl); 0.1 mM UTP (7.4 µl); UTP [alpha-^{33}P] (1 µl); RNase OUT (1 µl); T7 RNA polymerase (1 µl); DNA pGIBs (1 µg). Incubate each mix at 37 °C during 2 hours at 500 rpm. Add to each mix 2.5 V of 96 % EtOH and store it at - 20 °C for 2 hours. Centrifuge the samples at 12.000 rpm during

12 minutes and remove the supernatant. Dry the pellet at 30 °C during 12 minutes and resuspend the pellet in a final volume of 30 µl. An aliquot was used for specific radioactivity in a scintillation counter to determine the dpm (desintegrations per minute) of each single mix (*pGIBs-Thr, pGIBs-Phe, pGIBs-Lys).* Subsequently, a proportional unique mix containing the 3 TIVs (*in vitro* transcripts) will be used to obtain the transcription rate. GRO experiments were normalized taking into account the *in vitro* transcripts signals.

3. RNA isolation

Total RNA extraction was obtained by resuspending the cells in 500 µl LETS buffer (0.1 M LiCl, 10 mM EDTA, 0.2 % SDS, 10 mM Tris-HCl [pH 7.4]), 200 µl glass beads and 500 µl acid phenol: chloroform (5:1) and 3 µl of the *in vitro* transcripts. Cells breakage was performed using the Fast-Prep (Bio101, Inc.) device. Cells were centrifuged for 5 minutes at 12.000 rpm and contaminants were removed by adding chloroform:isoamilic alcohol (24:1). Supernatant was transferred into a new 2 ml tube and RNA was precipitated by adding 50 µl AcNa 3M pH 5.5 and 1 ml cold ethanol 96 % overnight at - 20 °C. After centrifugation at 13.000 rpm for 5 minutes, labeled RNA was washed with cold ethanol 70 % and dried. Samples were resuspended in 300 µl of cold sterile water and total labeled RNA was spectrophotometrically quantified. An aliquot was used to measure radioactivity (dpm) in a scintillation counter and all the *in vivo* labeled RNA was used for hybridization (0.35-3.5 x 10^7 dpm).

4. Membranes Hybridization

Hybridization was performed using nylon filters which were made using PCR-amplification whole ORF sequences as probes done at University of Valencia (Biochemistry and Molecular Biology Department). Nylon filters were previously pre-hybridized for 1 hour at 65 °C in hybridization buffer (Phosphate buffer 0.5 M pH 7.2 , 1 mM EDTA, 7 % SDS) and hybridizations were performed using 3 ml of the mentioned solution containing labeled RNA and incubated for 48 hours at 65 °C in a turning wheel. Subsequently, membranes were washed once with 1X SSC and 0.1 % SDS during 10 minutes and twice with 0.5 % SSC and 0.1 % SDS at 65 °C.

Filters were exposed for 1-2 days depending on the signal intensity measured with a Geiger counter to an imaging plate (BAS-MP, FujiFilm) read at 50 µm resolution in a Phosphorimager scanner (FLA-3000, FujiFilm).

For the measurement of mRNA levels, the second aliquot taken from the cell culture (20 ml) was kept frozen at -20 °C. Samples were thawed on ice and RNA was isolated following the same procedure conducted for the GRO with minor changes; after the samples were dried with the use of the speed-vac (Thermo Scientific), samples were resuspended in 100 µl sterile water and were dissolved for 1 hour at 30 °C with continuous shaking. RNA was purified using the RNeasy KIT (Qiagen) following the manufacturer's instructions.

Materials and Methods

To obtain labeled cDNA, about 100 µg of RNA were reverse transcribed by the addition of two different mixes. First, 14 µl of the mix; 100 µg of RNA, 1 µl Oligo dT (T_{15}VN) at 500 ng/µl, 1 µl RNase OUT and sterile water up to 14 µl. Second, 16 µl of the mix; 6 µl of 5X Buffer Maxima RT (Thermo Scientific), 3 µl 0.1 M DTT, 1.5 µl dNTPs (16 mM of A,G,T/0.1 mM of C), 4 µl ^{33}P-dCTP and 1 µl Maxima RT (Thermo Scientific). A total volume of 30 µl containing the RNA was incubated at 50 °C during 2 hours with continuous shaking at 650 rpm. The reaction was stopped adding 1 µl 0.5M EDTA pH 8.0. The labeled cDNA was purified by a S300-HR Ilustra Microspin column (GE). An aliquot was used for specific radioactivity in a scintillation counter. Membranes hybridization was done in the same conditions as described for the transcription rate, although, labeled cDNA was at 3.5 x 10^6 dpm. Filters were exposed for 7 and 16 hours.

A dot-blot procedure was used to estimate the proportion of poly $(A)^+$ mRNA in the total RNA and used this datum to normalize the different hybridizations of cDNAs. Three different dilutions of total RNA extracted (250, 125 and 63 ng/µl) of the three repeated experiments were spotted by the use of a BioGrid robot (Biorobotics) on a nylon filter. The filter was hybridized with 1 µl of 5´-labeled poly (dT) 10 µM, 2 µl of polynucleotide kinase (PNK, 10 U/µl) (Roche), 2 µl of 10X PNK (Kinase) buffer (Roche), 2 µl of [γ-^{32}P] ATP (3000 Ci/mmol, 10 µCi/µl) and sterile water up to 20 µl final volume. The filter was incubated for 1 hour at 37 °C and the enzyme was inactivated at 70 °C during 10 minutes. Nylon filters were previously pre-hybridized for 1 hour at 42 °C in hybridization buffer (Phosphate buffer

0.5M pH 7.2, 1mM EDTA, 7 % SDS) in a turning wheel and hybridizations were performed using 5 ml of the mentioned solution containing labeled RNA and incubated for 24 hours at 42 °C. Subsequently, membranes were washed as described above and exposed for 3 hours to an imaging plate. The acquisition of the images was performed using a Phosphoroimager FLA 3000 (Fujifilm) and its quantification was performed using the ArrayVision (Imaging Research) program. The intensity of the quantified signal was used as the amount of polyadenylated RNA of each sample divided by the total RNA value of each well. The proportion (mRNA / total RNA) obtained was multiplied by the value of (total RNA/cell volume) determined from extractions of total RNA and cell volume determinations (Coulter), thus determining the [mRNA]. The cell volume corresponds to the number of cells per ml multiplied by the volume of each cell.

Both GRO and cDNA belonging to the same sample were hybridized against the same nylon filter after blocking the filters with a boiling stripping reaction (SDS 0.1 %, Sodium phosphate 5 mM pH 7.0) during 10 minutes. For the 3 experiments, 3 different nylon filters were used. To quantify the samples, Arrayvision 7.0 (Imaging Research, Inc.) was used, considering the sARM density as signal.

Human Cells Lines 293T (HEK293T)

HEK293T Grow conditions

Human Embryonic Kidney 293 T (HEK293T) cells were maintained in Dulbecco's modified Eagle's medium (DMEM, Invitrogen) supplemented with 1 % penicillin/streptomycin (PEST, Invitrogen) and 10 % fetal bovine serum (FBS, Invitrogen) and incubated at 37 °C with 5 % CO_2. HEK293T cells were co-transfected with each desired DNA plasmid constructs using Lipofectamine-2000 (Invitrogen) according to the manufacturer's instructions. All plasmids were a kind gift from Dr. La Spada laboratory. Cells were incubated for 24-48 hours post-transfection and washed with PBS 7.4 pH for later use.

In vitro DUB assay using HEK293T cells

HEK293T cells were co-transfected with 8 µg of each desired DNA plasmid constructs (USP22-FLAG, ENY2-HA-FLAG, ATXN7L3-HIS and MYC-ATXN7-10Q or MYC-ATXN7-92Q). Cells were collected using 1 ml PBS and centrifuged for 3 minutes at 2.500 rpm at 4 °C. To obtain the cell lysate, 300 µl of RIPA buffer (Milipore) supplemented with protease cocktail inhibitor (Roche) was added to the cell pellet and the supernatant was collected after centrifugation at 14.000 rpm for 15 minutes at 4 °C.

For the Co-immunoprecipitation (Co-IP), a 1:1 mixture of protein A and protein G beads (10 µl of each) (Invitrogen) were added to the cell lysate and incubated for 1 hour at 4 °C under rotation. 20 µl of Flag-conjugated

bead slurry (Invitrogen) was added to the cell lysate and incubated for 2 hours at room temperature under rotation. Subsequently, the supernatant was removed with the use of a magnetic strip and beads were washed 3 times with TBS 7.6 pH. 12 µl of TBS was added to the beads followed by 8 µl of Flag peptide (5 µg/µl) (Invitrogen) and incubated it for 1 hour at 4 °C. Later, supernatant was removed and collected for later use.

For the *in vitro* deubiquitination assay (DUB assay), histones were prepared from HEK293T cells using the Histone extraction kit (Abcam) according to manufacturer´s instructions. Histones were quantified with Bradford assay (Biorad) and 1 µg of histone extracts were incubated with DUBm immunopurified complexes as described above for 2 hours at 37 °C. As a negative control, histone H2B was incubated solely in DUB buffer (100 mM Tris–HCl at pH 8.0, 1 mM EDTA, 1 mM DTT, 5 % glycerol, 1 mM PMSF and 1 % protease inhibitor). The reactions were stopped by the addition of TCA (10 % final concentration) and incubated overnight at 4 °C. Reactions were centrifuged for 45 minutes at 13.000 rpm and washed with 1 ml acetone. Cell pellets were resuspended in SDS 2X sample buffer and the reactions were analysed by Western blot using specific antibodies. Signal intensities of target bands were quantified by Image lab software (BioRad).

Column Fractionation and Analysis

Chromatography was carried out at 4 °C using an anion exchange MonoQ HR5/5 column 50 mm x 5 mm (Amersham Biosciences) equilibrated in buffer (50 mM Tris, pH 8, 50 mM NaCl) connected to a fast protein liquid

chromatography (FPLC) system LCC-500 FPLC (Amersham Biosciences) system following the indications as previously described (Lam et al., 2006).

HEK293T cells were co-transfected with 24 µg of each of the desired plasmids expressing both ENY2-FLAG-HA and MYC-ATXN7-10Q or MYC-ATXN7-92Q in 10 cm plates. Cells were collected using 1 ml PBS and centrifuged for 3 minutes at 2.500 rpm at 4 °C. 700 µl of each transfection were loaded for FPLC. Gel Filtration was performed with a Superose 6 10/300 GL column (Amersham Pharmacia) equilibrated in buffer (50 mM Tris, pH 8, 20 mM NaCl) at a flow rate of 0.5 ml/min. Fractions were collected every 0.5 ml and elution volumes of gel-filtration standards were 12.4 ml for Thyroglobulin (669 kDa), 15.8 ml for ADH (150 kDa) and 19.2 ml for cytochrome C (12.4 kDa). The column was washed with approximately 13 column volumes of buffer (50 mM Tris, pH 8, 20 mM NaCl) and bound proteins were eluted 20 ml linear NaCl salt gradient from 50 mM to 600 mM NaCl in 50 mM Tris, pH 8.0 at 1 ml/min. Fractions of 1 ml were collected, kept at 4 °C and prepared for SDS-PAGE Western blot. Samples were later stored at -80 °C.

Mice model

Mouse Cerebellum extraction and RNA isolation

Mice cerebellum extraction

Cerebellar tissue from mPrP-fxSCA7 92Q-BAC animals and wild-type littermates was harvested at age 30 weeks (10 weeks post-symptomatic).

RNA isolation

For RNA isolation from mice cerebellum, 50-100 mg of tissue was homogenized with 1 ml Trizol (Thermo Fisher) with the use of a 26 ½ gage needle until no particular matter was visible and incubated for 5 minutes at RT. 200 µl of chloroform were added to the samples, mixed vigorously for 15 seconds and left at RT for 3 minutes. Samples were centrifuged 4 °C for 15 minutes at 13.000 rpm. The clear aqueous layer was transferred into a fresh tube.

For RNA precipitation, 500 µl of isopropanol, 1/10 AcNa 3M (pH 5.5) and 1 µl glycogen were added to the samples and left for 30 minutes at -20 °C. Samples were centrifuged at 4 °C for 15 minutes and 13.000 rpm. After removing the supernatant, the RNA pellet was washed with 1 ml 75 % sterile ethanol, vortexed and centrifuged at 10.000 rpm for 15 minutes at 4 °C. Once the pellet was air-dried for 5-10 minutes at RT, pellet was resuspended in 40 µl of sterile water and measurement of RNA concentration was performed with the use of the spectrophotometer

(Nanodrop). Subsequently, 12 µg RNA were used to remove DNA from samples as follows; 3 µl DNase enzyme (Thermo Fisher), 10 µl 10X DNAse reaction buffer (Thermo Fisher) and nuclease free water up to a 100 µl final volume. The mixture was incubated in 37 °C water bath for 1 hour and 20 µl DNAse inactivation reagent (Thermo Fisher) was added and incubate at 37 °C for 5 minutes. Samples were centrifuged at 12.000 rpm for 2 minutes and supernatant (containing the RNA) was transferred into a new tube, measured with the nanodrop and stored at -80 °C for later use.

Real-time RT-PCR

Reverse transcription was performed on 1 µg of total cerebellar RNA using Turbo DNA free kit (Thermo Fisher) and High capacity cDNA reverse transcription Kit (Thermo Fisher) according to manufacturer instructions. The cDNAs were subjected to real-time PCR using primers for mice mitochondrial and ribosomal genes. To test the expression levels of the desired genes, 10 µl of the following mixture was used for the PCR amplification: 5 µl of Power SYBR green PCR master mix (Thermo Fisher), 3 µl of cDNA template (1/5 dilution), 0.35 µl of each forward and reverse primers at 10 mM concentration (DTT technologies) and 1.20 µl sterile water. mRNA levels were normalized to *GAPDH* gene.

Objectives

Objectives

During the development of this thesis, I have been involved in deciphering new aspects related to the deubiquitinase module (DUBm) from SAGA complex. My research was mainly involved in understanding the role of this module and its participation in gene expression, more specifically in transcription regulation. Focusing on this submodule, I have identified new partners of the transcription machinery that also participate in the regulation of gene expression in several aspects. Briefly, the main objectives of this thesis are the following:

- Functional characterization of the novel factors Asf1 and Mog1 involved in the ubiquitination/deubiquitination of histone H2B.
- The study of the molecular mechanisms of DUBm related diseases; Spinocerebellar Ataxia Type 7 (SCA7). To understand the principal mechanisms of this disease and its link with the DUBm activity.

Results and Discussion

CHAPTER 1

Functional characterization of the novel factors Asf1 and Mog1 involved in the ubiquitination/deubiquitination of histone H2B

Sus1 is a component of both the transcriptional co-activator SAGA complex and the nuclear pore-associated mRNA export complex (TREX-2) (revised in the introduction) (Rodríguez-Navarro et al., 2004). So far, Sus1 has been described as a component that participates in processes associated to the gene expression pathway such as activation of transcription, elongation and mRNA export (Köhler et al., 2006; Pascual-García et al., 2008). To find novel components of the histone H2B ubiquitination/deubiquitination machinery in yeast, we followed both biochemical and genetic approaches to find functional interactors of Sus1. In this chapter, I will describe the characterization of Asf1 and Mog1, as factors related to Sus1 that participate in the ubiquitination of histone H2B.

1. Deciphering the role of Asf1 in transcription

Asf1 is dispensable for Sus1 recruitment to *GAL1* gene, its induction and mRNA export

We have recently identified that Sus1, together with a component of the TREX-2 complex, Thp1, co-purifies with a histone chaperone named Asf1 (Pamblanco et al., 2014). During transcriptional activation, Asf1 associates

with the *GAL1*/*10* promoters and coding regions and it rapidly dissociates from these regions upon transcriptional repression. It travels with elongating RNA Pol II and it is necessary for RNA Pol II occupancy (Schwabish and Struhl, 2006). In these terms, Sus1 is also necessary for the correct expression of the *GAL1* gene since it is recruited to the *GAL1*/*GAL10* promoter following transcriptional activation (Cabal et al., 2006; Rodríguez-Navarro et al., 2004). Therefore, we aimed to investigate the recruitment and expression of Sus1 in the absence of *ASF1*.

Chromatin Immunoprecipitations (ChIP) experiments were performed in a strain expressing TAP-tagged Sus1 in wild-type (WT) and in the absence of *ASF1* (*asf1Δ*) to study the association of Sus1 to the *GAL1* promoter and ORF. For the *GAL1* induction, cells were incubated for 25 minutes in the presence of galactose. Our results reveal that Sus1-TAP recruitment to the promoter and gene body (ORF) of *GAL1* gene is not significantly affected in *asf1Δ* strain compared to the WT. Consequently, we also observe a normal *GAL1* expression in *asf1Δ* cells after galactose induction. However, when we compared Sus1-TAP recruitment to *GAL1* between the promoter and ORF, we observe a significant reduction in the association of Sus1-TAP to the ORF. These results indicate that Asf1 is dispensable for Sus1-TAP recruitment to *GAL1* gene, however, it affects the ratio of Sus1-TAP binding to *GAL1* promoter vs. coding regions (**Figure 13**) (Pamblanco et al., 2014).

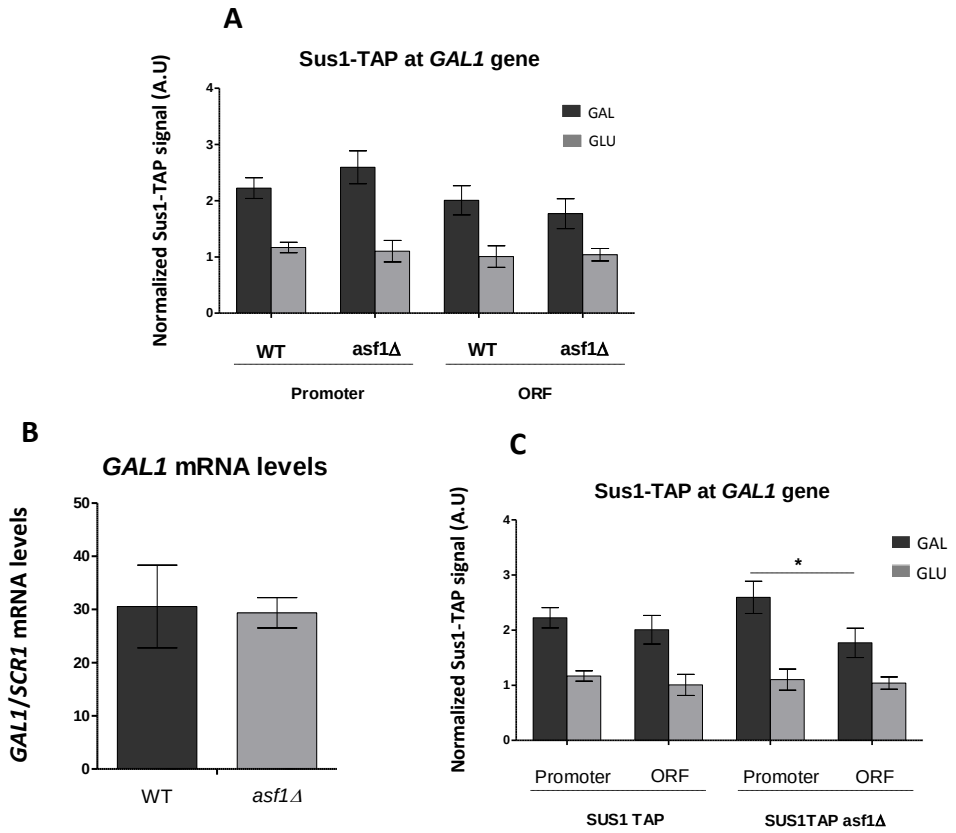

Figure 13. Asf1 is dispensable for Sus1 recruitment to *GAL1*. (A) Sus1-TAP recruitment to *GAL1* promoter and ORF was studied in the WT and *asf1Δ* cells following galactose induction after 25 minutes (B) *GAL1* induction in WT and *asf1Δ* cells was analysed after a 25 minute shift from 2 % raffinose to 2 % galactose growing media. The relative *GAL1* mRNA levels were determined by qPCR and normalized to the *SCR1* mRNA levels. Error bars represent SD for at least three independent experiments. (C) The same results represented in (A) were plotted to compare Sus1-TAP recruitment in *GAL1* promoter and ORF for each strain. The occupancy level was calculated as the signal ratio of the IP samples in relation to the input signal, minus the background of a no-antibody control. Error bars represent SD for at least three independent experiments. Statistical analysis was performed using the Student's t test and presented as a P-value (p) ($p < 0.05$ is considered as statistically significant).

Previous studies in our lab have demonstrated that *SUS1* interacts genetically with *ASF1*, since double mutant bearing deletions of both genes is correlated with growth impairment when compared with each

single mutant (Pamblanco et al., 2014, Doctoral thesis Dra. García-Oliver, 2013). These interactions may be indicative of a functional link among *SUS1* and *ASF1*, for instance, Sus1 participates in the export of mRNA, as its deletion leads to an accumulation of mRNAs in the nucleus (Rodríguez-Navarro et al., 2004). For this reason, we aimed to investigate whether Asf1 could participate in this process similarly to Sus1. Therefore, an analysis of the export of bulk poly $(A)^+$ mRNA in cells lacking *ASF1* was performed using *sus1Δ* strain as positive control. Our results show (**Figure 14**) that Asf1 is not necessary for mRNA export under the conditions tested in this study. As expected, *SUS1* deletion leads to an accumulation of mRNA in the nucleus (Pamblanco et al., 2014).

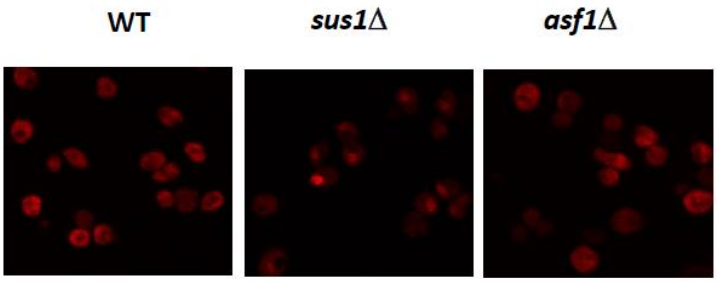

Figure 14 . FISH experiments in WT, *sus1Δ* and *asf1Δ* cells. Localization of poly $(A)^+$ RNA at 39 °C in YP+Glucose for 3 hours was performed using Cy3-labeled oligo (dT) probes.

Absence of *ASF1* reduces global levels of H2B ubiquitination and counteracts the effects of *SUS1* deletion

The monoubiquitination of histone H2B at Lys123 by the E2 ubiquitin conjugase Rad6 and the Bre1 ubiquitin ligase (Robzyk et al., 2000; Wood et al., 2003b) constitute one of the key steps in the control of gene expression since it regulates many processes such as chromatin dynamics, transcription initiation and elongation, silencing and DNA repair (Fuchs et al., 2014; Weake and Workman, 2008).

As well as H2B is monoubiquitinated, the ubiquitin mark also needs to be removed by the catalytic enzyme Ubp8 which is part of the DUBm. This step is required for a functional transcriptional activation and elongation (Daniel et al., 2004; Henry et al., 2003). Sus1 also participates in this process as being part of the DUBm (Köhler et al., 2006). In these lines, we investigated the role of Asf1 in H2Bub^{1} due to the physical and genetic interaction with Sus1. As represented in **Figure 15**, Western blot analysis from WT, *asf1Δ, sus1Δasf1Δ*, and *sus1Δ* strains indicate that deletion of *ASF1* leads to a significant reduction of H2Bub^{1} in both chromatin and total whole cell extracts. In contrast, *sus1Δ* mutant shows enrichment in H2Bub^{1} levels. The reduction observed in the single mutant *ASF1* is partially suppressed by the deletion of *SUS1* (double mutant *sus1Δasf1Δ*). These results reveal that Asf1 is required for maintaining correct levels of H2Bub^{1} (Pamblanco et al., 2014).

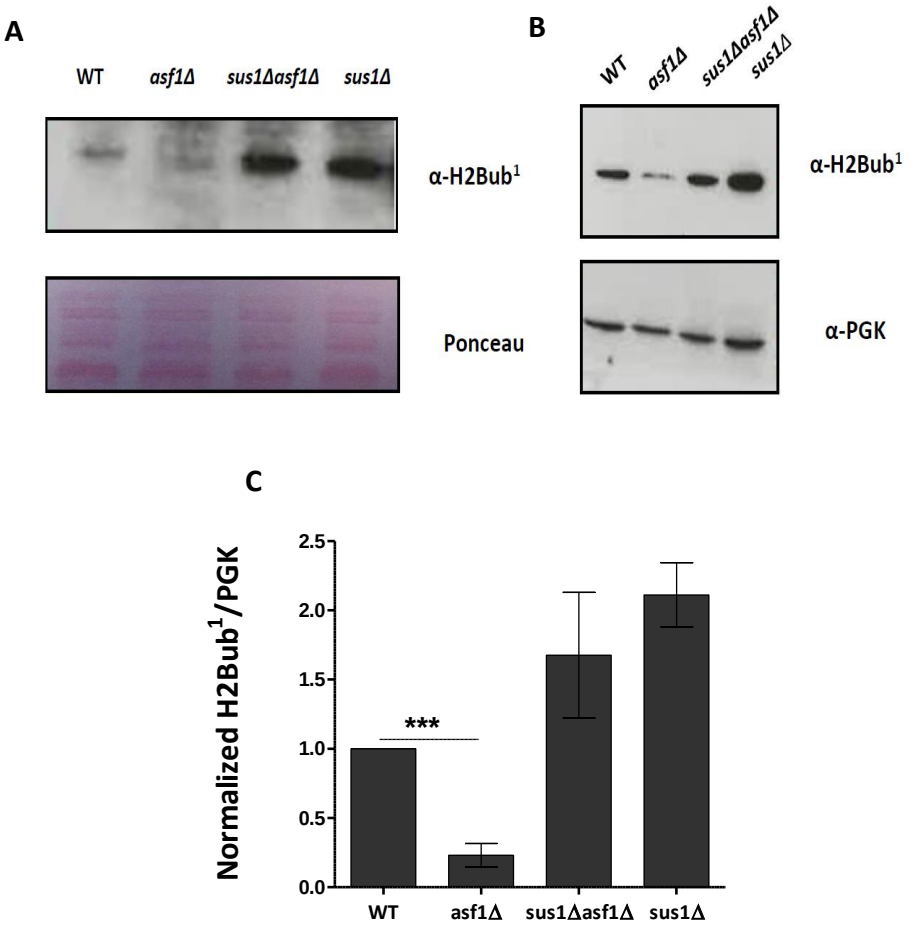

Figure 15. Asf1 is required for ubiquitination of histone H2B. A) Chromatin extracts corresponding to WT, *asf1Δ, sus1Δasf1Δ*, and *sus1Δ* strains. *asf1Δ* shows a decrease in H2Bub^1 levels compared with WT. On the contrary, *sus1Δasf1Δ* and *sus1Δ* mutants present an increase in H2Bub^1 levels. Ponceau S. staining of the membrane before blotting was used as loading control. B) Representative blot of WT, *asf1Δ, sus1Δasf1Δ*, and *sus1Δ* whole cell extracts. In this case, PGK abundance was used as loading control. C) Bar graphs indicates total H2Bub^1 levels normalized to *PGK* after quantification of WB signals. Error bars represent SD for at least three independent experiments. Statistical difference is considered as (*P = 0.01–0.05; **P = 0.001–0.01; ***P < 0.001).

2. Role of Mog1p in the control of gene expression

Sus1 interacts genetically with Mog1

Understanding the molecular basis of Sus1 function constitutes one of the main interests in our laboratory. Sus1 participates in different steps during gene expression as a component of the transcriptional co-activator SAGA complex and the TREX-2 mRNA export complex (Köhler et al., 2006; Pascual-García and Rodríguez-Navarro, 2009; Pascual-García et al., 2008; Rodríguez-Navarro et al., 2004). Outside the nucleus, Sus1 has also been shown to interact with cytoplasmic granules known as P-bodies (Cuenca-Bono et al., 2010). Due to our interest in deciphering new mechanisms that could link Sus1 with the coordination of different steps along gene expression, we investigated the genetic network of Sus1 interactions. The DRYGIN tool (database Repository of Yeast Genetic Interactions) provides valuable information in the context of genetic interactions of yeast mutants (http://drygin.ccbr.utoronto.ca). DRYGYN allows the identification of quantitative genetic interactions both positive and negative of *S. cerevisiae* double mutants. This information has been acquired by array studies by the laboratory of Dr. Charles Boone (University of Toronto) (Baryshnikova et al., 2010; Costanzo et al., 2010; Koh et al., 2010).

Searching DRYGIN database, we found out that the strongest genetic interaction of *SUS1* mutant is with *MOG1* (SGA score -0.53), a protein that so far has been described as a nuclear protein that interacts with Ran-GTP stimulating the release of GTP from Ran, indicating that Mog1 confers

directionality to nuclear import and export pathways (Baker et al., 2001; Steggerda and Paschal, 2000) (please see the introduction section).

This result suggests that *SUS1* and *MOG1* may present a functional relation which could implicate its contribution into similar biological processes. Therefore, we started to explore several possibilities that could explain the predicted genetic interaction. First, we used the web tool FuncAssociate 3.0 (http://llama.mshri.on.ca/funcassociate/) which from a set of genes or proteins is able to identify the Gene Ontology (GO) attributes of the gene set (Berriz et al., 2009). We used the set of genes genetically connected to *MOG1*, given by the DRYGYN tool to determine the *MOG1* "genetic network" and their GO using FuncAssociate 3.0. Our search shows that among the GO of genes genetically linked to *MOG1*, the components of the DUBm (Sus1, Sgf73, Ubp8 and Sgf11) have the highest score (**Table 2**). In addition, 6 genes related to mRNA export were also overrepresented among all GOs. Thus, through investigating *SUS1* genetic interactions, we hypothesize that *MOG1* could be linked to histone H2B deubiquitination and mRNA export.

FuncAssociate 3.0 : The Gene Set Functionator				
N	**X**	**P-value**	**Gene Ontology ID**	**Gene Ontology Attribute**
4	4	0.000001763	GO:0071819	DUBm complex
5	6	3,70E-04	GO:0016578	histone deubiquitination
4	5	0.000008561	GO:2001247	positive regulation of phophatidylcholine biosynthetic process
6	10	4,23E-04	GO:0031990	mRNA export from nucleus in response to heat stress
8	16	2,90E-05	GO:0000973	posttranscriptional tethering of RNA polymerase II gene DNA at nuclear periphery
5	10	0.00001377	GO:0033240	positive regulation of cellular amine metabolic process
9	19	6,89E-06	GO:0000972	transcription-dependent tethering of RNA polymerase II gene DNA at nucleus periphery

Table 2. Representative image of Mog1 GO attributes by FuncAssociate web tool.

MOG1 interacts genetically with factors involved in histone H2B ubi/deubiquitination

Our previous observations point out that *MOG1* is genetically linked with *SUS1*. In order to validate the possible genetic interaction between *MOG1* and *SUS1* suggested by the DRYGYN database, we created a double mutant and analysed the growth effects of *MOG1* deletion in cells lacking *SUS1*. As shown in **Figure 16**, *SUS1* and *MOG1* interact genetically. As it was mentioned above, not only *SUS1*, but also the rest of the DUBm components Ubp8, Sgf11 and Sgf73 showed genetic interaction with *MOG1*. We constructed double mutants bearing deletions for *MOG1* and the remaining three components from DUBm and monitored its effect in a cell growth assay as for *SUS1* deletion.

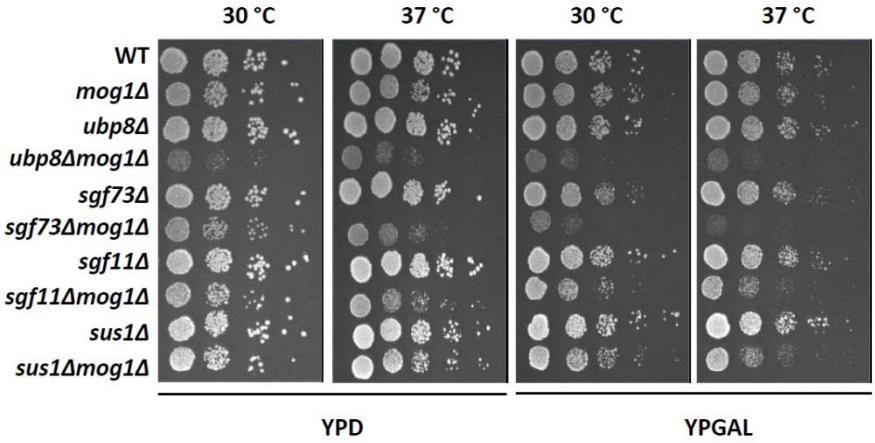

Figure 16. *MOG1* interacts genetically with all factors of the SAGA DUBm. Cells were diluted in 10^{-1} steps, and equivalent amount of cells were spotted onto YP+Glu (YPD) and YP+Gal (YPGal) plates. Cells were grown for 48 h at 30 °C and 37 °C.

Our results show that *mog1Δ* mutant does not present a growth defect compared to WT cells in all conditions tested. In contrast, we observe growth retardation in YP+glucose (YPD) medium when *MOG1* deletion is combined with *UBP8* and *SGF73*. This effect is also evident at 37 °C for *SGF11* and *SUS1*. Notably, the phenotype is always stronger when cells are grown in galactose-containing (YPGal) medium compared to single mutants (**Figure 16**). The strongest phenotype is observed for the combination in deletion of *MOG1* and *UBP8*, the catalytic enzyme of the DUBm, which places Mog1 in a key position in histone H2B deubiquitination. Overall, these genetic data suggest that Mog1 could participate in the process of histone H2B deubiquitination in yeast cells.

Past studies have shown that monoubiquitination of histone H2B ($H2Bub^1$) is a very dynamic process. The addition of an ubiquitin monomer to

histone H2B by the ubiquitin ligases Rad6, Bre1 and Lge1 (Robzyk et al., 2000; Song and Ahn, 2010; Wood et al., 2003b) plays important roles in transcription initiation and elongation. Both the addition by Rad6 and the removal of ubiquitin by Ubp8 enzyme from SAGA complex is essential for the transcriptional process (Daniel et al., 2004; Henry et al., 2003). Furthermore, H2Bub[1] is required for histone methylation by SET1C/COMPASS (Dover et al., 2002; Shilatifard, 2006; Sun and Allis, 2002) which constitutes one of the histone modification cross-talks necessary for the correct gene expression.

So, we decided to extend our genetic analysis with *mog1*Δ to factors involved in H2B ubiquitination. We created double mutants with deletions in *MOG1* together with *RAD6*, *BRE1* and *LGE1* subunits. We tested the genetic interaction by cell growth assay in YPD and YPGal plates at both 30 °C and 37 °C. Our analysis indicates that *mog1Δ* is epistatic to *bre1Δ* and *lge1Δ* compared with each single mutant in both YPD and YPGal, as its growth is slower in both conditions. On the contrary, the double mutant *rad6Δmog1Δ* do not present a significant enhancement of the growth defect when compared to the single *rad6Δ* (**Figure 17**). Interestingly, the growth defect of the double mutants *bre1Δmog1Δ* and *lge1Δmog1Δ* is comparable to that observed for single *RAD6* deletion. Based on these observations, we conclude that *MOG1* interacts in a synergistically dependent manner with *BRE1* and *LGE1* and might act at the same level than *RAD6*. Collectively, our genetic studies demonstrate that Mog1 is

genetically linked to the epigenetic process of histone H2B ubi/deubiquitination.

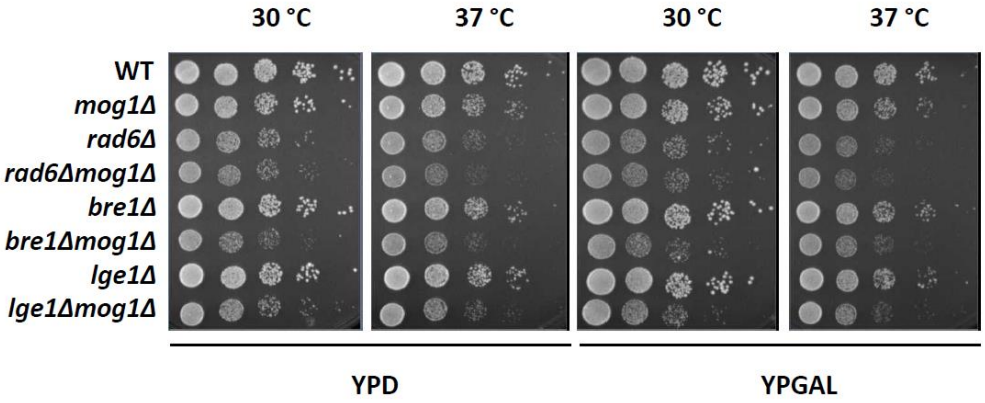

Figure 17. *MOG1* interacts genetically with the RAD6-dependent ubiquitination machinery. Cells were diluted in 10^{-1} steps, and equivalent amount of cells were spotted onto YP+Glu (YPD) and YP+Gal (YPGal) plates. Cells were grown for 48 hours at 30 °C and 37 °C.

Absence of *MOG1* reduces global levels of H2Bub^1 *in vivo*

The results presented so far demonstrate that *MOG1* interacts genetically with components from both H2B ubiquitinases and deubiquitinases. At this point, we wondered whether H2Bub^1 levels could be affected by the absence of *MOG1*. To test this possibility, we obtained total extracts from *mog1Δ*, *ubp8Δ*, *ubp8Δmog1Δ* and WT cells that were subjected to Western blot analysis with the required antibodies. As shown in **Figure 18**, deletion of *MOG1* reduces significantly the levels of H2Bub^1. As expected, the absence of *UBP8* strongly increases H2Bub^1 levels. As a control, we observed that unmodified H2B remains unaltered under the same conditions. Interestingly, the double mutant *ubp8Δmog1Δ* still led to

decreased levels of H2Bub[1], suggesting that Mog1 could act in early steps of monoubiquitination of H2B.

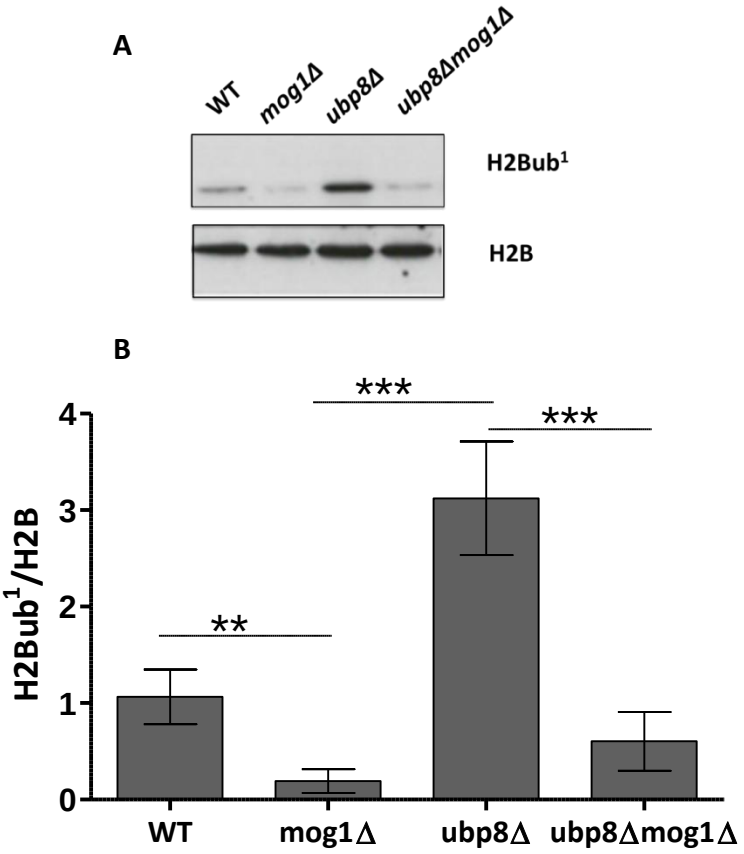

Figure 18. Absence of *MOG1* decreases H2Bub[1] levels. A) Total extracts from WT, *mog1Δ*, *ubp8Δ* and *ubp8Δmog1Δ* cells shows a decrease in H2Bub[1] levels in cells lacking *MOG1* as shown in the anti-H2Bub[1] Western blot (upper panel). As a control, immunoblot against total H2B indicates equal levels of H2B (lower panel). B) Bar graphs representing WT, *mog1Δ*, *ubp8Δ* and *ubp8Δmog1Δ* total extracts indicate H2Bub[1] levels normalized to total H2B after quantification. At least three independent experiments were performed for each case. Error bars represent SD and statistical difference is considered as (*P value = 0.01–0.05; **P value = 0.001–0.01; ***P value < 0.001).

Ubp8 preserves the association with its protein partners in *mog1Δ* cells

Deubiquitination of H2B is carried out by Ubp8 in the context of the SAGA DUB module (Daniel et al., 2004; Henry et al., 2003). It has been shown that all four DUBm subunits are required for activation of Ubp8 enzyme *in vitro* (Samara et al., 2010). One way to explain the reduction in H2Bub^1 levels upon *MOG1* deletion could be caused by the dissociation of Ubp8 from its DUBm partners. To tackle this aspect, we tagged Ubp8 with the TAP epitope in WT and *mog1*Δ cells and purified Ubp8 following the TAP technique. Ubp8 co-purifying proteins were detected by coomassie blue staining and the proteins were identified by LC-MS/MS. As a control, the presence of Ubp8 protein was monitored along the entire process by Western blot using α-TAP antibody (**Figure 19**, upper panel). Protein visualization by coomassie blue staining did not show any remarkable change in the band pattern between the WT and mutant strains (**Figure 19**, lower panel). Moreover, mass spectrometry analysis revealed that Ubp8 interacts with all SAGA subunits in the absence of *MOG1* suggesting that loss of *MOG1* does not affect Ubp8 association with the DUBm subunits and the rest of the SAGA complex (**Table 3**).

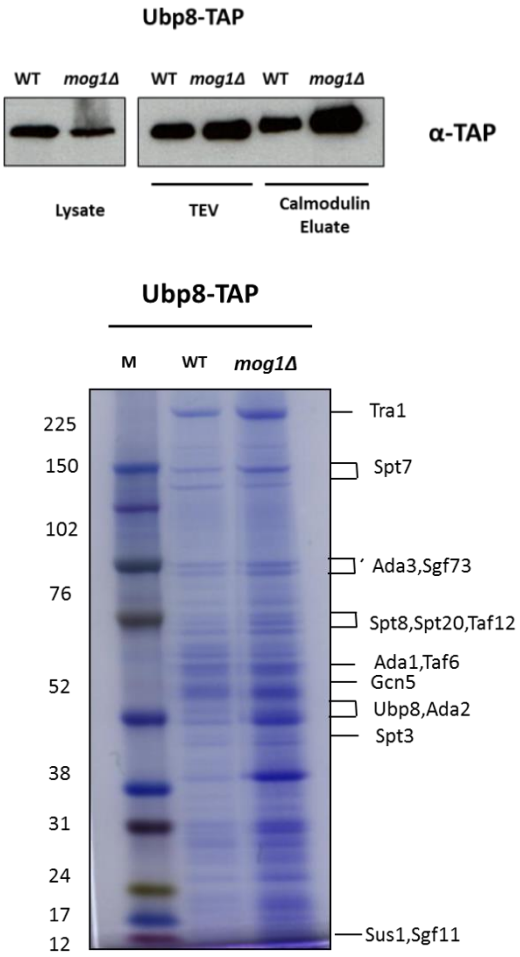

Figure 19. Analysis of Ubp8-TAP protein purifications in WT and in the absence of *MOG1*. Ubp8 was TAP-tagged in a WT and in *mog1Δ* strains. Ubp8 presence was confirmed by Western blot against anti-TAP antibody during the three steps of the purification: Lysate (before purification), TEV eluate (following first purification) and Calmodulin eluate (second purification) (upper panel). Calmodulin eluates from TAP purification were analysed in a polyacrylamide gradient gel (4-12%) and proteins were stained with Coomassie blue staining. Bands indicating SAGA subunits are indicated by its molecular weight following its mass spectrometry (lower panel).

Ubp8-TAP mog1 Δ		
Protein	**Cov (95%)**	**SAGA module**
SGF73	35	DUBm
SUS1	17	
SGF11	5	
UBP8	2	
TAF12	22	TAFm
TAF10	10	
TAF5	9	
TAF6	7	
TAF9	5	
SGF29	9	HATm
ADA2	5	
GCN5	1	
SPT7	10	SPTm
SPT20	10	
ADA1	4	
SPT3	4	
TRA1	3	

Table 3. LC-MS/MS analysis of Ubp8-TAP *mog1Δ* purification. The table contains the name of the proteins, corresponding to each protein and the number of peptide coverage (95 %) which reflects the percentage of matching amino acids from identified peptides with a confidence greater or equal to 95 % divided by the total number of amino acids in the sample.

Mog1 does not affect the localization of the DUB module and Ubp8 recruitment to actively transcribed genes

The DUBm as being part of the SAGA complex is preferentially localized in the nucleus where it plays an important role during different stages of transcription. Since Mog1 is a factor required for protein transport, it could be possible that the differences observed in H2Bub[1] levels in absence of Mog1 are due to a defect in DUBm nucleocytoplasmic transport. To exclude this possibility, Ubp8, Sus1 and Sgf11 were GFP-tagged in a WT and *mog1Δ* strains to monitor the localization of these

proteins in the absence of *MOG1*. Our data indicates that DUBm components preserve their intranuclear localization in the absence of *MOG1* when compared to WT (**Figure 20**). Our results show that Mog1 is not implicated in the transport of the DUBm.

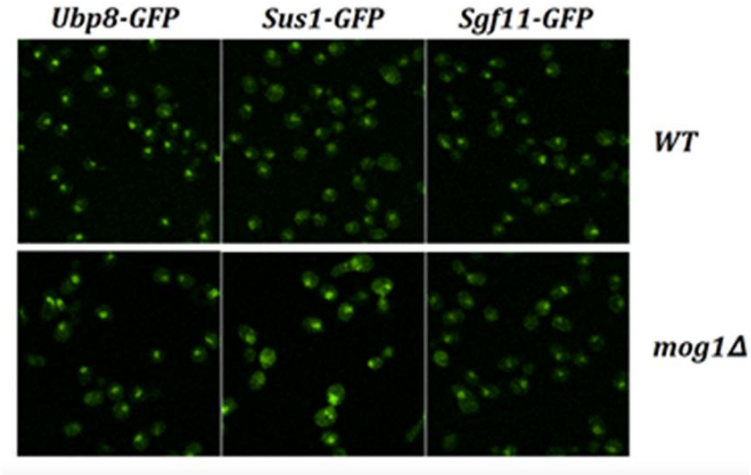

Figure 20. Localization of tagged GFP-DUBm components was analysed by fluorescence microscopy. Ubp8, Sus1 and Sgf11 were tagged with GFP in WT strain (upper panel) and in the absence of *MOG1* (lower panel) indicating that the absence of *MOG1* preserves the nuclear localization of the tested proteins.

Ubp8 has been shown to bind chromatin and this binding is supposed to be very dynamic (Bonnet et al., 2014; Daniel et al., 2004; Henry et al., 2003; Lee et al., 2005). Another way to explain the differences in H2Bub^{1} levels in WT and *mog1Δ* is by altering the dynamics of Ubp8 recruitment to chromatin. To test whether Mog1 could be affecting the association/dissociation of Ubp8 into chromatin, Ubp8 was TAP-tagged in a WT strain and in *mog1Δ* cells and subjected to Chromatin Immunoprecipitation (ChIP) followed by qPCR. The recruitment of Ubp8 to

the promoter and 5´ORF of three active transcribed genes; *ADH1*, *PMA1* and *YEF3* was analysed. Our data demonstrates that Mog1 is not affecting the recruitment of Ubp8, at least to the studied genes (**Figure 21**, upper panel). Additionally, Western blot analysis reveals that Ubp8 protein levels are maintained upon loss of *MOG1* (**Figure 21**, lower panel). Although we cannot exclude that Ubp8 activity is affected by *MOG1* deletion once bound to chromatin, our results suggest that Mog1 is affecting to the activity of other subunits implicated in the ubiquitination of histone H2B that causes decrease levels of H2Bub[1].

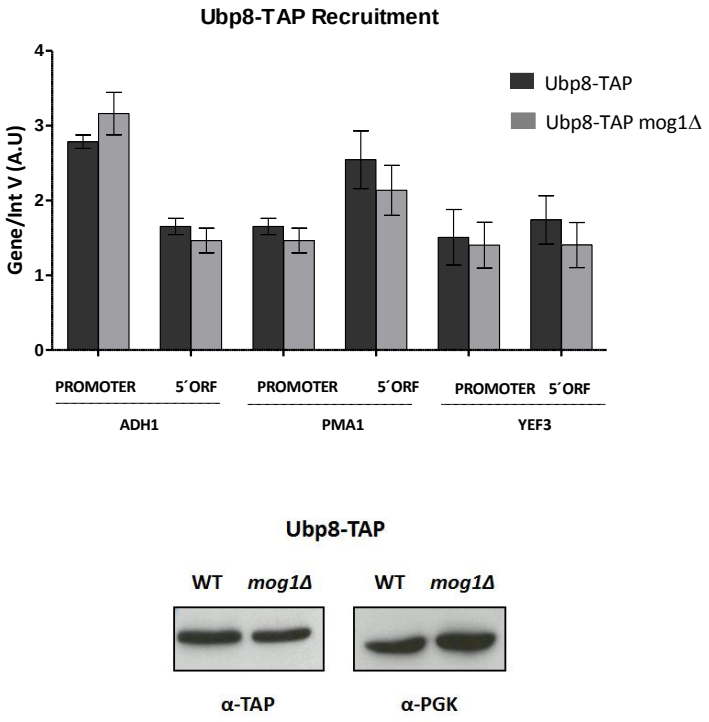

Figure 21. Mog1 preserves Ubp8 association to *ADH1*, *PMA1* and *YEF3* genes. Ubp8-TAP and Ubp8-TAP *mog1Δ* were subjected to ChIP and qPCR. The occupancy levels were calculated as the signal ratio of the IP samples in relation to the Input signal and normalized to an Intergenic region

(Chromosome V). Histograms indicate the mean and standard deviation for at least three independent experiments (upper panel). The Input level of Ubp8-TAP and Ubp8-TAP *mog1Δ* protein was detected from the inputs by Western blot using anti-TAP and anti-PGK antibody (lower panel).

Chromatin recruitment of Rad6 is decreased in *mog1Δ* cells

Different lysine modifications are placed on histones as the RNA Pol II travels along gene coding regions. These modifications are mainly associated with nucleosome dynamics and elongating forms of RNA Pol II (Fleming et al., 2008; Kouzarides, 2007). For instance, an example of active transcription occurs when histone H2B is monoubiquitinated (Osley, 2006). This histone H2B monoubiquitination implies the recruitment of the ubiquitin enzyme Rad6 and the ubiquitin ligase Bre1 into chromatin (Henry et al., 2003; Robzyk et al., 2000; Xiao et al., 2005). Because deletion of *MOG1* results in the reduction of H2Bub^{1}, we aimed to determine whether the association of the E2 ubiquitin conjugase that catalyses H2Bub^{1}, Rad6, to chromatin was altered in *mog1*Δ cells. To achieve this, we used chromatin Immunoprecipitation (ChIP) to determine the association of this subunit to the promoter and gene body of three highly transcribed constitutive genes *PMA1*, *ADH1* and *YEF3*. Rad6 was TAP-tagged and subjected to ChIP. Our results indicate that Mog1 affects the association of Rad6 specifically the 5´ORF of *PMA1*, *ADH1* and *YEF3* genes suggesting that Mog1 may regulate the binding of this protein to chromatin likely during elongation. Additionally, our Western blot analysis indicates that levels of TAP-tagged Rad6 are unaffected upon loss of *MOG1* (**Figure 22**).

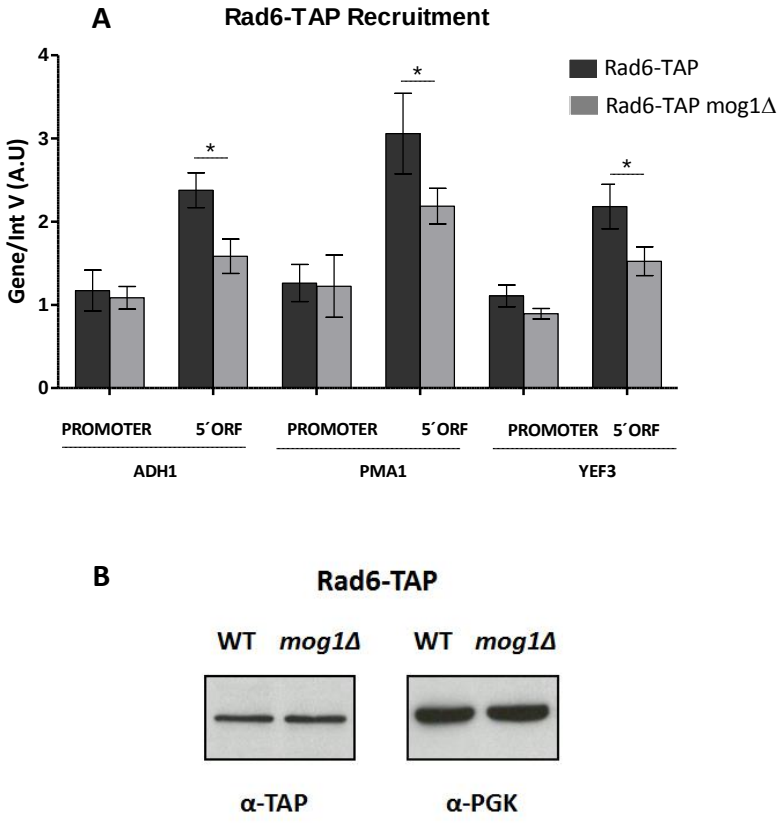

Figure 22. Mog1 affects the association of Rad6-TAP at coding regions. A) Mog1 affects the recruitment of the ubiquitinase Rad6 to the 5´ORF of *PMA1*, *ADH1* and *YEF3* genes. B) Inputs were subjected to Western Blot analysis against anti-TAP and anti-PGK (loading control) antibodies to monitor protein levels. Histograms indicate the mean and standard deviation for at least three independent experiments. Significance of the differences was obtained by the Student´s t-test (*P value = 0.01–0.05; **P value = 0.001–0.01; ***P value < 0.001).

Mog1 interacts genetically with the methyltransferases and affects H3K4me^3 levels

Several groups have demonstrated that monoubiquitination of histone H2B is required for histone H3K4me^3 by COMPASS complex through a so-called "cross-talk" modification pathway (Dover et al., 2002; Henry and Berger, 2002; Lee et al., 2007; Sun and Allis, 2002; Vitaliano-Prunier et al., 2008). Indeed, when the cell presents an absence of H2Bub^1, H3K4me^3 levels are no longer detectable (Shahbazian et al., 2005b). As it has been reported, H3K4me^3 is a hallmark for active transcription and studies have correlated active transcription with the existence of H3K4me^3 at transcriptional start sites (Barski et al., 2007).

In order to link *mog1Δ* phenotype of low H2Bub^1 with histone H3 methylation, we analysed the genetic interaction between *MOG1* and the methyltransferases subunits *SET1*, *SET2* and *DOT1* which are implicated in the methylation of histone H3 at its lysines K4, K36 and K79, respectively (Kim et al., 2013; Krogan et al., 2003a; van Leeuwen et al., 2002; Nguyen and Zhang, 2011). Our cell growth assay shows that *MOG1* interacts genetically with *SET2* mutant in both YPD and YPGal, however, the interation between MOG1 and *SET1* and *DOT1* is more determinant in YPGal containing medium (**Figure 23**).

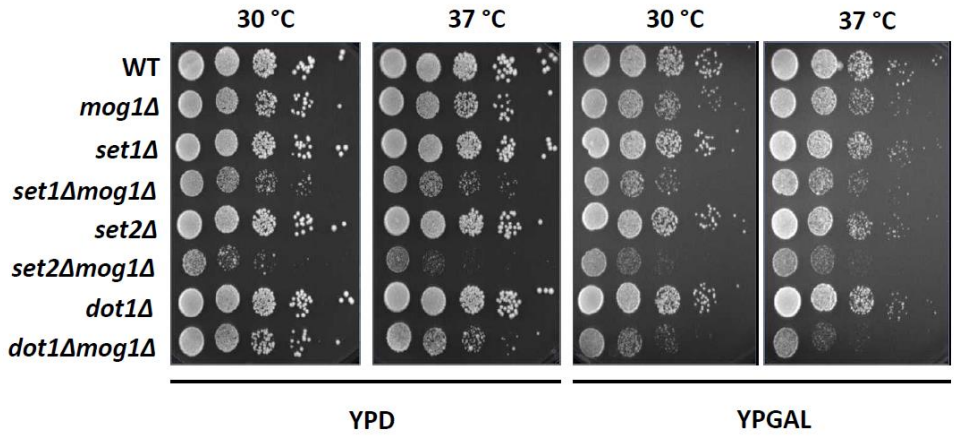

Figure 23. *MOG1* interacts genetically with the H3 methyltransferases *SET1*, *SET2* and *DOT1*. Cells were diluted in 10^{-1} steps, and equivalent amount of cells were spotted onto YP+Glu (YPD) and YP+Gal (YPGal) plates. Cells were grown for 48 hours at 30 °C and 37 °C.

In line with our results regarding the lower levels detected of H2Bub^{1} in *mog1Δ* cells, we asked whether this reduction could also be reflected in the trimethylation levels of H3K4, thus, linking Mog1 with the H2Bub^{1}-H3K4me^{3} histone cross-talk. To test this possibility, we performed Western blot analyses to detect H3K4me^{3} from total extracts obtained from WT*, mog1Δ*, *set1Δ* and *spp1Δ* strains, since Set1 and Spp1 are both components of the COMPASS complex and its deletion is linked to reduced levels of H3K4me^{3} (Ramakrishnan et al., 2016; Schneider et al., 2005). As shown in **Figure 24**, absence of *MOG1* leads to a significant decrease in H3K4me^{3} levels compared to WT cells. As predicted, lack of *SPP1* and *SET1* follows the expected pattern, reducing H3K4me^{3} levels. Total levels of H3

were used as control, where unmodified H3 levels were determined for all strains. Our results point towards a new possible role of Mog1 in the H2Bub^{1}-H3K4me^{3} histone cross-talk since deletion of *MOG1* affects both H2Bub^{1} and H3K4me^{3}.

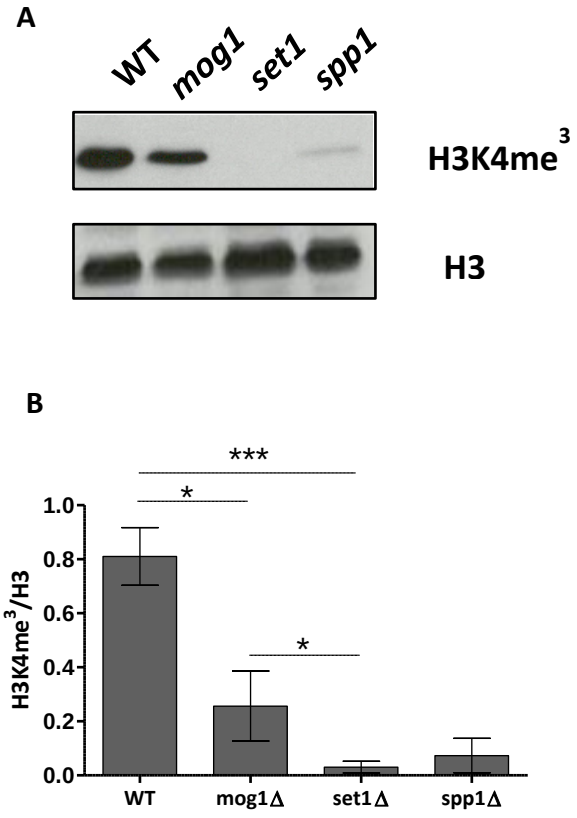

Figure 24. Mog1 promotes H3K4me^{3}. A) Expression levels of total extracts from WT, mog1Δ, set1Δ and spp1Δ were analysed by Western blot using H3K4me^{3} and H3 antibodies. B) Representative graph of H3K4me^{3} levels after H3 normalization show the mean and standard deviations of at least three independent experiments. P-value was calculated using Student´s t-test (*P = 0.01–0.05; **P = 0.001–0.01; ***P < 0.001).

Set1 recruitment to chromatin is decreased in absence of *MOG1*

As presented in the introduction, H2Bub[1] on lysine K123 in yeast mediates a trans-histone regulatory pathway that leads to di- and trimethylation of histone H3 at its lysine 4 and 79 (Dover et al., 2002; Sun and Allis, 2002). H3K4me has been associated with active transcription and requires the recruitment to chromatin of the methyltransferase Set1 found in the COMPASS complex (Miller et al., 2001; Shilatifard, 2006). Due to the decreased levels of H3K4me^3 found in *mog1Δ* cells, we tested whether this fact could be linked with a poor recruitment of Set1 into chromatin. We tested its association with the promoter and gene body of *PMA1*, *ADH1* and *YEF3* genes. Our ChIP experiments show that Set1 recruitment is dramatically decreased in the absence of *MOG1*, however, Set1 protein levels are unaffected in cells lacking *MOG1* (**Figure 25**). Notably, the strongest effect of *MOG1* deletion on Set1 recruitment is observed at coding regions. This observation indicates that Mog1 may also be affecting the methyltransferase activity of Set1 which is manifested with low levels of H3K4me^3.

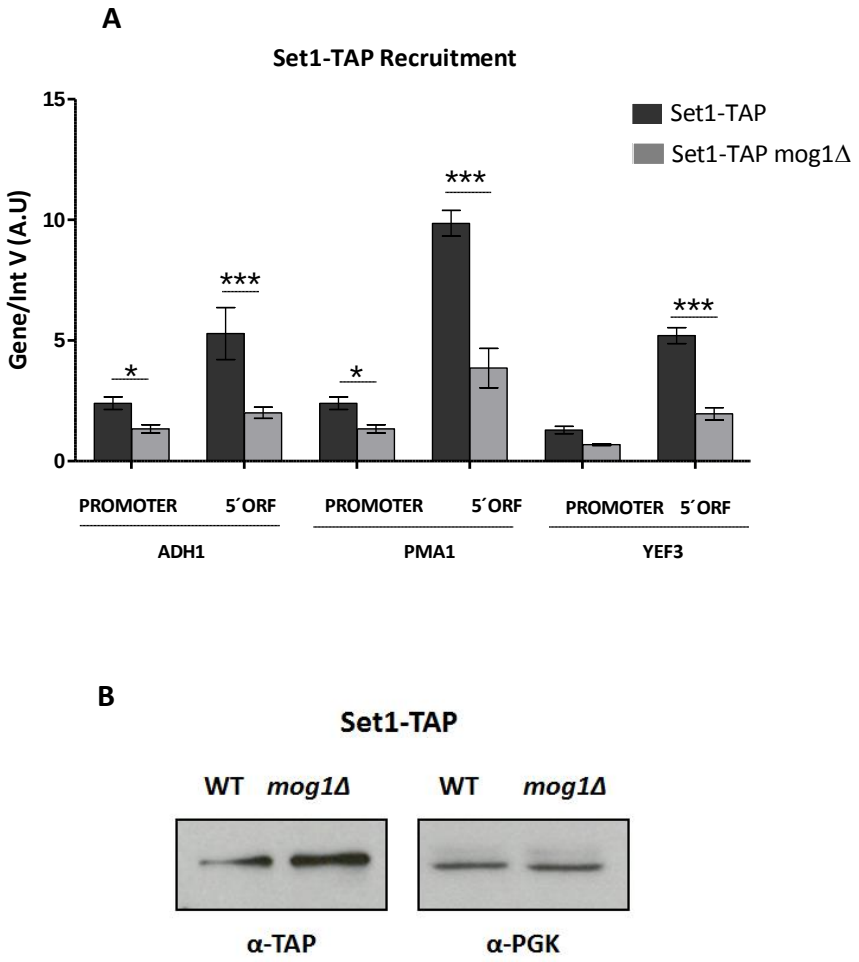

Figure 25. Set1-TAP recruitment to *PMA1*, *ADH1* and *YEF3* genes is affected upon loss of *MOG1*. A) ChIP experiments of Set1-TAP tagged strains reveal that Set1 association to the promoter and 5´ORF of the studied genes is affected in cells lacking *MOG1*. B) Inputs were subjected to Western Blot analysis against anti-TAP and anti-PGK (loading control) antibodies to monitor protein levels. Histograms indicate the mean and standard deviation for at least three independent experiments. Significance of the differences was obtained by the Student´s t-test and presented as P-values (*P = 0.01–0.05; **P = 0.001–0.01; ***P < 0.001).

Mog1 associates with active genes

As it has been postulated, the recruitment of several factors into chromatin is associated with active genes transcribed by RNA Pol II (Bannister and Kouzarides, 2011). To support the role of Mog1 in chromatin modifications, we also determined Mog1-HA recruitment by ChIP and qPCR to the actively transcribed *PMA1* and *YEF3* genes. As indicated in **Figure 26**, our results reveal that Mog1 can bind to the 5´ORF of the highly transcribed *PMA1* and *YEF3* compared to the WT strain (No Tag).

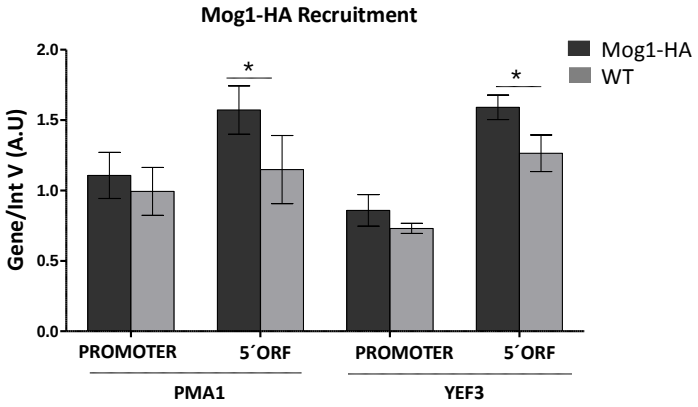

Figure 26. Mog1-HA is recruited to the 5´region of actively transcribed genes. Mog1 was HA-tagged and subjected to ChIP assay using HA antibody. The occupancy levels was calculated as the signal ratio of the IP samples in relation to the Input signal and normalized to an Intergenic region. Statistical analysis was obtained by the Student´s t-test and presented as a P-value (*P<0.05).

Our data indicates that Mog1 is significantly enriched only at the 5´ORF compared to an untagged strain. However, the absolute fold enrichment value is low. This is compatible with a transient interaction between Mog1 and coding regions and also with Mog1's role in protein transport.

Genome-wide analysis links *MOG1* absence with decreased levels of transcription and mRNA concentration.

Our previous results suggest that Mog1 could be playing a role in transcription regulation and in downstream steps such as mRNA export. Thus, we decided to explore on a genomic scale the effects on transcription and mRNA levels in cells lacking *MOG1*. In collaboration with Dr. José Enrique Pérez laboratory from University of Valencia, we used the GRO technique (García-Martínez et al., 2004, 2011) which allows the measurement of the TRs (Transcription rate) for all yeast ORFs, mRNA levels (RA) and mRNA stability (RS) by the use of nylon microarrays and *in vivo* radioactive labeling of nascent RNA when cells are in an exponential phase. As explained in the materials and methods section, this method is divided into two different steps, on one hand, an aliquot taken from a cell culture allows calculating the density of elongating RNA polymerases along the entire gene, while another aliquot from the same cell culture provides information about mRNA amounts using the same DNA ChIP.

Indeed, this method allows the calculation of mRNA stability (RS) for each gene which is obtained by dividing mRNA amount by TR for every gene when considering steady-state mRNA levels. This implies that the mRNA amount does not change, it keeps constant, because the rate of synthesis equals the rate of degradation (Pérez-Ortín et al., 2007).

As a first step, we measured with the use of a cell counter Coulter, the cell volume of both WT and *mog1Δ* mutant. This step is required to normalize

nascent transcription (nTR) from each strain according to its cellular volume (Pérez-Ortín et al., 2013). This normalization will allow obtaining the SR rate (mRNA synthesis rate). The obtained cell volumes for WT and *mog1Δ* strains were 0.02 and 0.019, respectively.

To obtain the nTR, we first generated three different types of *in vitro*-synthesized RNAs transcripts using control probes from Bacillus (*pGIBs-Thr, pGIBs-Phe, pGIBs-Lys,* from now on called p-GIBs) which will be later used to normalize the DPM signals corresponding to each gene (please see methods section). In parallel, cells were collected and permeabilized with sarkosil for its later *in vivo* transcription adding [α-^{33}P] rUTP. Before RNA isolation, 3 µl of the *in vitro*-synthesized RNAs transcripts were added to each sample and subsequently we performed the described protocol. Lastly, we measured with the scintillation counter the incorporated radioactivity which is proportional to the amount of elongating RNA polymerases. As shown in the graph (**Figure 27**) mutant *mog1Δ* incorporates lower levels of radioactivity suggesting that lower levels of elongating forms of RNA polymerases are actively transcribing.

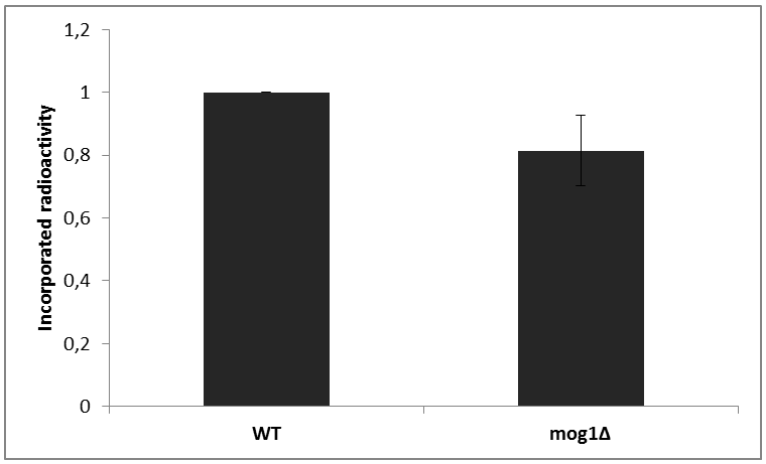

Figure 27. Incorporated radioactivity during GRO reaction. Bars representing the median of three independent experiments indicate the total radioactivity incorporated during the genomic run-on process relative to the wild-type strain. Errors bars represent the standard deviation showing no significant differences.

Taking the GRO signals from each gene, we obtained the nTR (production of new mRNA molecules) by correcting every signal with the p-GIBs values. As mentioned in the introduction, the term TR reflects two different parameters, on one hand, the nTR measures the *in situ* RNA polymerases transcriptional activity and, on the other, the SR (mRNA synthesis rate) measures the contribution of transcription to the cellular mRNA concentration. To obtain the SR, we corrected the nTR data considering the total cellular volume of each strain. Taking into account our previous explanation, we determined the SR of *mog1Δ* strain using the median of all ORFs with the use of the statistical package R. Boxplots diagrams

represent the SR for each of the three conditions tested; the value assigned to each boxplot indicates the median relative to the WT strain (BY4741) (**Figure 28**). First, we focused into the total genes; our data indicates that there exists a decreased in the synthesis of mature RNA compared to the WT strain. Our second approach was to validate if absence of *MOG1* affected SAGA-dominated genes due to the link we previously found between Mog1 and the DUBm from SAGA complex. Our analysis demonstrates a decrease in SAGA-dominated genes, however, this fact is not significant compared to the TFIID-dominated genes. This data suggests that Mog1 may be acting as a general factor in transcription.

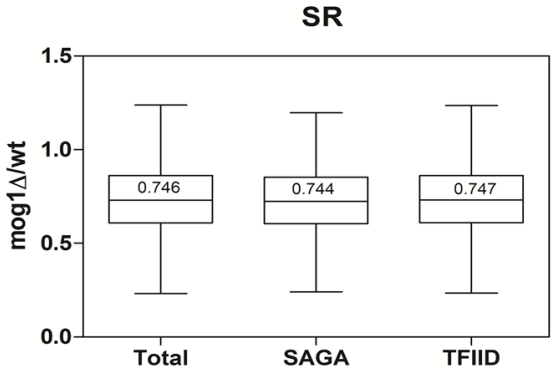

Figure 28. Boxplots diagrams representing the SR of *mog1Δ* relative to a BY4741 strain. Each boxplot contains the median for the three groups of genes tested. Error bars represent the standard deviation.

As mentioned before, a second aliquot was taken from both WT and *mog1Δ* cell cultures to determine the concentration of mRNA for each condition. This value was adjusted by the concentration of polyadenylated

RNA explained in the methods section. In this line, a dot-blot procedure was used to estimate the proportion of poly $(A)^+$ mRNA in the total RNA and used this datum to normalize the different hybridizations of cDNAs.

As shown in **Figure 29**, the concentration of mRNA in *mog1Δ* relative to the WT strain is lower for the total genes, SAGA and TFIID-dominated genes. Hence, this result suggests that in mutant *mog1Δ* there exists a general decrease in mRNA concentration consistent with the lower SR previously observed.

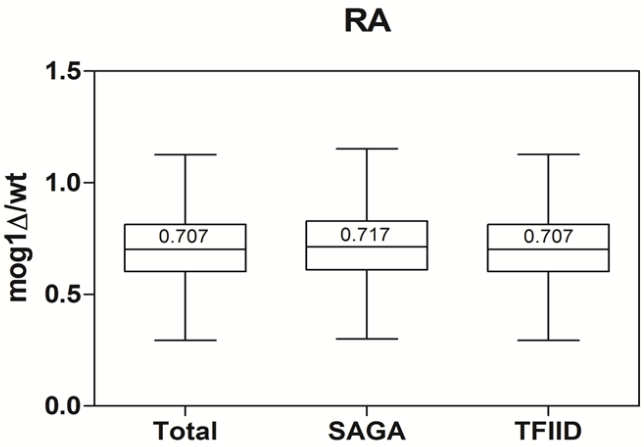

Figure 29. Boxplots diagrams representing the RA of *mog1Δ* relative to a BY4741 strain. Each boxplot contains the median for the three group of genes tested. Error bars represent the standard deviation.

From the SR and RA data one would predict that transcription is affected at early steps leading to a low concentration of most transcripts. To verify that stability is not the main way to regulate mRNA concentration in *mog1Δ*, we also calculated RS. As it was previously mentioned, assuming a

steady-state level, it is possible to predict the RS (mRNA stability) by the formula RS=RA/SR using the previous data. **Figure 30** illustrates by a boxplot diagram the RS for each of the three conditions tested (total genes, SAGA and TFIID-dominated genes); the value assigned to each boxplot indicates the median relative to the WT strain (BY4741). Assuming that the synthesis and degradation rate are equivalent, the RS may compensate the changes in transcription and mRNA concentration. In our case, *mog1Δ* mutant presents a decreased in the synthesis rate (SR) as well as in mRNA concentration (RA) (**Figure 28** and **29**), therefore, the RS is maintained compared to the WT strain (**Figure 30**).

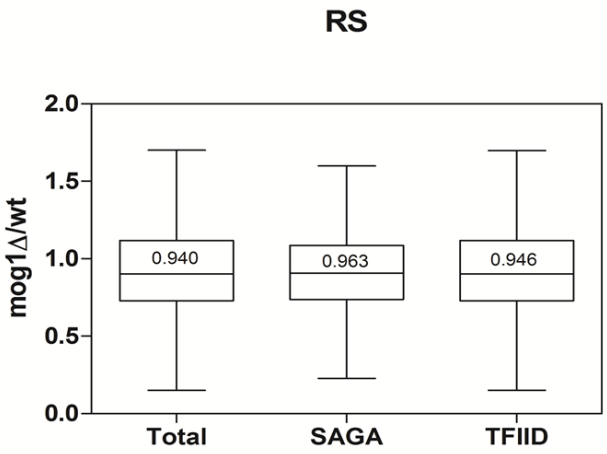

Figure 30. Boxplots diagrams representing the RS of *mog1Δ* relative to a BY4741 strain. Each boxplot contains the median for the three group of genes tested. Error bars represent the standard deviation.

To get further insight into the behaviour of transcription and mRNA decay in *mog1Δ*, we analysed the distribution of SR, RA and RS and differentiate the set of genes between up and down-regulated genes. Taking into account all the genes tested, we obtained two major representations; genes down-regulated (fold change mutant/WT < 0.58) and up-regulated (fold change >1.7) for all the conditions tested (SR, RA and RS) (**Table 4**). As shown in the table, most of the genes are down-regulated for both SR and RA, however, our data indicates that the RS is not affected since genes up (315) and down-regulated (374) are considered to be equally distributed. If we compare the genes that show < 0.58 fold-change compared to WT for both SR and RA, we only observe overlapping in 197 genes (**Figure 31**). This set is not enriched in any GO using the web tool Funcassociate 3.0 (http://llama.mshri.on.ca/funcassociate/). Moreover, when we studied the distribution of SAGA and TFIID-dominated genes among the three set of genes obtained by the Venn diagram (Table 5, SR=640, RA=670 and common=197) no differences in SAGA or TFIID-regulated genes is observed since the proportion of SAGA-regulated genes represents the expected percentage in the genome (10 %). From this data, we can first conclude that neither SR nor RA affect specifically SAGA or TFIID-dependent genes suggesting that Mog1 could present a global effect in transcription.

Fold change	SR	RA	RS
Down-regulated <0.58	844	874	374
Up-regulated >1.7	83	12	315

Table 4. Distribution of down and up-regulated genes between SR, RA and RS. Arbitrary values were taken for gene distribution; Down-regulated genes were considered with levels lower than 0.58 fold change while up-regulated with levels higher than 1.7 fold change.

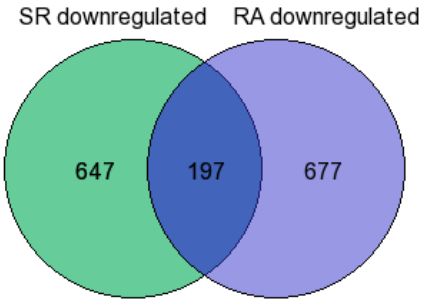

Figure 31. Venn diagram representing SR and RA down-regulated data.

	SAGA-dominated	TFIID-dominated
SR	63	637
RA	55	670
SR/RA	17	191

Table 5. SAGA and TFIID- dominated genes distribution among SR, RA and SR/RA overlapping genes.

As represented in **Figure 31**, only 197 genes present both low SR and RA, so it is expected that the other genes that are affected by SR or RA would show difference in their stability. To analyse these possibilities, we tested the non-overlapping set of genes among the down-regulated RA and SR which presumably would present differences in their stability. To do so, we first compared the unique SR (647) and RA (677) with the genes that show downregulated RS through a Venn diagram (**Figure 32**) (http://genevenn.sourceforge.net/). This analysis demonstrates that most genes that show down RS leads to down RA, while no overlapping exists among SR and RS down-regulated genes meaning that these genes do not present instability. Nevertheless, the comparison between RA and RS demonstrates that 208 genes present instability which probes that lower levels of RA with no affected SR have an impact on the RS (**Figure 32. A**). This scenario is also reproduced when we compared SR and RA down-regulated genes versus RS up-regulated genes (**Figure 32.B**). In this case, 262 genes overlap between SR and RS with no overlapping among RA and RS, which indicates that lower levels of transcription and equal levels of RA lead to increase RS having an impact on the stability.

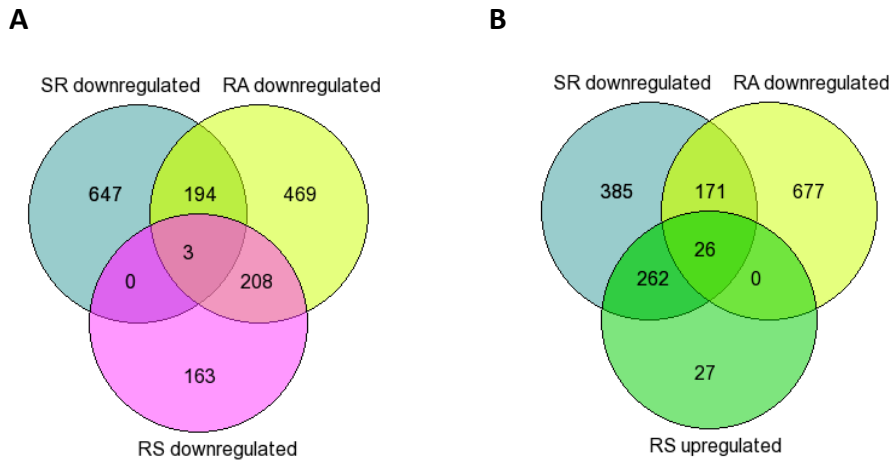

Figure 32. Venn diagram representation of SR, RA and RS genes. A) Comparison between SR, RA and RS down-regulated genes. B) Comparison between SR and RA down-regulated with RS up-regulated genes.

Overall, our data demonstrate that mutant *mog1Δ* leads to a decrease in global transcription and mRNA concentration with no major impact on stability and that it is required for maintaining the correct epigenetic environment necessary to establish the appropriated transcriptional rate during gene expression. Indeed, no differences between TFIID and SAGA-dominated genes are found in *mog1Δ* suggesting that Mog1 may act through the whole genome.

Mog1 interacts genetically with TREX-2 components and it is involved in mRNA export

As it has been previously introduced, TREX-2 facilitates mRNA export by its association with the nuclear pore complex (NPC). In this line, it has been established that proteins involved in early steps of gene expression interact with the NPC, the export machinery and factors involved in mRNA biogenesis which play a role in chromatin dynamics (Rodríguez-Navarro and Hurt, 2011). The interaction among TREX-2 complex and SAGA regulates gene recruitment to the NPC after transcription activation to facilitate transcription processivity (Cabal et al., 2006; Pascual-García et al., 2008). The connection among TREX-2 and SAGA is a clear example of transcription coupled to mRNA export which is fundamental for the process of mRNA biogenesis.

The epigenetic cross-talk H2Bub^{1}-H3K4me^{3} has been linked to the COMPASS subunit Swd2 (Vitaliano-Prunier et al., 2008) and it has been found that Swd2 plays an important role in coordinating this cross-talk with mRNA processing by recruiting the export factors Mex67 and Yra1 to the mRNP (Vitaliano-Prunier et al., 2012). Furthermore, in our lab we demonstrated a role for Sus1 in coordinating H2Bub^{1} with mRNA export (Köhler et al., 2006; Pascual-García and Rodríguez-Navarro, 2009a; Pascual-García et al., 2008), and in this thesis we found new functional links between Sus1 and Mog1. So, it is possible that Mog1 participates in multiple steps during the gene expression process as part of these orchestrated mechanisms. To get insights into this possibility, we first

studied *mog1Δ* genetic interaction with TREX-2 subunits. To achieve this, we created double mutants bearing *MOG1* and TREX-2 subunits deletion and carried out cell growth assay. As shown in **Figure 33**, *MOG1* interacts genetically with *THP1* and *SEM1* as the double mutants present growth impairment compared to its single deletions. This phenotype is observed at both 30 °C and 37 °C with more severe growth impairment in YPGal plates. This result points towards a mechanism in which Mog1 could be implicated in the same biological process as TREX-2 subunits.

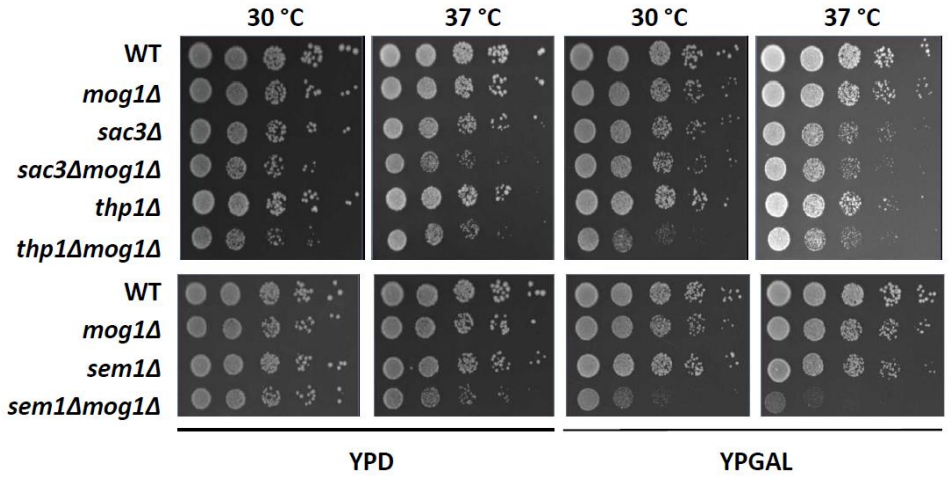

Figure 33. Mog1 interacts genetically with TREX-2 subunits. Double disruption strains *sac3Δmog1Δ*, *thp1Δmog1Δ* and *sem1Δmog1Δ* exhibits growth impairment. Cells were diluted in 10^{-1} steps and the same amount of cells was spotted onto YPD or YPGal plates. Cells were grown for 48 hours at 30 °C and 37 °C.

Based on this genetic interaction between *MOG1* and some subunits of TREX-2 and that past work has demonstrated that *MOG1* mutation causes nuclear accumulation of poly $(A)^+$ RNA in *S. pombe* (Oki et al., 2007; Tatebayashi et al., 2001) we decided to explore the possible implication of

Mog1 in mRNA export. Previous studies showed no nuclear accumulation of mRNA in *S. cerevisiae* (Oki and Nishimoto, 1998) at 37 °C, however we tested the localization of poly $(A)^+$ RNA by *in situ* hybridization using Cy3 labeled oligo (dT) probes in WT, *mog1Δ* and *sus1Δ* (positive control) at 30 °C and after 2 h incubation at 39 °C, since higher incubation temperature has been reported to amplify mRNA export defects (Gwizdek et al., 2006; Iglesias et al., 2010). Analysis of nuclear mRNA export shows an mRNA export defect in *mog1Δ* cells at 39 °C compared to WT control; however the % of cells showing mRNA export block is clearly lower than for *sus1Δ* (**Figure 34**). As previously reported, mutant *sus1Δ* presents mRNA export defect (Rodríguez-Navarro et al., 2004) in both conditions. In all, our data indicate that *mog1Δ* mutant present mRNA export defect under certain conditions, thus, we propose that Mog1 might be implicated in coordinating different steps of the gene expression pathways from $H2Bub^1$ to mRNA export.

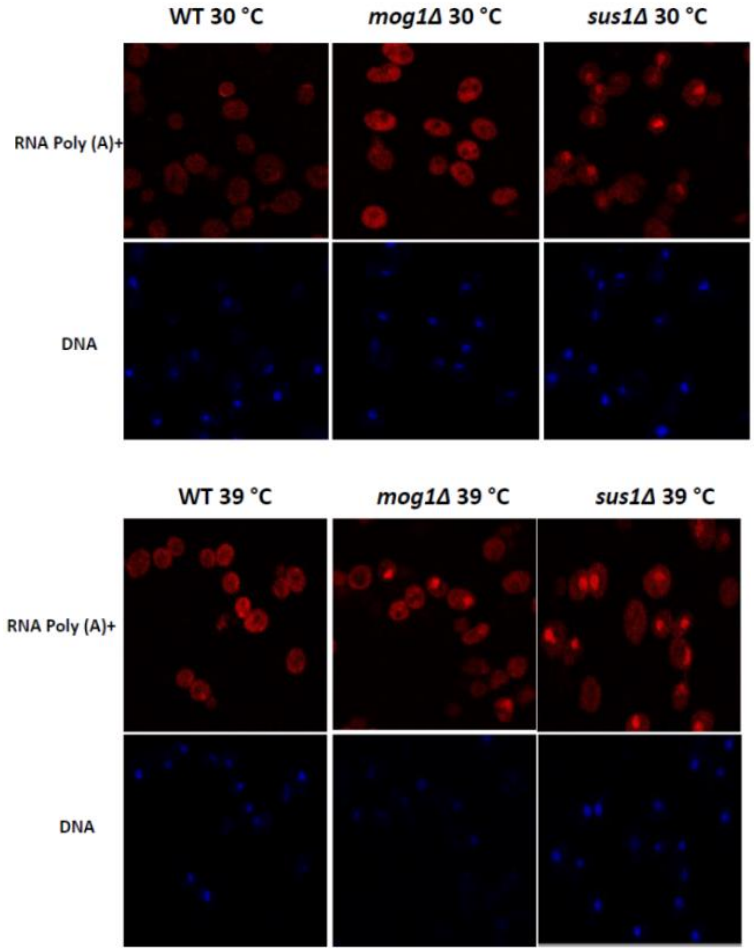

Figure 34. *mog1Δ* cells exhibit impaired mRNA export. WT, *mog1Δ* and *sus1Δ* mRNA export was assessed by in situ hybridization after shifting from 30 °C (upper panel) and at 39 °C for 2 hours (lower panel).

Levels of Swd2 are reduced in absence of *MOG1*

As mentioned earlier, Swd2 (also known as Cps35) is a COMPASS subunit involved in coordinating H2Bub^{1}-H3K4me^{3} cross-talk and downstream events such as recruitment of Mex67 and Yra1 to the nascent mRNP (Vitaliano-Prunier et al., 2008, 2012). For instance, it has been established that di- and trimethylation of H3K4 depend on monoubiquitination of histone H2B which is achieved by Rad6 and Bre1 catalytic activity (Dehé et al., 2005; Dover et al., 2002; Robzyk et al., 2000; Sun and Allis, 2002; Wood et al., 2003b). Indeed, the monoubiquitination of histone H2B promotes the ubiquitination of Swd2 subunit having an impact on the H3K4 di- and trimethylation thus participating in the cross-talk among H2Bub^{1} and H3K4me^{3} (Vitaliano-Prunier et al., 2008). Due to the results previously shown in this thesis likely connecting Mog1 with histone cross-talk we asked whether this protein could affect the role of Swd2 in this coordination. To achieve this purpose, we decided to investigate whether Mog1 is necessary for Swd2 chromatin recruitment by ChIP followed by qPCR to the promoter and 5'ORF of *PMA1*, *ADH1* and *YEF3* genes (**Figure 35. A**). Our data demonstrates that Swd2 association to the coding regions of *PMA1* and *ADH1* genes is decreased in the absence of *MOG1*.

Notably, specifically for Swd2 we observe a reproducible reduction in the levels of the protein which points to a role of Mog1 in regulating Swd2 stability, therefore having a direct impact in H2Bub^{1} and H3K4me^{3} histone crosstalk with mRNP biogenesis (**Figure 35. B**)

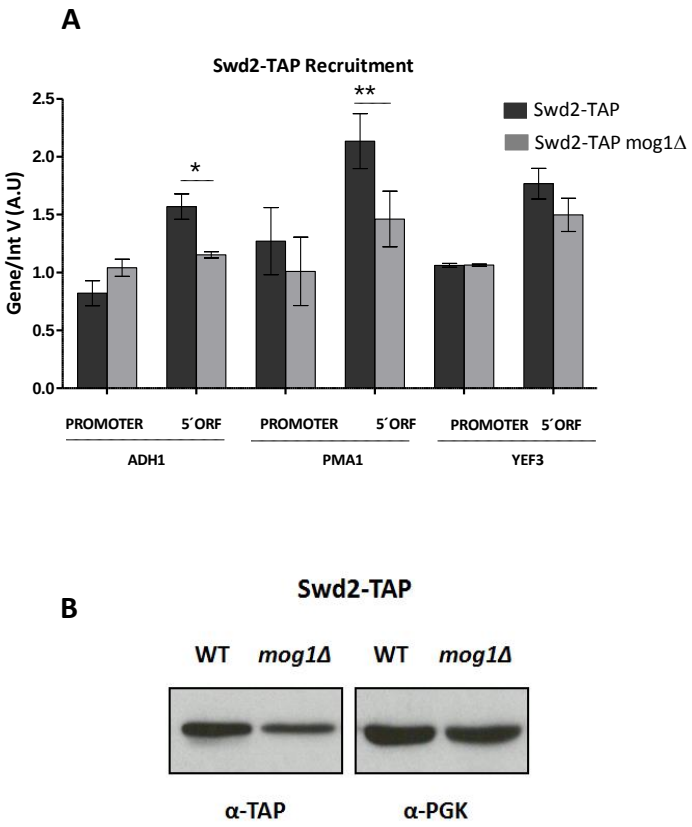

Figure 35. Swd2-TAP association to chromatin is affected in *mog1Δ* cells. A) ChIP and qPCR analysis using specific primers for *PMA1*, *ADH1* and *YEF3* promoter and 5´ORF genes show that Swd2-TAP recruitment is decreased in cells lacking *MOG1*. The occupancy levels was estimated as the signal ratio of the IP samples in relation to the Input signal and normalized to the Intergenic region of chromosome V. Statistical analysis was obtained by the Student´s t-test and presented as a P-value (*P = 0.01–0.05; **P = 0.001–0.01). At least three independent experiments were used to normalize the samples. B) Inputs were subjected to Western blot against anti-TAP and anti-PGK (loading control).

Mog1 co-purifies with components of the transcription machinery

Mog1 has been described so far as a nuclear protein that interacts with GTP-Gsp1 protein and stimulates nucleotide release from Gsp1, thus, its

main function resides in nuclear protein import (Baker et al., 2001; Steggerda and Paschal, 2000). Information found in BIOGRID database (www.thebiogrid.org) indicates that Mog1 presents 185 interactors (physical and genetic), among them, several nucleoporines and Ran GTPases have been identified. To gain insight into Mog1 protein interactions we used the TAP tag to purify Mog1-containing complexes and performed mass spectrometry analysis (LC-MS/MS) on the purification product. The presence of Mog1 was confirmed by Western blot which indicates that Mog1 was detected along the entire process (**Figure 36**).

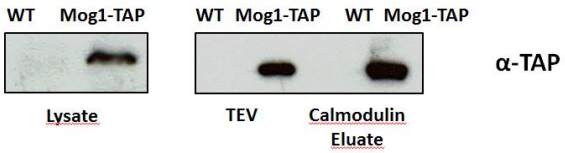

Figure 36. Mog1-TAP and no-tag (WT) purification. Mog1 protein was confirmed by Western blot against anti-TAP antibody during the three steps of the purification: Lysate (before purification), TEV eluate (following first purification) and Calmodulin eluate (second purification).

Our mass spectrometry results confirm that Mog1 co-purifies with the GTP-binding proteins Gsp1 and Gsp2 along with several nucleoporins (Nup60, Nup2 and Nsp1) as was previously predicted. Surprisingly, we were able to identify peptides for several components from the SAGA complex. Additionally, two subunits of the COMPASS (Set1C) complex, Shg1 and Sdc1, were also identified which could explain the relation among Mog1 and the methyltransferase function of COMPASS on histone H3. Indeed, some peptides for the ubiquitin ligase Bre1 were also

identified in the protein mixture of Mog1-interactors, suggesting that Mog1 and Bre1 might be also cooperating in the same process. Furthermore, we also detected a physical interaction among Mog1 protein and histones H2B, H3 and H4 which gives support to the interaction between Mog1, chromatin and some complexes involved in its modification (**Table 6**).

	Protein	% Cov (95)	Function/Complex
Mog1 partners	YRA1	70	RNA annealing protein YRA1
	MOG1	67	Nuclear import protein MOG1
	NUG1	48	Nuclear GTP-binding protein
	LSG1	45	Large subunit GTPase
	GSP1	27	GTP-binding nuclear protein GSP1/CNR1
	GSP2	19	GTP-binding nuclear protein GSP2
Histones	H4	54	Histone
	H2B1	47	Histone
	H3	37	Histone
SAGA	TAF10	45	SAGA/TFIID
	TAF9	22	SAGA/TFIID
	TAF4	16	TFIID
	TAF5	14	SAGA/TFIID
	TAF6	13	SAGA/TFIID
	TRA1	12	SAGA/TFIID
	TAF12	12	SAGA/TFIID
	SPT5	11	SAGA/TFIID
	SPT7	9	SAGA
	SPT20	6	SAGA
	ADA2	6	SAGA
	SGF73	5	SAGA
	SPT3	4	SAGA
	SGF29	3	SAGA
	GCN5	3	SAGA
NUPs	NUP60	33	Nucleoporin
	NUP2	27	Nucleoporin
	NSP1	7	Nucleoporin
COMPASS	SDC1	15	COMPASS
	SHG1	13	COMPASS
Rad6/Bre1/Lge1	SPT5	11	Transcription elongation factor
	BRE1	5	E3 ubiquitin-protein ligase

Table 6. LC-MS/MS analysis of Mog1 purification. The table contains the name of the proteins, the function/complex corresponding to each protein and the number of peptide coverage (95 %) which reflects the percentage of matching amino acids from identified peptides with a confidence greater or equal to 95 % divided by the total number of amino acids in the sample.

Interestingly, our results show that Mog1 co-purifies with the DUBm component Sgf73, however, Sus1, Ubp8 and Sgf11 were not detected. This observation is very interesting and might indicate that Mog1 could interact with a SAGA complex lacking the DUBm. This could be a way to regulate that the opposite effects on H2BK123 exhorted by Rad6 and Ubp8 are controlled thus ensuring correct timing for gene expression. To test whether Mog1 interacts with Sgf73 and not with the rest of the DUBm, we constructed Mog1-TAP Sgf73-HA Ubp8-PK, Sgf73-HA Ubp8-Pk and Ubp8-PK strains to immunoprecipitate Mog1 with the TAP antibody and analysed by Western blot the interaction with Sgf73 and Ubp8 (**Figure 37. A**). Additionally, we tested Mog1 interaction with other SAGA subunit, such as the HATm-containing protein Ada2 using the following strains: Mog1-TAP Ada2-HA Ubp8-PK, Ada2-HA Ubp8-Pk and Ubp8-PK (**Figure 37. B**). Our co-IPs experiments allowed the confirmation of Mog1 interaction with Sgf73 and Ada2. On the contrary, Mog1 was not able to co-purify with Ubp8 under the same conditions. Overall, our results demonstrates that Mog1 is able to co-purify with Sgf73 and Ada2, however, we were not able to detect protein Ubp8 suggesting that Mog1 could function as a modulator of histone H2B deubiquitination by impeding the binding of an active DUBm with SAGA complex.

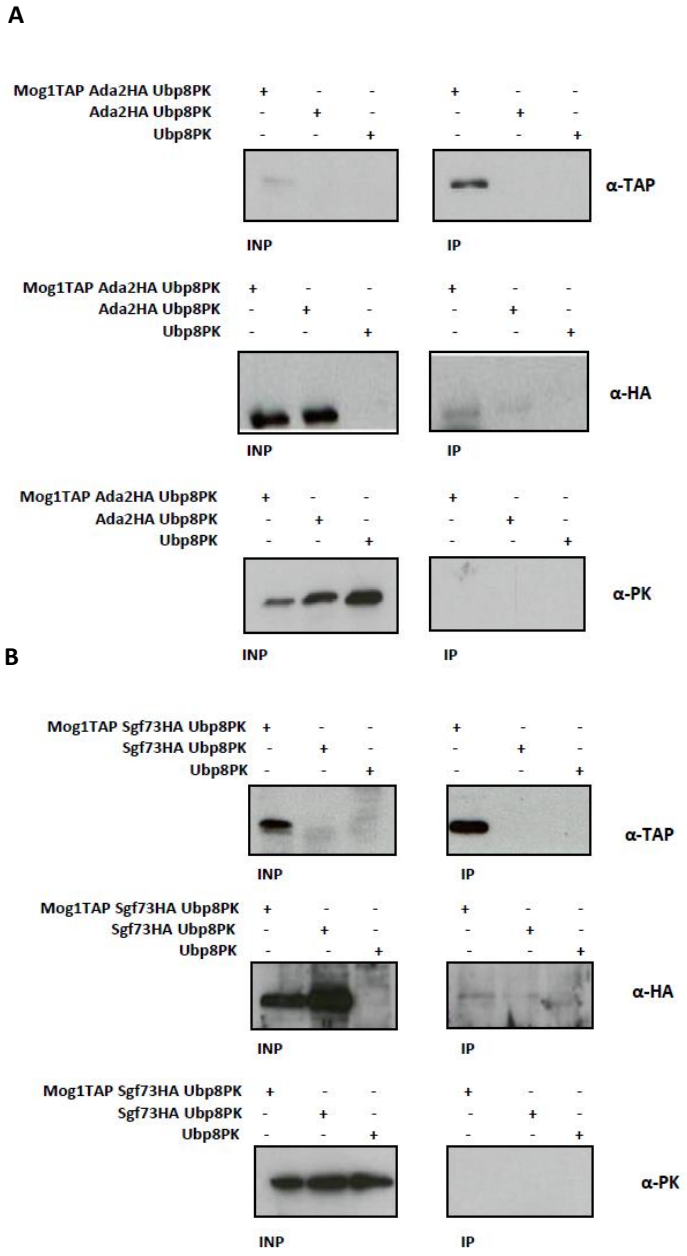

Figure 37. Mog1-TAP interacts with components from SAGA complex. Mog1-TAP was subjected to immunoprecipitation (IP) using anti-TAP antibody to monitor its interaction with Ada2-HA (A) and Sgf73-HA (B) using anti-HA. In both cases, Ubp8 protein from DUBm was not detected by Western blot.

Discussion

During this part of my thesis, I have been involved in the study of the DUBm and its implication in transcriptional regulation. In our study, we have been able to demonstrate that the histone chaperone Asf1 and Mog1 protein are both implicated in maintaining correct levels of monoubiquitinated histone H2B (H2Bub^{1}), hence having an impact on chromatin dynamics.

In the context of gene expression regulation, the assembly and disassembly of chromatin by histones chaperones is an essential step for biological processes such as DNA transcription, repair, replication and recombination (Akey and Luger, 2003; Mousson et al., 2007). Asf1 has been described as a histone chaperone implicated in these processes actively participating in the regulation of gene expression (English et al., 2006). We were able to demonstrate that Asf1 co-purifies with components of the NPC, SAGA and TREX-2 subunits (Pamblanco et al., 2014), thus, focusing on the connection between SAGA and TREX-2 complexes, we analysed the possible contribution of Asf1 to mRNA export. Although our results do not show an mRNA export deficiency in *asf1Δ* cells, neither a misregulation in *GAL1* expression, it is possible that there are some minor defects in transcription and export in these cells. In fact, we observed several cells in *ASF1* mutant that presented a partial mRNA export block compared to the WT, however, our experiments did not allow us to demonstrate that this difference was significant. A possible way to

observe a more concrete phenotype could be to have a synchronized culture of *asf1Δ* cells since Asf1 is involved in chromatin assembly throughout the cell cycle (Sutton et al., 2001b). An analysis revealed that Asf1 is associated to coding regions of transcriptionally active genes and that *asf1Δ* mutant cells lead to a decrease in RNA Pol II association at several coding regions, such as *GAL10 and PYK1*, thus suggesting that Asf1 could be considered as a RNA Pol II elongation factor (Schwabish and Struhl, 2006). Due to the fact that Sus1 plays a key role in coupling transcription activation with mRNA export and it is recruited to SAGA-dependent genes such as *GAL1* (Pascual-García and Rodríguez-Navarro, 2009b; Pascual-García et al., 2008), we investigated the possible contribution of Asf1 to Sus1 recruitment. According to our result, Sus1 recruitment to *GAL1* promoter and ORF is not affected by the absence of *ASF1.* However, we were able to observe a significant difference between Sus1 levels at *GAL1* promoter compared to the gene body in *asf1*Δ cells. Although our results indicate that this imbalance does not affect to *GAL1* expression, our results suggest that *ASF1* deletion may, in someway, affect to the chromatin environment, hence, showing a difference among Sus1 recruitment to *GAL1* promoter and gene body. In order to clarify this fact, a more in-depth study should be conducted to analyse whether fine tune regulation of *GAL*1 gene is affected in *asf1Δ* cells.

Sus1 as being part of the DUBm from SAGA complex plays a major role in the deubiquitination of histone H2B (Galán and Rodríguez-Navarro, 2012; Köhler et al., 2006) a modification that is necessary for a correct

transcription activation and elongation (Daniel et al., 2004; Henry et al., 2003). Therefore, one of our purposes was to investigate whether Asf1 is required for H2Bub^{1}. Our work confirms that H2Bub^{1} depends on Asf1 since deletion of this protein leads to decreased H2Bub^{1} levels, in contrast to *SUS1* mutant. The double mutant bearing *SUS1* and *ASF1* deletions partially suppresses the phenotype of the single mutant which suggests that they may contribute in the same process. It would be interesting to study whether Asf1 contributes to the ubiquitination of histone H2B or instead, prevents H2Bub^{1} from being deubiquitinated. Together, our findings suggest that Asf1 is linked to TREX-2 and the nuclear pore complex; therefore, this connection may affect chromatin histone modifications such as monoubiquitination of H2B. This work has been published in the journal <u>*Nucleus*</u> under the title "*Unveiling novel interactions of histone chaperon Asf1 linked to TREX-2 factors Sus1 and Thp1*" and I have contributed as a first co-authorship.

In this work, we also show for the first time that Mog1 contributes to the coordination of transcription regulation. Mog1 was previously described as a coordinator of the RanGTP cycle, hence, it binds to Ran GTPase and participates in the nuclear protein import pathway (Baker et al., 2001; Oki and Nishimoto, 1998). Due to our interest in finding new factors involved in coordination of gene expression steps, we found genetic interaction between *SUS1* and *MOG1*. The strong genetic interaction between *MOG1* and components from the DUBm confirmed our predicted results and suggested that Mog1 could be implicated in a similar biological process.

The DUBm from SAGA complex deubiquitinates histone H2B and absence of its subunits leads to increased levels of histone H2Bub^1 (Ingvarsdottir et al., 2005; Köhler et al., 2006, 2008; Lee et al., 2005; Shukla et al., 2006). Therefore, we first explored whether Mog1 could contribute in maintaining correct levels of H2Bub^1 and demonstrated that Mog1 is implicated in this process as our data shows that absence of *MOG1* results in decreased levels of H2Bub^1. Moreover, the genetic interaction between *MOG1* and the ubiquitinases *LGE1* and *BRE1* also supports the role of Mog1 in H2Bub^1. Rad6 is the ubiquitin ligase responsible for monoubiquitination of histone H2B and it is recruited to both promoters and 5´ORF (Kao et al., 2004; Song and Ahn, 2010; Wood et al., 2003b; Xiao et al., 2005). According to this, absence of *MOG1* results in a poor association of Rad6 to the 5´ORF of the highly transcribed genes *PMA1*, *ADH1* and *YEF3* suggesting that Mog1 stimulates the recruitment or activity of Rad6. However, differences in H2Bub^1 could be due to a poor recruitment or activity of Rad6 or instead, to an excess of Ubp8 enzyme activity. To discriminate between both scenarios, we performed Ubp8 ChIP and show no differences compared to WT. Furthermore, Ubp8 physical interactions and localization are not affected in *mog1Δ*. In all, we propose that Mog1 modulates upstream events that lead to H2Bub^1, however, a more detailed study of Ubp8 enzymatic activity would be needed in order to clarify this aspect. Additionally, it would be interesting to investigate whether chromatin-associated H2Bub^1 is affected upon *MOG1* deletion.

It has been previously established that H2Bub^{1} by Rad6/Bre1 modulates H3K4me^{2} and H3K4me^{3}, in fact, lack of H2Bub^{1} results in absence or decrease of these epigenetic marks (Dover et al., 2002; Lee et al., 2007; Shahbazian et al., 2005b; Sun and Allis, 2002). Additionally, histone cross-talk is associated with transcription elongation (Bannister and Kouzarides, 2011). Our results indicate that absence of *MOG1* leads to decreased levels of H3K4me^{3}, which is expected from a factor required for the efficiency of H2Bub^{1}. Although the genetic interaction observed between *MOG1* and the methyltransferases *SET1*, *DOT1* and *SET2* only occurs in some conditions it might account for a downstream role for Mog1 in the control of histone H3 methylation. Although we have focused on H3K4me^{3} mediated by COMPASS complex, it is plausible to think that Mog1 participates in the process of other histone cross-talk. These results are consistent with the fact that Mog1 is required for the recruitment of COMPASS subunits Set1 and Swd2 to active genes. Interestingly, previous research has shown that Swd2 is a key factor involved in modulating H2Bub^{1}-H3K4me^{3} histone cross-talk to couple with mRNA metabolism (Lee et al., 2007; Vitaliano-Prunier et al., 2008). Our observation that protein levels of Swd2 are diminished in the absence of *MOG1* may indicate that Swd2 stability is regulated by Mog1 leading to a dysfunctional activity of the histone cross-talk. In agreement with this, absence of Mog1 also affects mRNA export. In this line, H2Bub^{1} has been shown to be required for mRNA export in some experimental conditions. Thus, it is likely that Mog1 is a novel coordinator of H2Bub^{1}-H3K4me^{3} coupled with mRNA

biogenesis and export. Past studies have shown that absence of *MOG1* does not result in mRNA accumulation in the nucleus in *S. cerevisiae* (Oki and Nishimoto, 1998), however, later studies confirmed a defect in mRNA export in *S. pombe* (Oki et al., 2007; Tatebayashi et al., 2001). Consistent with this finding, we were able to detect an accumulation of poly $(A)^+$ RNA in mutant *mog1Δ.* This finding is also supported by the genetic interaction among *MOG1* and TREX-2 subunits. Interestingly, the work by Vitaliano-Prunier *et al.,* demonstrated that defects in H2B ubiquitination or H2B-dependent modification of Swd2 result in nuclear accumulation of poly $(A)^+$ RNA (Vitaliano-Prunier et al., 2012) which raises the possibility that Mog1 could participate in mRNA export through its role in H2B ubiquitination. It would be crucial to address whether Mog1 participates in the modification of Swd2 to coordinate this pathway. Current work in our lab is trying to solve this interesting question.

Our results also leave an open question regarding the role of Mog1 in PAF complex activity. The fact that Mog1 mainly affects the recruitment of Rad6 and Set1 to coding regions, supports its role during transcription elongation and RNA Pol II processivity. Paf1 is required for monoubiquitination of histone H2B and for the recruitment of COMPASS complex, thus having an impact on H3 methylation (Krogan et al., 2003b; Wood et al., 2003b). In addition, recent research has proposed that Rtf1 subunit from PAF complex can promote H2B ubiquitination by a direct interaction with Rad6 (Van Oss et al., 2016). Thus, it would be interesting

to study whether Mog1 contributes to PAF complex activity, hence facilitating ubiquitination of H2BK123 during transcription elongation.

As expected of a factor whose absence affect epigenetic regulation, our genome-wide analysis also supports the idea that Mog1 is implicated in transcription. We observe low levels in transcription rate (SR) and mRNA concentration (RA) in *mog1Δ* cells. Additionally, the fact that the majority of genes are down-regulated in *mog1Δ* and that no differences among SAGA and TFIID-dominated genes exist, we suggest that Mog1 could act in a global manner in transcription. To corroborate this result, it would be interesting to study the recruitment of Rpb1 subunit to chromatin. Consistent with this transcriptional role, Mog1 can co-purify with several complexes of the transcription machinery such as SAGA and COMPASS. Remarkably, Mog1 interacts with the DUBm subunit Sgf73, however, our results suggest that it is not able to interact with the rest of the DUBm (Sus1, Ubp8 and Sgf11). Maintaining the balance of ubiquitin ligases and deubiquitinases activities is required for the correct gene expression. In this line, Schulze and colleagues demonstrated that Ubp8 deubiquitinates H2BK123ub^{1} at H3K4me^{3}-marked regions (Schulze et al., 2011). Indeed, recent studies have revealed that the DUBm subunit, Sgf11 ZnF domain targets the nucleosome core particle (NPC) acidic patch (Morgan et al., 2016). However, the exact mechanism by which ubi/deubiquitination activities are coordinated is still a matter of debate. Recently, researchers have established that Bre1 RING domain is required for stimulating Rad6 catalytic activity over H2BK123 and this occurs in competition with the

DUBm subunit Sgf11 (Gallego et al., 2016). Thus, the deubiquitinated nucleosome may only be available for reubiquitination once the DUBm is dissociated. A provocative scenario would be that Mog1 in association with the ubiquitinases Rad6/Bre1, prevents the transition from $H2Bub^{1}$ to $H2B\text{-}deub^{1}$ by impeding the incorporation of the DUBm to SAGA until $H3K4me^{3}$ is not completed, thus preventing H2B from being deubiquitinated before the cross-talk is complete.

Taken together, we propose that Mog1 acts as a modulator of gene expression having an impact on the coordination of chromatin modification with downstream steps (**Figure 38**). The most likely hypothesis is that Mog1 acts synergistically with epigenetic regulators such as SAGA, Rad6 and COMPASS complex, hence, contributing to post-translational modifications such as $H2Bub^{1}$ and consequently to histone H3 methylation, marks related with transcription initiation and elongation coupled to mRNA export (Rodríguez-Navarro and Hurt, 2011; Shilatifard, 2006). However, an exact mechanism that could place Mog1 in the context of gene expression is still a matter of study. We also consider that it would be interesting to invest time in studying the new role of Mog1 in epigenetic control in higher eukaryotes, since Mog1 mutations are linked to Brugada syndrome (BS). It would be fascinating to see whether the role of Mog1 in gene expression is conserved and is part of the molecular bases leading to the pathology of BS. Overall, our study demonstrates that Mog1 functions not only for nuclear import but also in coordinating different steps of gene expression.

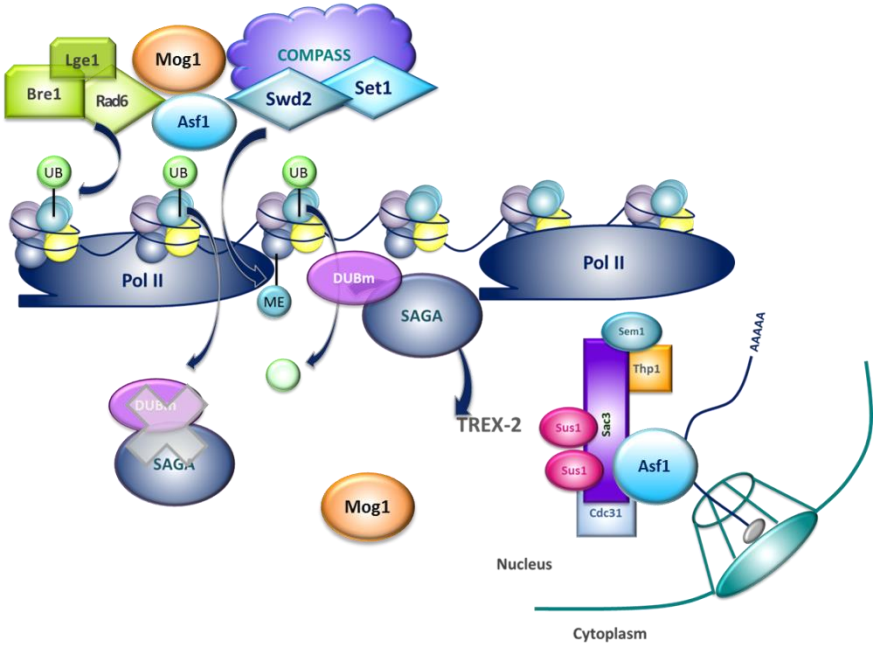

Figure 38. Squematic draw of the possible role of Mog1 and Asf1 during gene expression coordination. Mog1 cooperates with the ubiquitin ligases Rad6/Bre1/Lge1 to ubiquitinate histone H2B at lysine 123 which subsequently promotes trimethylation of histone H3 at lysine 4 by COMPASS complex subunit Set1. Mog1 may also contribute to the stabilization of Swd2 COMPASS subunit thus facilitating H3K4me^{3}. Mog1 also interacts with a SAGA complex lacking the DUBm subunits Sus1, Ubp8 and Sgf11 which suggests that it prevents the transition from H2BK123 to deubiquitinated H2B and hence, impeding the incorporation of the DUBm to SAGA until the cross-talk H2Bub^{1}-H3K4me^{3} is completed. Finally, Mog1 coordinates mRNA export together with TREX-2 complex to ensure the coupling between epigenetic cross-talk and mRNA export. Histone chaperon Asf1 interacts with TREX-2 complex and several nucleoporines, indeed, it is implicated in maintaining correct levels of H2Bub^{1}.

CHAPTER 2

Molecular mechanisms of the DUBm related disease Spinocerebellar Ataxia type 7 (SCA7)

In order to complete this part of the work, I performed an internship at the University of San Diego (California) in the laboratory of Dr. Albert La Spada where I worked with human cell lines and mice. The metabolome analysis was carried out at the CIPF in collaboration with the metabolic department using yeast as a model system.

Metabolic Profile of WT and polyQ-ATXN7

As mentioned in the introduction, SCA7 is an autosomal-dominant neurodegenerative rare disease produced by a polyglutamine expansion in the N-terminal of the ATXN7 protein (David et al., 1997). Although many groups are focusing on the study of the molecular mechanisms surrounding SCA7 disease, an effective cure and treatment is not yet available. For this reason, an implementation of new therapies that could contribute to the progression of the disease is necessary. In order to get insight into the discovery of new biomarkers, several researchers have previously associated the appearance of biochemical alterations in SCAs using NMR-based metabolomics as a tool (Griffin et al., 2004). Therefore, one of our goals was to investigate new possible biomarkers in SCA7 disease using *S. cerevisiae* as a model organism of SCA7 by ^{1}H nuclear

magnetic resonance (NMR) spectroscopy, a tool that has been optimised in yeast in our lab (Palomino-Schätzlein et al., 2013). Energy metabolism has been shown to influence histone and DNA modifications, thus affecting gene expression and having an impact on human health and disease (Donohoe and Bultman, 2012; Martinez-Pastor et al., 2013). Thus, in the case of finding promising changes in yeast, we could make a step forward and translate our study to higher organisms.

As a first stage and following the methodology previously explained (please see Methods section), we transformed the yeast mutant *sgf73Δ* with a plasmid encoding the WT human version of ATXN7 containing 10Q (WT-ATXN7) and the pathogenic human version of ATXN7 containing the polyglutamine (113Q) tract in *S. cerevisiae* (polyQ-ATXN7). We evaluated the aqueous extract from both WT-ATXN7 and the polyQ-ATXN7. NMR analysis allowed the identification and quantification of 39 different polar metabolites (**Table Annex 1**). In order to get an overview of the metabolic changes between both groups, multivariate analysis in form of principal component analysis (PCA) was performed using the metabolite concentration tables as input data. The resulting score plot of the first two principal components (t (1) and t (2)) accounting for 76 % of the total variability is represented in **Figure 39**. According to our results, no clear separation in space of the samples from WT-ATXN7 and polyQ-ATXN7 in *sgf73Δ* cells could be observed, which seems to indicate that the differences in the metabolic profile between both strains are relatively small.

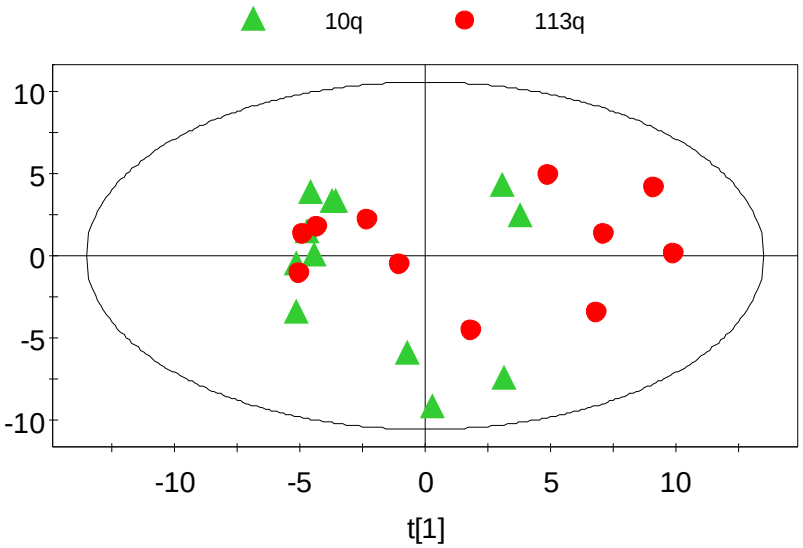

Figure 39. PCA score plot of the first two principal components t(1) and t(2) of *S. cerevisiae* aqueous extracts of 10Q (green)and 113Q (red) mutant. R = 0.76, Q = 0.56, UV scaling.

Despite the fact that we did not detect a changed pattern at the PCA model, for a deeper analysis we performed a univariate statistical analysis comparing normalized metabolite levels in both strains. As a result, we were able to differentiate different metabolites which showed a p-value lower than 0.05 (**Table 7**), including serine, valine, b-glucose, thiamine phosphate and proline. Although most of these amino acids changes do not seem specific to any remarkable route, the detection of b-glucose could be indicative of this metabolic pathway.

	10Q		113Q		
Metabolite	mean	SD	mean	SD	p-value
Serine	5.0099	0.4180	5.5631	0.6529	0.0217
Valine	13.4477	2.7260	11.0865	2.1341	0.0274
b-glucose	0.7250	0.3206	1.1354	0.5303	0.0317
Thiamine phosphate	0.9055	0.0871	1.0327	0.1867	0.0439
Proline	5.5248	0.3260	6.0715	0.8340	0.0460

Table 7. Selected metabolite concentrations of WT-ATXN7 (10Q) and the polyQ-ATXN7 (113Q). Concentrations values were normalized to total intensity.

Expression levels of mitochondrial and ribosomal genes are not affected in SCA7 mice cerebellum

It has been reported that strains lacking genes *SGF73*, *SGF11* and *UBP8* which belong to the deubiquitination module of the SAGA/SLIK complexes present a replicative life span (RLS) extension phenotype (McCormick et al., 2014). Moreover, this group also discovered a genetic and physical interaction between the DUBm components and the Sir-2 deacetylase, suggesting that extended *sgf73Δ* RLS are due to an altered Sir-2 deacetylase function. Given that polyQ expanded ATXN7 causes SCA7 disease, it has been proposed that polyQ-ATXN7 could affect the function of USP22 and SIRT1 (yeast Sir-2) in SCA7 disease (McCormick et al., 2014)

In order to acquire further knowledge in the role of Sgf73 in RLS regulation, La Spada laboratory conducted a ChIP-seq experiment to

determine the DNA binding sites of Sgf73 (Thesis of Dr. Amanda Manson). From the genomic regions bound to Sgf73, 31 genes were related to RLS and 19 of them were identified as ribosomal protein (RP) genes. 9 out of the 19 RP genes were down-regulated in *sgf73Δ* mutants. Indeed, they also found a significant reduction in the expression levels of cell metabolism genes in cells lacking *SGF73*.

To determine if there exists a possible connection between genes down-regulated in *sgf73Δ* mutant cells (associated with an increased in RLS) and SCA7 disease, we performed an expression analysis of ribosomal and mitochondrial genes from the cerebellum of SCA7 mice compared to a WT population. Two different set of mice were manipulated for the experiment 1) mice containing the polyglutamine expansion (92Q) and 2) WT mice (non-transgenic) grown until week 30. Transgenic mice were produced in Dr. La Spada lab (Furrer et al., 2011) which were designated as WT "PrP-SCA7-c24Q" and mutant "PrP-SCA7-c92Q" (La Spada et al., 2001). A total of 16 cerebellums corresponding to both non-transgenic and SCA7-92Q were extracted by the technical service at the University of San Diego to measure the expression levels of the ribosomal (*RPL10*, *RPL19*, *RPL18a*, *RPL23*, *RPL27*, *RPL8*, *RPL35*, *RPL37a*, *RPL6* and *RPS26*) and mitochondrial (*IDH3G*, *IDH3B*, *SLC20A1*, *SLC01C1*, *HEPH*, *CP*, *TMEM33*, *MPC2*, *RPS25*) genes.

As shown in our results, expression levels of the RP and mitochondrial genes remains unaltered among WT and polyQ-mice (**Figure 40**). These results suggests that although these genes present a down-regulation in

sgf73Δ mutant in yeast (Thesis Dr. Amanda Mason) it does not appear to be correlated with a downregulation in SCA7 disease, at least in the cerebellum of the tested mice.

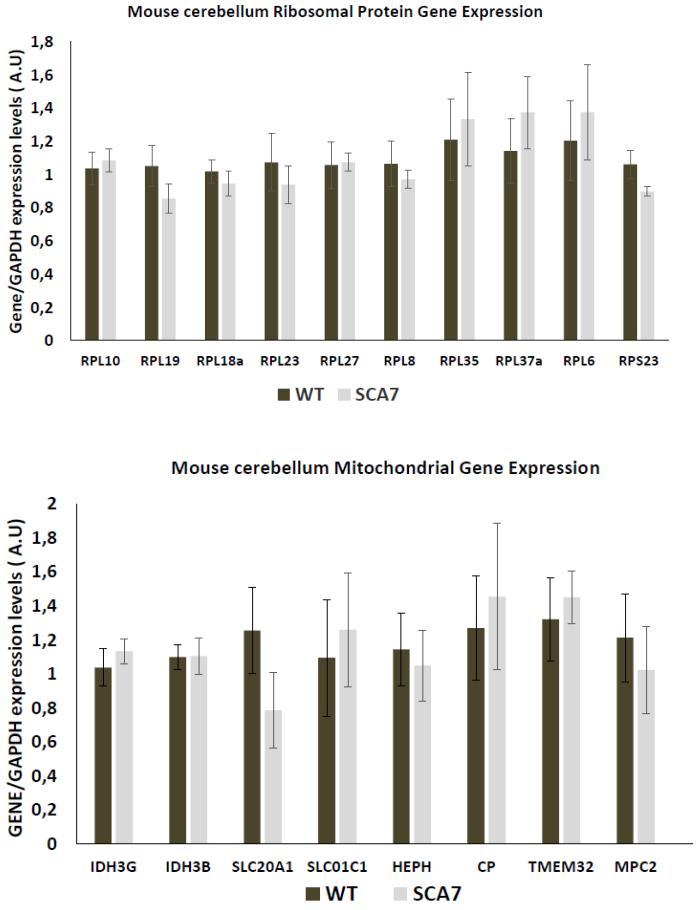

Figure 40. Real-time RT-PCR analysis of total RNA extracted from transgenic mice cerebellum at 30 weeks (10 weeks post-symptomatic). Specific primers were used to study the expression levels of mitochondrial and RP genes in "PrP-SCA7-c24Q" and mutant "PrP-SCA7-c92Q". mRNA levels are quantified using an n=8 for both WT and mutant SCA7 mice after normalization to *GAPDH* gene. No significant differences (p-value <0.05) are observed between the two populations. Each bar represents the mean value +/- SD.

PolyQ repetitions in ATXN7 protein preserves DUB activity of SAGA complex in human cell lines

The SAGA DUBm from the SAGA co-activator complex in yeast is composed of four proteins Ubp8, Sus1, Sgf11 and Sgf73 (Köhler et al., 2006; Lee et al., 2005; Rodríguez-Navarro et al., 2004). The human homologues of these proteins are; USP22, ENY2, ATXN7L3 and ATXN7, respectively (Helmlinger et al., 2004; Zhao et al., 2008) which form part of the TFTC/STAGA module. Both in yeast and humans ySAGA/hSTAGA contain two enzymatic activities; the deubiquitinase activity performed by yUbp8/hUSP22 (Daniel et al., 2004; Henry et al., 2003) and the acetylase activity conducted by yGcn5/hGCN5 (Grant et al., 1997). It has been previously reported that for a correct Ubp8 activation, Ubp8 needs to be assembled into the DUBm together with the rest of the components (Köhler et al., 2008). Protein ATXN7 plays an important role in the functioning of the deubiquitinase Ubp8, since its absence has been correlated with increased levels of histone $H2Bub^{1}$ (Lee et al., 2009), however, another group has shown that ATXN7 is dispensable for the DUB activity in a Drosophila model (Mohan et al., 2014).

Although some laboratories have recently focused on the possible effect that the polyQ expansion may produce in the DUB activity of SAGA (Lan et al., 2015; Yang et al., 2015), one of our goals was also to elucidate whether expanded ATXN7 had an effect on the *in vitro* DUB activity of the SAGA complex using recombinant mammalian DUBm components in HEK293T cells.

For this purpose, HEK293T cells were co-transfected with plasmids expressing the four components of the human DUBm; USP22-FLAG, ATXN7L3-HIS, ENY2-FLAG-HA and MYC-ATXN7-10Q (WT) or MYC-ATXN7-92Q (mutant). USP22-Flag was immunoprecipitated and purified histones were used as substrate and incubated with the immunoprecipitated complex for 2 hours at 37 °C. Immunoblots analyses of the purified proteins were performed by Western blot using specific antibodies. Our results show that co-expressing the four proteins from the DUBm permits the activity of USP22, as there is a reduction in the levels of $H2Bub^{1}$ (**Figure 41**) compared to controls; cells without USP22 expression and a negative control where only histones were incubated with DUB buffer. However, no significant differences were identified on the DUB activity of USP22 between mutant and WT-ATXN7 under the conditions tested in this study. As a negative control a plasmid with no tag (empty Flag) was used in the experiment. We observed a tendency that ATXN7-92Q shows lower levels of $H2Bub^{1}$, however, this difference is not statistically significant. Our results suggest that the *in vitro* activity of the DUBm do not seem to be affected in HEK293T cells, at least in the conditions tested in this study.

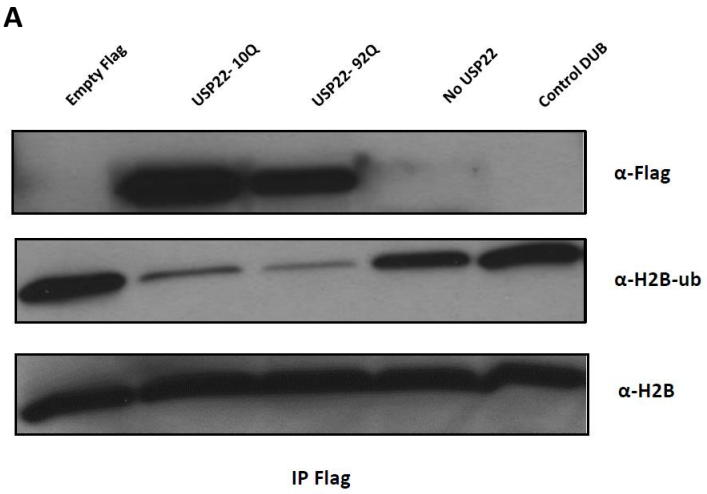

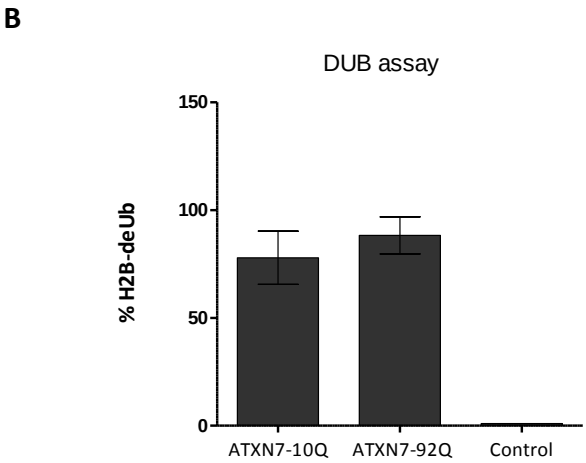

Figure 41. Deubiquitination activity of USP22 using HEK293T cell lines. Plasmids expressing the distinct subunits of the DUBm (USP22-FLAG, ENY2-FLAG-HA, ATXN7L3-HIS and MYC-ATXN7-10Q (WT) or MYC-ATXN7-92Q (mutant)) were transiently co-expressed in HEK293T cell lines. Immunopurified DUBm was subjected to an *in vitro* deubiquitination assay. USP22-FLAG was immunoprecipitated using Flag beads and the immunopurified protein was tested by WB with the anti-Flag antibody. The deubiquitination reaction was analysed by Western blot using antibodies directed against H2B-ub and total H2B (A). (B) Representation of the % of H2B-deubiquitinated confirms very similar deubiquitinating activity of USP22 between the two complexes; WT-ATXN7 and mutant-ATXN7. Error bars represent the SD for at least three independent experiments.

PolyQ-ATXN7 seem to affect the association between ENY2 and TREX-2 complex

We aimed to examine whether the presence of the polyglutamine tract in the ATXN7 protein affects the association of protein-protein among SAGA and TREX-2 complex. Although previous studies have suggested that mutant ATXN7 affects transcription through its association with STAGA/TFTC (McMahon et al., 2005; Palhan et al., 2005), little is known about the pathology observed in SCA7 and its link with altered protein-protein interactions. To test the hypothesis that polyglutamine ATXN7 causes pathology by aberrant or lack of protein interactions, we co-transfected HEK293T cells with plasmids expressing ENY2-FLAG-HA together with MYC-ATXN7-10Q or MYC-ATXN7-92Q to follow the association of ENY2 with its common partners in the presence of mutant ATXN7 using gel-filtration chromatography.

The profile of copurifying proteins in the WT and mutant ATXN7 obtained after gel filtration (**Figure 42. A** and **C**) suggests that ATXN7 co-purifies with SAGA complex which elutes with an approximately size of 1.8 MDa (Grant et al. 1997). On the other hand, when we performed Western blots with the fractions against anti-Flag, allowing ENY2 detection, our blots show that ENY2 is distributed along the whole gradient with enriched fractions that could match with SAGA and TREX-2 similar to what have been shown for yeast Sus1 (**Figure 42. B** and **D**) (Rodríguez-Navarro et al., 2004). In this study, we were able to demonstrate that yeast Sus1 (human ENY2) belongs to both complexes, SAGA and TREX-2, linking transcription

by the SAGA co-activator complex with mRNA export. Our results seem to indicate that polyQ-ATXN7 alters ENY2 association pattern as compared to WT ATXN7-10Q. According to our data, our hypothesis would be based on the possible protein-protein disruption by the existence of poly-Q ATXN7 which could affect mRNA export having an impact on gene expression regulation.

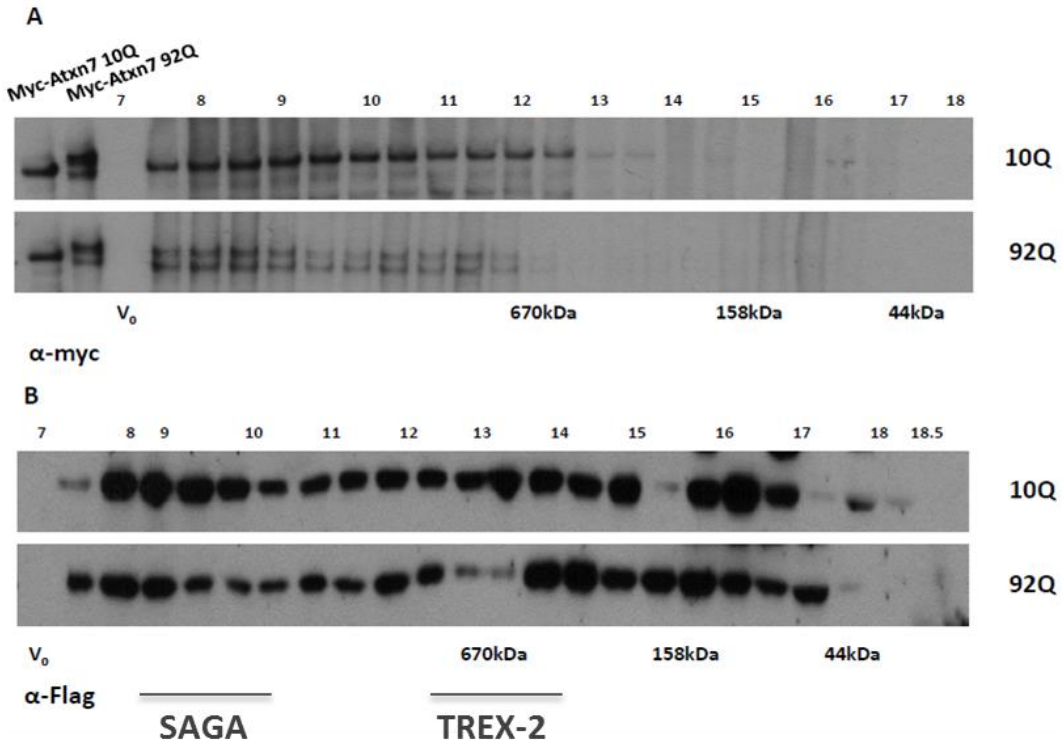

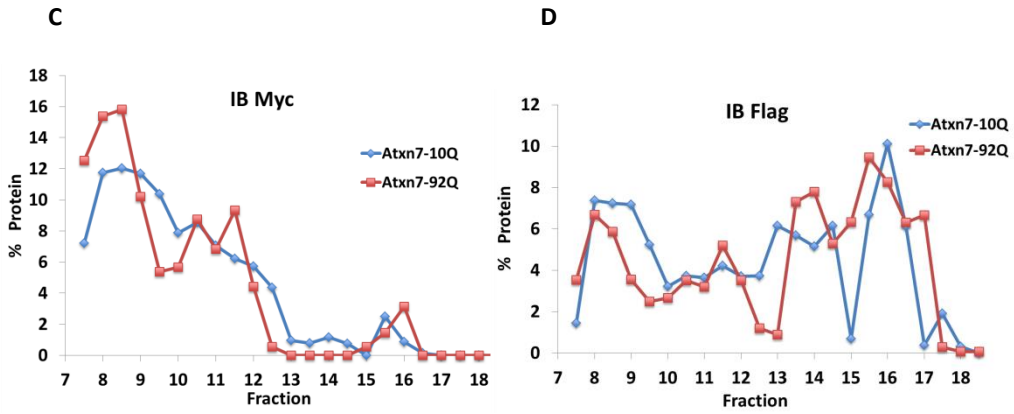

Figure 42. Identification of ENY2 and ATXN7 interacting proteins by gel filtration chromatography. A) Western blot analysis against anti-myc of eluted fractions corresponding to the co-transfection of HEK293T cells with plasmids expressing ENY2-FLAG-HA with MYC-ATXN7-10Q or MYC-ATXN7-92Q. B) Same as A) but applying Western Blot analysis against anti-Flag to detect ENY2 protein. C) and D) show the percentage of ATXN7 and ENY2 proteins detected in each fraction. As demonstrated in the plots, ENY2 detection decreases in fractions 12-13 which corresponds to TREX-2 eluting fractions. IB; Immunoblot.

Discussion

It is still unknown the main mechanisms by which polyglutamine expansions lead to neurodegenerative disease such as Spinocerebellar Ataxia type 7 (SCA7). Although the discovery of ATXN7 and its participation in transcription has clarified several aspects of the disease, there still exists a lack of evidence regarding the role of ATXN7 in the development of the disease. We found interesting to cover several aspects that remain unanswered regarding to SCA7, thus, we have mainly focused into the role of polyQ-ATXN7 and its possible contribution to transcriptional dysregulation together with complementary experiments that could reveal new features of the disease.

In our lab, we had previously optimized a protocol for NMR using yeast *S. cerevisiae* (Palomino-Schätzlein et al., 2013). Thus, we considered the possibility of linking SCA7 with changes in metabolic routes using this strategy. The first purpose of our work was to identify which metabolites were differentially identified between the two strains (ATXN7-10Q and ATXN7-113Q) in the conditions tested (SC medium containing glucose as a carbon source), in addition to the implementation of the experiment for further studies. Although the results present in this study do not show a strong differentiation between the WT-ATXN7 (10Q) and polyQ-ATXN7 (113Q), some metabolic changes were detected. The changes in the amino acidic pattern are usually difficult to interpret since changes in the amino acids found in our study (serine, valine, proline) participate in many different routes and do not seem to be specific to any precise pathway. Nevertheless, it seems interesting to observe the higher levels of glucose found in the polyQ-ATXN7 which may indicate that there exists an alteration in the energetic metabolism. Most of the metabolites detected in the analysis correspond mostly to yeast fermentation whose final product is ethanol. This fact is reflected in **Table ANNEX 1**. since we were able to detect higher levels of ethanol, lactate and acetate in both conditions. However, also several metabolites from the TCA cycle such as citrate and succinate were detected, even if at much lower concentrations.

Yeast *S. cerevisiae* is known to present a mixed respiratory-fermentative metabolism depending on the type and concentration availability of sugars and/or oxygen (Rodrigues et al., 2006). Oxygen depletion commonly

controls the switch from respiration to fermentation, but in the case of *S. cerevisiae*, this change is controlled in response to external glucose level (Otterstedt et al., 2004). However, it has been observed that this yeast specie catabolizes glucose mostly by a fermentative process (Rodrigues et al., 2006). In a situation where glucose concentration is low, the mitochondria will have more affinity for pyruvate which will lead to respiration. However, in case of higher concentrations of glucose, more pyruvate will be formed favoring alcoholic fermentation in the cytosol. One way to implement our analysis would be to decrease glucose concentration in the yeast culture medium favoring the switch from fermentation to respiration thus detecting metabolites formed in the mitochondria which could give us further knowledge on SCA7 disease and its role in the metabolic pathways. On the other hand, it would also be reasonable to use other organisms such as cell lines, mice or human patients to detect differences among the two populations. A recent study has provided insights into the metabolic/cellular changes in various SCAs, including SCA7, in the cerebellar vermis and pons of a cohort of patients detecting biomarkers that reflect dynamics aspects of cellular metabolism (Adanyeguh et al., 2015).

To understand mechanisms that could explain the role of polyQ-ATXN7 in transcription deregulation, we based one of our experiments on a previous research performed in yeast. Throughout my research, one of our goals was to explore whether downregulated genes found in *sgf73Δ* mutants corresponded to transcriptional alterations in SCA7 mice. Hence, a set of

genes corresponding to RP and mitochondrial genes that showed downregulation in *SGF73* mutant cells were analysed indicating that unaltered expression levels were found in mice cerebellum. As it is described in the literature, SCA7 is the only SCA characterized by neuronal cell death in the retina resulting in blindness (Yoo et al., 2003; Yvert et al., 2000). Hence, it would be interesting to get insight into the possible role of the expression of RP and mitochondrial genes in the retina of SCA7 population. Scientists have associated severe chromatin decondensation in rod photoreceptors in SCA7 mouse model with increased recruitment of TFTC/STAGA to specific promoters (Helmlinger et al., 2006). In accordance with this finding, a prior microarray showed that mutant polyQ-ATXN7 causes retinal dysfunction by altering mRNA expression of photoreceptor genes (Abou-Sleymane et al., 2006). While we were not able to see a dysregulation in mRNA expression levels from RP and mitochondrial genes, it would be interesting to clarify if these changes could be seen in the retina of SCA7 mice.

Our investigation has also been directed towards the role of polyQ-ATXN7 and its contribution with the deubiquitinase (DUB) activity of STAGA complex. Given the importance of Sgf73 in the DUBm conformation and function, we aimed to understand if the presence of polyQ expansions in ATXN7 affected the *in vitro* DUB activity in human cell lines and in consequence, transcription dysregulation. Our results reveal that the polyQ expansions in the N-terminal region of ATXN7 do not affect the DUB activity of STAGA complex in HEK293T cell lines. These results are in

agreement with previous research which elucidated key cellular roles of polyQ-ATXN7 in the deubiquitination activity and its contribution to the pathogenesis of the disease. This research concluded that the presence of polyQ-ATXN7 in astrocytes do not alter the enzymatic activity of the DUBm, nevertheless, they suggest that polyQ expansions contribute to SCA7 by initiating aggregates that sequester the DUBm from its substrates (Lan et al., 2015). Similarly, previous evidence suggests that polyQ-ATXN7 tends to form nuclear aggregates in central nervous system (CNS) neurons by self-association or by interaction with other factors such as transcription factors (Holmberg et al., 1998; Yvert et al., 2000). Another study proposed that polyQ expansions in ATXN7 sequesters USP22 into inclusions leading to an increase of $H2Bub^1$ levels which implies that it interferes with the normal function of USP22 and consequently with the DUBm (Yang et al., 2015). Our observed unchanged levels of $H2Bub^1$ might be due to the existence of compensatory DUBs enzymes. For instance, a recent study has discovered that two $H2Bub^1$ DUB enzymes function independently of SAGA and compete with USP22 for ATXNL3 and ENY2 for DUB activity (Atanassov et al., 2016). Previous research has attributed the existence of polyQ-ATXN7 with transcriptional dysregulation (Chou et al., 2010), thus, another possibility is that transcriptional dysregulation caused by an impairment of the DUB activity might be found in those tissues affected by the disease, such as cone-rode receptors and cerebellum. Mutations in ATXN7 have been correlated with H3 hyperacetylation and with an increase in the recruitment of TFTC/STAGA to specific promoters

of rod-specific genes (Helmlinger et al., 2006). Using astrocytes as model organism another study proved that polyQ expansion decreased ATXN7 occupancy and correlated this fact with increased levels of H2Bub^{1} at the REELIN promoter (McCullough et al., 2012). In light of these findings, it could be possible that our *in vitro* results do not represent a perfect *in vivo* environment in the cell, it is likely that an *in vivo* study would provide us with more detailed analysis.

Linking our previous result with the importance of the correct structural composition of STAGA complex for transcription activation, we also contemplated the option that polyQ-ATXN7 could affect the assembly of STAGA complex or even, the assembly between STAGA and TREX-2 complex. As it is known, the association between yeast Sus1 (hENY2) and yeast Sgf73 (hATXN7) is fundamental for the correct mRNA export. On one hand, yeast Sgf73 mediates the regulation of H2Bub^{1} levels, and consequently it has been demonstrated to be necessary for mRNA export since it affects the integrity of the TREX-2 mRNA export complex (Kohler et al. 2008). On the other hand, *SUS1* deletion prevents the localization of Sac3 and Thp1 at the NPC which demonstrates that Sgf73 together with Sus1 are necessary for the efficient targeting of Sac3 and Thp1 to the nuclear pore complex (Kohler et al. 2008). Based on this evidence, our results point towards new mechanisms that suggest that the expanded ATXN7 could affect the association of ENY2 with its TREX-2 partners, Sac3 and Thp1, consequently, affecting the mRNA export towards the NPC for the correct gene expression. A suitable approach to clarify this possibility

could be the tagging of ENY2 with a TAP tag together with polyQ or WT ATXN7 and perform tandem purification for the later detection of the TREX-2 components by Western blot or LC-MS/MS mass spectrometry. Additionally, we would like to test whether the polyQ-ATXN7 affects the association of Sus1 with its TREX-2 partners in *S. cerevisiae*. Our findings for SCA7 open new possibilities to link the pathology of the disease with transcription and mRNA export, therefore, ATXN7 is a known transcription factor (Helmlinger et al., 2004) that may alter the activity of some proteins when the polyQ tract is present in the protein. For this reason, a complete understanding of how mutant ATXN7 affects the association of SAGA-TREX-2 members is necessary in order to establish new therapeutic approaches that could prevent the progression of the disease.

Overall, during this part of my research, we have tried to cover different aspects to find new mechanisms in SCA7 disease using different model organism such as yeast *S. cerevisiae,* cell lines and mice. Our hypothesis is that polyQ-ATXN7 maintains the correct activity of the DUBm, however, it seems to alter the association of ENY2 with TREX-2 components, thus having an impact on gene regulation. Further research would be needed in order to clarify this promising preliminary result (**Figure 43**).

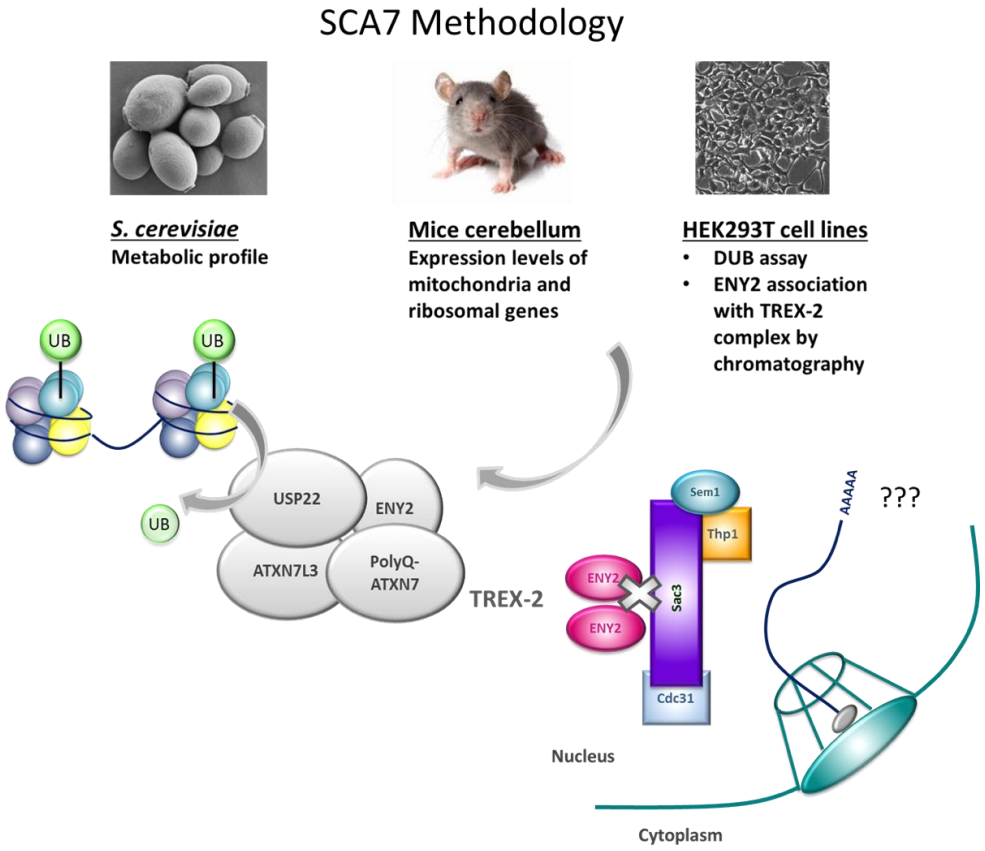

Figure 43. Schematic representation of SCA7 models of disease. Different approaches have been performed in order to get insight into new molecular mechanisms of SCA7 disease; *S. cerevisiae*, mice cerebellum and HEK293T cell lines. We propose that the polyQ-ATXN7 is able to activate the DUBm, thus having normal levels of H2Bub[1]. However, in the presence of the polyglutamine tract within ATXN7 protein, ENY2 seems to dissociate from its TREX-2 partners which could suggest that polyQ-ATXN7 may impact in gene regulation, for instance, in mRNA export.

Future perspectives

Future Perspectives

Molecular and biochemical approaches have contributed to our understanding of the different steps that occur in gene expression. Although much research has been useful in deciphering the role of different factors implicated in regulatory circuits governing gene expression, we are still far from resolving this complicated network. Thus, the precise regulation of each stage is indispensable for the cell to function correctly.

During the development of this work, we have mainly focused on understanding the function of the SAGA co-activator complex in transcription and mRNA export. Along this complex, our interest has been mainly directed towards Sus1 protein, a component from the DUBm. This interesting protein belongs to both SAGA and the mRNA export TREX-2 complex (Rodríguez-Navarro et al., 2004), which serves as an example of a protein capable of modulating independent processes that are coupled within gene expression. The study of Sus1 protein has helped us to the discovery of Mog1 protein as a new modulator of gene expression (manuscript under preparation). Although this protein has been previously identified as an effector of protein import (Oki and Nishimoto, 1998), its link with gene expression had not been described. In this thesis, we have been able to show that Mog1 participates in histone modifications such as monoubiquitination of histone H2B and trimethylation of H3K4, hence, having a role in histone cross-talk. Indeed, it participates with several factors implicated in the transcription pathway such as the ubiquitinases, SAGA and COMPASS complex. Moreover, our study has enabled us to

reveal that Mog1 is also linked with TREX-2 complex and in turn, to mRNA export. Therefore, it is possible that Mog1 participation in upstream processes such as histone modifications affects downstream steps including mRNA export. Despite the fact that Mog1 is not a transcription factor, it may act transiently along transcription, thus, facilitating the binding or catalytic activities of several factors. Further analysis will allow us to conclude whether GTPase domain of Mog1 is implicated in this intriguing process. Its vicinity to the NPC to accomplish its role in nuclear import, could be connected to our findings, hence, a better understanding of the various facets of Mog1 is therefore essential for understanding the transcription process in which it is engaged.

Beside the amount of the different histone chaperones that participate in chromatin dynamics, we found that Asf1 co-purifies with the TREX-2 components Sus1 and Thp1 and indeed, it participates in the ubiquitination of histone H2B (Pamblanco M, Oliete-Calvo et al., 2014). Whether Asf1 promotes ubiquitination of histone H2B or instead, it prevents H2B from being deubiquitinated is a hallmark in our research.

The correct regulation of histone modifications is a key step in gene expression; therefore, misregulation of the activity of the enzymes involved in this pathway can result in the pathogenesis of human diseases. On these lines, the participation of the DUBm component, human ATXN7 (ySgf73), in SCA7 disease is a clear example of how transcriptional factors lead to human malignancies. Our research has demonstrated that although the DUBm catalytic activity remains unaltered in our analysis,

specific SAGA-TREX-2 deregulation might contribute to the development of the disease.

We hope that future research will help to unravel the unknown mechanisms involved in histone modifications, histone chaperones and chromatin remodeling complexes, hence, contributing to the better understanding of gene expression.

Conclusions

Conclusions

The main conclusions of this work are the following:

1. Asf1 affects global levels of monoubiquitinated histone H2B, however, it does not alter Sus1 chromatin binding to *GAL1* at both promoter and ORF. Indeed, Asf1 is not necessary for *GAL1* expression or for mRNA export.
2. Mog1 interacts genetically with components involved in the ubiquitination and deubiquitination of histone H2B and it is required to maintain the levels of monoubiquitinated histone H2B. Moreover, it affects the association of the ubiquitinase Rad6 to the chromatin.
3. Mog1 interacts genetically with the methyltransferase Set2 and with Set1 and Dot1 under certain conditions. Furthermore, it affects the recruitment of the COMPASS complex Set1 and Swd2 subunits and seems to participate in Swd2 stability. In addition, Mog1 regulates trimethylated levels of H3K4, thus, it participates in the $H2Bub^{1}$-$H3K4me^{3}$ cross-talk.
4. Mog1 is recruited to chromatin and it interacts physically with transcription factors including several subunits from the SAGA and COMPASS complexes. Mog1 associates with the DUBm subunit Sgf73, in contrast, it does not interact with the rest of the DUBm.
5. Mog1 interacts genetically with Thp1, Sus1 and Sem1 subunits from TREX-2 complex and it is implicated in mRNA export.
6. Cells lacking *MOG1* present a decrease in the transcription rate (SR) and mRNA amount (RA) with unaltered mRNA stability (RS).

Conclusions

7. SCA7 mice present unchanged expression levels of mitochondrial and ribosomal genes.
8. SCA7 cell line model presents a correct deubiquitinase activity but contains alterations in the association between ENY2 and TREX-2 complex.

Annexes

Annexes

metabolite	left limit (ppm)	right limit (ppm)	mean	SD	mean	SD
Acetate	1.925	1.916	55.188	6.856	55.472	8.684
a-Glucose	5.259	5.228	0.539	0.249	0.730	0.306
Alanine	1.500	1.470	88.510	6.857	81.310	15.090
Arginine	3.265	3.224	69.956	5.492	71.372	3.221
	1.69	1.614	31.311	2.273	32.856	8.064
Asparagine	2.914	2.8879	0.350	0.097	0.718	1.087
Aspartic acid	2.840	2.795	11.481	0.788	11.194	0.444
ATP	8.557	8.539	0.895	0.071	1.195	0.574
b-Glucose	4.668	4.631	0.725	0.321	1.135	0.530
Citrate	2.654	2.639	1.950	0.336	2.025	0.465
CMP/CTP	6.130	6.115	0.380	0.070	0.484	0.184
Ethanol	1.164	1.210	26.666	6.932	31.133	4.656
Galactitol	4.000	3.965	9.587	0.839	10.105	1.035
Glutamic acid	2.375	2.335	91.069	3.308	88.978	8.419
Glutamine	2.48	2.4234	11.564	2.940	13.852	7.506
Glutathione	4.588	4.552	5.483	0.448	5.948	0.911
	2.977	2.931	2.574	0.248	2.709	0.662
Glycerol	3.585	3.540	94.235	17.011	87.247	22.186
	3.580	3.570	23.904	5.359	21.697	7.119
	3.572	3.564	25.789	5.901	23.463	7.781
Glycine	3.559	3.553	11.339	2.679	10.401	3.725
GMP	8.230	8.210	1.532	0.091	1.811	0.507
	5.955	5.935	0.802	0.100	0.935	0.292
Glycerophosphocholine	3.240	3.230	19.199	1.417	19.012	0.783
Histidine	7.11	7.07	3.172	0.138	3.562	0.771
Isoleucine	0.948	0.939	2.051	0.086	2.209	0.578
Lactate	1.345	1.320	14.971	2.118	15.292	2.703
Leucine	0.983	0.961	5.868	1.116	5.032	1.211
Lysine	3.050	3.000	79.610	6.571	79.726	2.778
Methionine	2.656	2.64	2.009	0.348	2.095	0.506
Myo-inositol	4.075	4.055	1.739	0.155	2.142	0.662

NAD	9.355	9.335	2.636	0.175	3.264	1.430
	9.160	9.135	2.116	0.106	2.306	0.464
	8.856	8.803	2.319	0.116	2.500	0.619
Phenylalanine	7.457	7.315	8.697	0.590	10.185	3.333
Proline	2.03	2.003	4.541	0.275	6.552	7.302
	4.165	4.122	5.525	0.326	6.072	0.834
Serine	3.860	3.847	5.010	0.418	5.563	0.653
Succinate	2.415	2.400	3.942	0.907	3.771	0.796
Trehalose	5.215	5.180	0.906	0.087	1.033	0.187
Thiamine phosphate	2.500	2.485	2.651	0.191	2.941	0.854
Thiamine phosphate	5.463	5.442	0.886	0.168	1.003	0.246
Tryptophan	7.754	7.728	0.736	0.086	1.108	0.832
	7.560	7.530	0.838	0.151	1.161	0.753
Tyrosine	6.920	6.890	3.523	0.160	3.641	0.445
UDP N-acetylglucosamine	5.540	5.501	0.489	0.143	0.674	0.430
UDP-glucose	5.635	5.588	0.321	0.197	0.567	0.578
Valine	1.057	1.035	13.448	2.726	11.087	2.134
	1.005	0.983	13.241	2.771	10.854	2.247
α-D glucoronic acid	3.500	3.490	0.257	0.266	0.290	0.268
β-D glucoronic acid	3.275	3.267	1.134	0.102	1.307	0.425

Table annex 1. Identified and quantified metabolites in aqueous yeast extracts. Spectral integration regions for quantification are indicated on the right side.

Bibliography

Bibliography

Abou-Sleymane, G., Chalmel, F., Helmlinger, D., Lardenois, A., Thibault, C., Weber, C., Mérienne, K., Mandel, J.-L., Poch, O., Devys, D., et al. (2006). Polyglutamine expansion causes neurodegeneration by altering the neuronal differentiation program. Hum. Mol. Genet. *15*, 691–703.

Abruzzi, K.C., Lacadie, S., and Rosbash, M. (2004). Biochemical analysis of TREX complex recruitment to intronless and intron-containing yeast genes. EMBO J. *23*, 2620–2631.

Adanyeguh, I.M., Henry, P.-G., Nguyen, T.M., Rinaldi, D., Jauffret, C., Valabregue, R., Emir, U.E., Deelchand, D.K., Brice, A., Eberly, L.E., et al. (2015). In vivo neurometabolic profiling in patients with spinocerebellar ataxia types 1, 2, 3, and 7. Mov. Disord. Off. J. Mov. Disord. Soc. *30*, 662–670.

Adkins, M.W., Howar, S.R., and Tyler, J.K. (2004). Chromatin disassembly mediated by the histone chaperone Asf1 is essential for transcriptional activation of the yeast PHO5 and PHO8 genes. Mol. Cell *14*, 657–666.

Adkins, M.W., Carson, J.J., English, C.M., Ramey, C.J., and Tyler, J.K. (2007). The histone chaperone anti-silencing function 1 stimulates the acetylation of newly synthesized histone H3 in S-phase. J. Biol. Chem. *282*, 1334–1340.

Ahmed, S., Brickner, D.G., Light, W.H., Cajigas, I., McDonough, M., Froyshteter, A.B., Volpe, T., and Brickner, J.H. (2010). DNA zip codes control an ancient mechanism for gene targeting to the nuclear periphery. Nat. Cell Biol. *12*, 111–118.

Akey, C.W., and Luger, K. (2003). Histone chaperones and nucleosome assembly. Curr. Opin. Struct. Biol. *13*, 6–14.

Aleman, T.S., Cideciyan, A.V., Volpe, N.J., Stevanin, G., Brice, A., and Jacobson, S.G. (2002). Spinocerebellar ataxia type 7 (SCA7) shows a cone-rod dystrophy phenotype. Exp. Eye Res. *74*, 737–745.

Allard, S., Utley, R.T., Savard, J., Clarke, A., Grant, P., Brandl, C.J., Pillus, L., Workman, J.L., and Côté, J. (1999). NuA4, an essential transcription

adaptor/histone H4 acetyltransferase complex containing Esa1p and the ATM-related cofactor Tra1p. EMBO J. *18*, 5108–5119.

Allfrey, V.G., and Mirsky, A.E. (1964). Structural Modifications of Histones and their Possible Role in the Regulation of RNA Synthesis. Science *144*, 559.

Atanassov, B.S., Mohan, R.D., Lan, X., Kuang, X., Lu, Y., Lin, K., McIvor, E., Li, W., Zhang, Y., Florens, L., et al. (2016). ATXN7L3 and ENY2 Coordinate Activity of Multiple H2B Deubiquitinases Important for Cellular Proliferation and Tumor Growth. Mol. Cell *62*, 558–571.

Avvakumov, N., Nourani, A., and Côté, J. (2011). Histone chaperones: modulators of chromatin marks. Mol. Cell *41*, 502–514.

Baker, S., and Grant, P. (2007). The SAGA continues: expanding the cellular role of a transcriptional co-activator complex. Oncogene *26*, 5329–5340.

Baker, R.P., Harreman, M.T., Eccleston, J.F., Corbett, A.H., and Stewart, M. (2001). Interaction between Ran and Mog1 is required for efficient nuclear protein import. J. Biol. Chem. *276*, 41255–41262.

Bannister, A.J., and Kouzarides, T. (2011). Regulation of chromatin by histone modifications. Cell Res. *21*, 381–395.

Barski, A., Cuddapah, S., Cui, K., Roh, T.-Y., Schones, D.E., Wang, Z., Wei, G., Chepelev, I., and Zhao, K. (2007). High-resolution profiling of histone methylations in the human genome. Cell *129*, 823–837.

Baryshnikova, A., Costanzo, M., Kim, Y., Ding, H., Koh, J., Toufighi, K., Youn, J.-Y., Ou, J., San Luis, B.-J., Bandyopadhyay, S., et al. (2010). Quantitative analysis of fitness and genetic interactions in yeast on a genome scale. Nat. Methods *7*, 1017–1024.

Batta, K., Zhang, Z., Yen, K., Goffman, D.B., and Pugh, B.F. (2011). Genome-wide function of H2B ubiquitylation in promoter and genic regions. Genes Dev. *25*, 2254–2265.

Bibliography

Baudin, A., Ozier-Kalogeropoulos, O., Denouel, A., Lacroute, F., and Cullin, C. (1993). A simple and efficient method for direct gene deletion in Saccharomyces cerevisiae. Nucleic Acids Res. *21*, 3329–3330.

Beck, M., and Hurt, E. (2017). The nuclear pore complex: understanding its function through structural insight. Nat. Rev. Mol. Cell Biol. *18*, 73–89.

Berriz, G.F., Beaver, J.E., Cenik, C., Tasan, M., and Roth, F.P. (2009). Next generation software for functional trend analysis. Bioinforma. Oxf. Engl. *25*, 3043–3044.

Bhaumik, S.R., and Green, M.R. (2001). SAGA is an essential in vivo target of the yeast acidic activator Gal4p. Genes Dev. *15*, 1935–1945.

Bhaumik, S.R., Smith, E., and Shilatifard, A. (2007). Covalent modifications of histones during development and disease pathogenesis. Nat. Struct. Mol. Biol. *14*, 1008–1016.

Bian, C., Xu, C., Ruan, J., Lee, K.K., Burke, T.L., Tempel, W., Barsyte, D., Li, J., Wu, M., Zhou, B.O., et al. (2011). Sgf29 binds histone H3K4me2/3 and is required for SAGA complex recruitment and histone H3 acetylation. EMBO J. *30*, 2829–2842.

Bischoff, F.R., and Ponstingl, H. (1991). Catalysis of guanine nucleotide exchange on Ran by the mitotic regulator RCC1. Nature *354*, 80–82.

Bönisch, C., Nieratschker, S.M., Orfanos, N.K., and Hake, S.B. (2008). Chromatin proteomics and epigenetic regulatory circuits. Expert Rev. Proteomics *5*, 105–119.

Bonnet, J., Wang, C.-Y., Baptista, T., Vincent, S.D., Hsiao, W.-C., Stierle, M., Kao, C.-F., Tora, L., and Devys, D. (2014). The SAGA coactivator complex acts on the whole transcribed genome and is required for RNA polymerase II transcription. Genes Dev. *28*, 1999–2012.

Brickner, D.G., Cajigas, I., Fondufe-Mittendorf, Y., Ahmed, S., Lee, P.-C., Widom, J., and Brickner, J.H. (2007). H2A.Z-Mediated Localization of Genes

at the Nuclear Periphery Confers Epigenetic Memory of Previous Transcriptional State. PLoS Biol. *5*.

Brown, C.E., Lechner, T., Howe, L., and Workman, J.L. (2000). The many HATs of transcription coactivators. Trends Biochem. Sci. *25*, 15–19.

Brown, C.E., Howe, L., Sousa, K., Alley, S.C., Carrozza, M.J., Tan, S., and Workman, J.L. (2001). Recruitment of HAT complexes by direct activator interactions with the ATM-related Tra1 subunit. Science *292*, 2333–2337.

Brownell, J.E., Zhou, J., Ranalli, T., Kobayashi, R., Edmondson, D.G., Roth, S.Y., and Allis, C.D. (1996). Tetrahymena histone acetyltransferase A: a homolog to yeast Gcn5p linking histone acetylation to gene activation. Cell *84*, 843–851.

Buratowski, S. (2003). The CTD code. Nat. Struct. Biol. *10*, 679–680.

Buratowski, S. (2009). Progression through the RNA polymerase II CTD cycle. Mol. Cell *36*, 541–546.

Cabal, G.G., Genovesio, A., Rodriguez-Navarro, S., Zimmer, C., Gadal, O., Lesne, A., Buc, H., Feuerbach-Fournier, F., Olivo-Marin, J.-C., Hurt, E.C., et al. (2006). SAGA interacting factors confine sub-diffusion of transcribed genes to the nuclear envelope. Nature *441*, 770–773.

Capelson, M., and Corces, V.G. (2004). Boundary elements and nuclear organization. Biol. Cell *96*, 617–629.

Carrozza, M.J., Li, B., Florens, L., Suganuma, T., Swanson, S.K., Lee, K.K., Shia, W.-J., Anderson, S., Yates, J., Washburn, M.P., et al. (2005). Histone H3 methylation by Set2 directs deacetylation of coding regions by Rpd3S to suppress spurious intragenic transcription. Cell *123*, 581–592.

Casolari, J.M., Brown, C.R., Komili, S., West, J., Hieronymus, H., and Silver, P.A. (2004). Genome-wide localization of the nuclear transport machinery couples transcriptional status and nuclear organization. Cell *117*, 427–439.

Chakrabarti, S., Wu, X., Yang, Z., Wu, L., Yong, S.L., Zhang, C., Hu, K., Wang, Q.K., and Chen, Q. (2013). MOG1 rescues defective trafficking of Na(v)1.5 mutations in Brugada syndrome and sick sinus syndrome. Circ. Arrhythm. Electrophysiol. *6*, 392–401.

Chávez, S., Beilharz, T., Rondón, A.G., Erdjument-Bromage, H., Tempst, P., Svejstrup, J.Q., Lithgow, T., and Aguilera, A. (2000). A protein complex containing Tho2, Hpr1, Mft1 and a novel protein, Thp2, connects transcription elongation with mitotic recombination in Saccharomyces cerevisiae. EMBO J. *19*, 5824–5834.

Chekanova, J.A., Abruzzi, K.C., Rosbash, M., and Belostotsky, D.A. (2008). Sus1, Sac3, and Thp1 mediate post-transcriptional tethering of active genes to the nuclear rim as well as to non-nascent mRNP. RNA N. Y. N *14*, 66–77.

Chen, S., Peng, G.-H., Wang, X., Smith, A.C., Grote, S.K., Sopher, B.L., and La Spada, A.R. (2004). Interference of Crx-dependent transcription by ataxin-7 involves interaction between the glutamine regions and requires the ataxin-7 carboxy-terminal region for nuclear localization. Hum. Mol. Genet. *13*, 53–67.

Chen, Y.C., Gatchel, J.R., Lewis, R.W., Mao, C.-A., Grant, P.A., Zoghbi, H.Y., and Dent, S.Y.R. (2012). Gcn5 loss-of-function accelerates cerebellar and retinal degeneration in a SCA7 mouse model. Hum. Mol. Genet. *21*, 394–405.

Cho, E.J., Kobor, M.S., Kim, M., Greenblatt, J., and Buratowski, S. (2001). Opposing effects of Ctk1 kinase and Fcp1 phosphatase at Ser 2 of the RNA polymerase II C-terminal domain. Genes Dev. *15*, 3319–3329.

Chou, A.-H., Chen, C.-Y., Chen, S.-Y., Chen, W.-J., Chen, Y.-L., Weng, Y.-S., and Wang, H.-L. (2010). Polyglutamine-expanded ataxin-7 causes cerebellar dysfunction by inducing transcriptional dysregulation. Neurochem. Int. *56*, 329–339.

Clapier, C.R., and Cairns, B.R. (2009). The biology of chromatin remodeling complexes. Annu. Rev. Biochem. *78*, 273–304.

Costanzo, M., Baryshnikova, A., Bellay, J., Kim, Y., Spear, E.D., Sevier, C.S., Ding, H., Koh, J.L.Y., Toufighi, K., Mostafavi, S., et al. (2010). The genetic landscape of a cell. Science *327*, 425–431.

Cremer, T., and Cremer, C. (2001). Chromosome territories, nuclear architecture and gene regulation in mammalian cells. Nat. Rev. Genet. *2*, 292–301.

Cuenca-Bono, B., García-Molinero, V., Pascual-García, P., García-Oliver, E., Llopis, A., and Rodríguez-Navarro, S. (2010). A novel link between Sus1 and the cytoplasmic mRNA decay machinery suggests a broad role in mRNA metabolism. BMC Cell Biol. *11*, 19.

Cuthbert, G.L., Daujat, S., Snowden, A.W., Erdjument-Bromage, H., Hagiwara, T., Yamada, M., Schneider, R., Gregory, P.D., Tempst, P., Bannister, A.J., et al. (2004). Histone deimination antagonizes arginine methylation. Cell *118*, 545–553.

Daniel, J.A., Torok, M.S., Sun, Z.-W., Schieltz, D., Allis, C.D., Yates, J.R., and Grant, P.A. (2004). Deubiquitination of histone H2B by a yeast acetyltransferase complex regulates transcription. J. Biol. Chem. *279*, 1867–1871.

Das, C., Tyler, J.K., and Churchill, M.E.A. (2010). The histone shuffle: histone chaperones in an energetic dance. Trends Biochem. Sci. *35*, 476–489.

Das, C., Roy, S., Namjoshi, S., Malarkey, C.S., Jones, D.N.M., Kutateladze, T.G., Churchill, M.E.A., and Tyler, J.K. (2014). Binding of the histone chaperone ASF1 to the CBP bromodomain promotes histone acetylation. Proc. Natl. Acad. Sci. U. S. A. *111*, E1072–E1081.

David, G., Abbas, N., Stevanin, G., Dürr, A., Yvert, G., Cancel, G., Weber, C., Imbert, G., Saudou, F., Antoniou, E., et al. (1997). Cloning of the SCA7 gene reveals a highly unstable CAG repeat expansion. Nat. Genet. *17*, 65–70.

David, G., Dürr, A., Stevanin, G., Cancel, G., Abbas, N., Benomar, A., Belal, S., Lebre, A.S., Abada-Bendib, M., Grid, D., et al. (1998). Molecular and clinical correlations in autosomal dominant cerebellar ataxia with progressive macular dystrophy (SCA7). Hum. Mol. Genet. *7*, 165–170.

De Nadal, E., Zapater, M., Alepuz, P.M., Sumoy, L., Mas, G., and Posas, F. (2004). The MAPK Hog1 recruits Rpd3 histone deacetylase to activate osmoresponsive genes. Nature *427*, 370–374.

Dehé, P.-M., Pamblanco, M., Luciano, P., Lebrun, R., Moinier, D., Sendra, R., Verreault, A., Tordera, V., and Géli, V. (2005). Histone H3 lysine 4 mono-methylation does not require ubiquitination of histone H2B. J. Mol. Biol. *353*, 477–484.

Desai, A., and Hyman, A. (1999). Microtubule cytoskeleton: No longer an also Ran. Curr. Biol. CB *9*, R704-707.

Dillon, S.C., Zhang, X., Trievel, R.C., and Cheng, X. (2005). The SET-domain protein superfamily: protein lysine methyltransferases. Genome Biol. *6*, 227.

Donohoe, D.R., and Bultman, S.J. (2012). Metaboloepigenetics: Interrelationships between energy metabolism and epigenetic control of gene expression. J. Cell. Physiol. *227*, 3169–3177.

Dover, J., Schneider, J., Tawiah-Boateng, M.A., Wood, A., Dean, K., Johnston, M., and Shilatifard, A. (2002). Methylation of histone H3 by COMPASS requires ubiquitination of histone H2B by Rad6. J. Biol. Chem. *277*, 28368–28371.

Duina, A.A., Miller, M.E., and Keeney, J.B. (2014). Budding Yeast for Budding Geneticists: A Primer on the Saccharomyces cerevisiae Model System. Genetics *197*, 33–48.

Dujon, B. (1996). The yeast genome project: what did we learn? Trends Genet. TIG *12*, 263–270.

Durairaj, G., Sen, R., Uprety, B., Shukla, A., and Bhaumik, S.R. (2014). Sus1p facilitates pre-initiation complex formation at the SAGA-regulated genes independently of histone H2B de-ubiquitylation. J. Mol. Biol. *426*, 2928–2941.

Durand, A., Bonnet, J., Fournier, M., Chavant, V., and Schultz, P. (2014). Mapping the deubiquitination module within the SAGA complex. Struct. Lond. Engl. 1993 *22*, 1553–1559.

D'Urso, A., and Brickner, J.H. (2014). Mechanisms of epigenetic memory. Trends Genet. TIG *30*, 230–236.

Ehrenhofer-Murray, A.E. (2004). Chromatin dynamics at DNA replication, transcription and repair. Eur. J. Biochem. *271*, 2335–2349.

Elgin, S.C.R., and Grewal, S.I.S. (2003). Heterochromatin: silence is golden. Curr. Biol. CB *13*, R895-898.

Ellisdon, A.M., Dimitrova, L., Hurt, E., and Stewart, M. (2012). Structural basis for the assembly and nucleic acid binding of the TREX-2 transcription-export complex. Nat. Struct. Mol. Biol. *19*, 328–336.

Emili, A., Schieltz, D.M., Yates, J.R., and Hartwell, L.H. (2001). Dynamic interaction of DNA damage checkpoint protein Rad53 with chromatin assembly factor Asf1. Mol. Cell *7*, 13–20.

English, C.M., Adkins, M.W., Carson, J.J., Churchill, M.E.A., and Tyler, J.K. (2006). Structural Basis for the Histone Chaperone Activity of Asf1. Cell *127*, 495–508.

Faza, M.B., Kemmler, S., Jimeno, S., González-Aguilera, C., Aguilera, A., Hurt, E., and Panse, V.G. (2009). Sem1 is a functional component of the nuclear pore complex-associated messenger RNA export machinery. J. Cell Biol. *184*, 833–846.

Fischer, T., Strässer, K., Rácz, A., Rodriguez-Navarro, S., Oppizzi, M., Ihrig, P., Lechner, J., and Hurt, E. (2002). The mRNA export machinery requires

the novel Sac3p-Thp1p complex to dock at the nucleoplasmic entrance of the nuclear pores. EMBO J. *21*, 5843–5852.

Fischer, T., Rodríguez-Navarro, S., Pereira, G., Rácz, A., Schiebel, E., and Hurt, E. (2004). Yeast centrin Cdc31 is linked to the nuclear mRNA export machinery. Nat. Cell Biol. *6*, 840–848.

Fleming, A.B., Kao, C.-F., Hillyer, C., Pikaart, M., and Osley, M.A. (2008). H2B ubiquitylation plays a role in nucleosome dynamics during transcription elongation. Mol. Cell *31*, 57–66.

Fuchs, G., and Oren, M. (2014). Writing and reading H2B monoubiquitylation. Biochim. Biophys. Acta *1839*, 694–701.

Fuchs, G., Hollander, D., Voichek, Y., Ast, G., and Oren, M. (2014). Cotranscriptional histone H2B monoubiquitylation is tightly coupled with RNA polymerase II elongation rate. Genome Res. *24*, 1572–1583.

Furrer, S.A., Mohanachandran, M.S., Waldherr, S.M., Chang, C., Damian, V.A., Sopher, B.L., Garden, G.A., and La Spada, A.R. (2011). Spinocerebellar ataxia type 7 cerebellar disease requires the coordinated action of mutant ataxin-7 in neurons and glia, and displays non-cell-autonomous bergmann glia degeneration. J. Neurosci. Off. J. Soc. Neurosci. *31*, 16269–16278.

Galán, A., and Rodríguez-Navarro, S. (2012). Sus1/ENY2: a multitasking protein in eukaryotic gene expression. Crit. Rev. Biochem. Mol. Biol. *47*, 556–568.

Gallego, L.D., Ghodgaonkar Steger, M., Polyansky, A.A., Schubert, T., Zagrovic, B., Zheng, N., Clausen, T., Herzog, F., and Köhler, A. (2016). Structural mechanism for the recognition and ubiquitination of a single nucleosome residue by Rad6-Bre1. Proc. Natl. Acad. Sci. U. S. A. *113*, 10553–10558.

García-Martínez, J., Aranda, A., and Pérez-Ortín, J.E. (2004). Genomic run-on evaluates transcription rates for all yeast genes and identifies gene regulatory mechanisms. Mol. Cell *15*, 303–313.

García-Martínez, J., Pelechano, V., and Pérez-Ortín, J.E. (2011). Genomic-wide methods to evaluate transcription rates in yeast. Methods Mol. Biol. Clifton NJ *734*, 25–44.

García-Oliver, E., García-Molinero, V., and Rodríguez-Navarro, S. (2012). mRNA export and gene expression: the SAGA-TREX-2 connection. Biochim. Biophys. Acta *1819*, 555–565.

García-Oliver, E., Pascual-García, P., García-Molinero, V., Lenstra, T.L., Holstege, F.C.P., and Rodríguez-Navarro, S. (2013). A novel role for Sem1 and TREX-2 in transcription involves their impact on recruitment and H2B deubiquitylation activity of SAGA. Nucleic Acids Res. *41*, 5655–5668.

Garden, G.A., and La Spada, A.R. (2008). Molecular Pathogenesis and Cellular Pathology of Spinocerebellar Ataxia Type 7 Neurodegeneration. Cerebellum Lond. Engl. *7*, 138–149.

Garden, G.A., Libby, R.T., Fu, Y.-H., Kinoshita, Y., Huang, J., Possin, D.E., Smith, A.C., Martinez, R.A., Fine, G.C., Grote, S.K., et al. (2002). Polyglutamine-expanded ataxin-7 promotes non-cell-autonomous purkinje cell degeneration and displays proteolytic cleavage in ataxic transgenic mice. J. Neurosci. Off. J. Soc. Neurosci. *22*, 4897–4905.

Gardner, R.G., Nelson, Z.W., and Gottschling, D.E. (2005). Ubp10/Dot4p regulates the persistence of ubiquitinated histone H2B: distinct roles in telomeric silencing and general chromatin. Mol. Cell. Biol. *25*, 6123–6139.

Gasser, S.M. (2002). Visualizing chromatin dynamics in interphase nuclei. Science *296*, 1412–1416.

Georgakopoulos, T., Gounalaki, N., and Thireos, G. (1995). Genetic evidence for the interaction of the yeast transcriptional co-activator proteins GCN5 and ADA2. Mol. Gen. Genet. MGG *246*, 723–728.

Gietz, R.D., Schiestl, R.H., Willems, A.R., and Woods, R.A. (1995). Studies on the transformation of intact yeast cells by the LiAc/SS-DNA/PEG procedure. Yeast Chichester Engl. *11*, 355–360.

Goffeau, A., Barrell, B.G., Bussey, H., Davis, R.W., Dujon, B., Feldmann, H., Galibert, F., Hoheisel, J.D., Jacq, C., Johnston, M., et al. (1996). Life with 6000 genes. Science *274*, 546, 563–567.

González-Aguilera, C., Tous, C., Gómez-González, B., Huertas, P., Luna, R., and Aguilera, A. (2008). The THP1-SAC3-SUS1-CDC31 complex works in transcription elongation-mRNA export preventing RNA-mediated genome instability. Mol. Biol. Cell *19*, 4310–4318.

Görlich, D., and Kutay, U. (1999). Transport between the cell nucleus and the cytoplasm. Annu. Rev. Cell Dev. Biol. *15*, 607–660.

Govind, C.K., Zhang, F., Qiu, H., Hofmeyer, K., and Hinnebusch, A.G. (2007). Gcn5 Promotes Acetylation, Eviction, and Methylation of Nucleosomes in Transcribed Coding Regions. Mol. Cell *25*, 31–42.

Govind, C.K., Qiu, H., Ginsburg, D.S., Ruan, C., Hofmeyer, K., Hu, C., Swaminathan, V., Workman, J.L., Li, B., and Hinnebusch, A.G. (2010). Phosphorylated Pol II CTD recruits multiple HDACs, including Rpd3C(S), for methylation-dependent deacetylation of ORF nucleosomes. Mol. Cell *39*, 234–246.

Grant, P.A., Duggan, L., Côté, J., Roberts, S.M., Brownell, J.E., Candau, R., Ohba, R., Owen-Hughes, T., Allis, C.D., Winston, F., et al. (1997). Yeast Gcn5 functions in two multisubunit complexes to acetylate nucleosomal histones: characterization of an Ada complex and the SAGA (Spt/Ada) complex. Genes Dev. *11*, 1640–1650.

Green, E.M., Jiang, Y., Joyner, R., and Weis, K. (2012). A negative feedback loop at the nuclear periphery regulates GAL gene expression. Mol. Biol. Cell *23*, 1367–1375.

Grewal, S.I.S., and Moazed, D. (2003). Heterochromatin and epigenetic control of gene expression. Science *301*, 798–802.

Griffin, J.L., Cemal, C.K., and Pook, M.A. (2004). Defining a metabolic phenotype in the brain of a transgenic mouse model of spinocerebellar ataxia 3. Physiol. Genomics *16*, 334–340.

Guet, D., Burns, L.T., Maji, S., Boulanger, J., Hersen, P., Wente, S.R., Salamero, J., and Dargemont, C. (2015). Combining Spinach-tagged RNA and gene localization to image gene expression in live yeast. Nat. Commun. *6*, 8882.

Gwizdek, C., Iglesias, N., Rodriguez, M.S., Ossareh-Nazari, B., Hobeika, M., Divita, G., Stutz, F., and Dargemont, C. (2006). Ubiquitin-associated domain of Mex67 synchronizes recruitment of the mRNA export machinery with transcription. Proc. Natl. Acad. Sci. U. S. A. *103*, 16376–16381.

Hahn, S. (2004). Structure and mechanism of the RNA polymerase II transcription machinery. Nat. Struct. Mol. Biol. *11*, 394–403.

Han, Y., Luo, J., Ranish, J., and Hahn, S. (2014). Architecture of the Saccharomyces cerevisiae SAGA transcription coactivator complex. EMBO J. *33*, 2534–2546.

Hands, S.L., and Wyttenbach, A. (2010). Neurotoxic protein oligomerisation associated with polyglutamine diseases. Acta Neuropathol. (Berl.) *120*, 419–437.

Hansen, J.C. (2002). Conformational dynamics of the chromatin fiber in solution: determinants, mechanisms, and functions. Annu. Rev. Biophys. Biomol. Struct. *31*, 361–392.

Harlen, K.M., and Churchman, L.S. (2017). The code and beyond: transcription regulation by the RNA polymerase II carboxy-terminal domain. Nat. Rev. Mol. Cell Biol.

Hassan, A.H., Prochasson, P., Neely, K.E., Galasinski, S.C., Chandy, M., Carrozza, M.J., and Workman, J.L. (2002). Function and selectivity of bromodomains in anchoring chromatin-modifying complexes to promoter nucleosomes. Cell *111*, 369–379.

Helmlinger, D., Hardy, S., Sasorith, S., Klein, F., Robert, F., Weber, C., Miguet, L., Potier, N., Van-Dorsselaer, A., Wurtz, J.-M., et al. (2004).

Ataxin-7 is a subunit of GCN5 histone acetyltransferase-containing complexes. Hum. Mol. Genet. *13*, 1257–1265.

Helmlinger, D., Hardy, S., Abou-Sleymane, G., Eberlin, A., Bowman, A.B., Gansmüller, A., Picaud, S., Zoghbi, H.Y., Trottier, Y., Tora, L., et al. (2006). Glutamine-Expanded Ataxin-7 Alters TFTC/STAGA Recruitment and Chromatin Structure Leading to Photoreceptor Dysfunction. PLoS Biol. *4*.

Henry, K.W., and Berger, S.L. (2002). Trans-tail histone modifications: wedge or bridge? Nat. Struct. Biol. *9*, 565–566.

Henry, K.W., Wyce, A., Lo, W.-S., Duggan, L.J., Emre, N.C.T., Kao, C.-F., Pillus, L., Shilatifard, A., Osley, M.A., and Berger, S.L. (2003). Transcriptional activation via sequential histone H2B ubiquitylation and deubiquitylation, mediated by SAGA-associated Ubp8. Genes Dev. *17*, 2648–2663.

Holmberg, M., Duyckaerts, C., Dürr, A., Cancel, G., Gourfinkel-An, I., Damier, P., Faucheux, B., Trottier, Y., Hirsch, E.C., Agid, Y., et al. (1998). Spinocerebellar ataxia type 7 (SCA7): a neurodegenerative disorder with neuronal intranuclear inclusions. Hum. Mol. Genet. *7*, 913–918.

Hu, F., Alcasabas, A.A., and Elledge, S.J. (2001). Asf1 links Rad53 to control of chromatin assembly. Genes Dev. *15*, 1061–1066.

Huang, C., and Yu, Y.-T. (2013). Synthesis and labeling of RNA in vitro. Curr. Protoc. Mol. Biol. *Chapter 4*, Unit4.15.

Huertas, P., and Aguilera, A. (2003). Cotranscriptionally formed DNA:RNA hybrids mediate transcription elongation impairment and transcription-associated recombination. Mol. Cell *12*, 711–721.

Huisinga, K.L., and Pugh, B.F. (2004). A genome-wide housekeeping role for TFIID and a highly regulated stress-related role for SAGA in Saccharomyces cerevisiae. Mol. Cell *13*, 573–585.

Hwang, W.W., Venkatasubrahmanyam, S., Ianculescu, A.G., Tong, A., Boone, C., and Madhani, H.D. (2003). A conserved RING finger protein

required for histone H2B monoubiquitination and cell size control. Mol. Cell *11*, 261–266.

Iglesias, N., Tutucci, E., Gwizdek, C., Vinciguerra, P., Von Dach, E., Corbett, A.H., Dargemont, C., and Stutz, F. (2010). Ubiquitin-mediated mRNP dynamics and surveillance prior to budding yeast mRNA export. Genes Dev. *24*, 1927–1938.

Ingvarsdottir, K., Krogan, N.J., Emre, N.C.T., Wyce, A., Thompson, N.J., Emili, A., Hughes, T.R., Greenblatt, J.F., and Berger, S.L. (2005). H2B ubiquitin protease Ubp8 and Sgf11 constitute a discrete functional module within the Saccharomyces cerevisiae SAGA complex. Mol. Cell. Biol. *25*, 1162–1172.

Jani, D., Lutz, S., Marshall, N.J., Fischer, T., Köhler, A., Ellisdon, A.M., Hurt, E., and Stewart, M. (2009). Sus1, Cdc31, and the Sac3 CID region form a conserved interaction platform that promotes nuclear pore association and mRNA export. Mol. Cell *33*, 727–737.

Kao, C.-F., Hillyer, C., Tsukuda, T., Henry, K., Berger, S., and Osley, M.A. (2004). Rad6 plays a role in transcriptional activation through ubiquitylation of histone H2B. Genes Dev. *18*, 184–195.

Kelly, S.M., and Corbett, A.H. (2009). Messenger RNA export from the nucleus: a series of molecular wardrobe changes. Traffic Cph. Den. *10*, 1199–1208.

Kim, J., Guermah, M., McGinty, R.K., Lee, J.-S., Tang, Z., Milne, T.A., Shilatifard, A., Muir, T.W., and Roeder, R.G. (2009). RAD6-Mediated transcription-coupled H2B ubiquitylation directly stimulates H3K4 methylation in human cells. Cell *137*, 459–471.

Kim, J., Kim, J.-A., McGinty, R.K., Nguyen, U.T.T., Muir, T.W., Allis, C.D., and Roeder, R.G. (2013). The n-SET domain of Set1 regulates H2B ubiquitylation-dependent H3K4 methylation. Mol. Cell *49*, 1121–1133.

Kimura, A., Umehara, T., and Horikoshi, M. (2002). Chromosomal gradient of histone acetylation established by Sas2p and Sir2p functions as a shield against gene silencing. Nat. Genet. *32*, 370–377.

Koehler, C., Bonnet, J., Stierle, M., Romier, C., Devys, D., and Kieffer, B. (2014). DNA binding by Sgf11 protein affects histone H2B deubiquitination by Spt-Ada-Gcn5-acetyltransferase (SAGA). J. Biol. Chem. *289*, 8989–8999.

Koh, J.L.Y., Ding, H., Costanzo, M., Baryshnikova, A., Toufighi, K., Bader, G.D., Myers, C.L., Andrews, B.J., and Boone, C. (2010). DRYGIN: a database of quantitative genetic interaction networks in yeast. Nucleic Acids Res. *38*, D502-507.

Köhler, A., Pascual-García, P., Llopis, A., Zapater, M., Posas, F., Hurt, E., and Rodríguez-Navarro, S. (2006). The mRNA export factor Sus1 is involved in Spt/Ada/Gcn5 acetyltransferase-mediated H2B deubiquitinylation through its interaction with Ubp8 and Sgf11. Mol. Biol. Cell *17*, 4228–4236.

Köhler, A., Schneider, M., Cabal, G.G., Nehrbass, U., and Hurt, E. (2008). Yeast Ataxin-7 links histone deubiquitination with gene gating and mRNA export. Nat. Cell Biol. *10*, 707–715.

Köhler, A., Zimmerman, E., Schneider, M., Hurt, E., and Zheng, N. (2010). Structural basis for assembly and activation of the heterotetrameric SAGA histone H2B deubiquitinase module. Cell *141*, 606–617.

Komarnitsky, P., Cho, E.J., and Buratowski, S. (2000). Different phosphorylated forms of RNA polymerase II and associated mRNA processing factors during transcription. Genes Dev. *14*, 2452–2460.

Kornberg, R.D. (1974). Chromatin structure: a repeating unit of histones and DNA. Science *184*, 868–871.

Kouzarides, T. (2007). Chromatin modifications and their function. Cell *128*, 693–705.

Krogan, N.J., Kim, M., Ahn, S.H., Zhong, G., Kobor, M.S., Cagney, G., Emili, A., Shilatifard, A., Buratowski, S., and Greenblatt, J.F. (2002). RNA

Polymerase II Elongation Factors of Saccharomyces cerevisiae: a Targeted Proteomics Approach. Mol. Cell. Biol. *22*, 6979–6992.

Krogan, N.J., Kim, M., Tong, A., Golshani, A., Cagney, G., Canadien, V., Richards, D.P., Beattie, B.K., Emili, A., Boone, C., et al. (2003a). Methylation of histone H3 by Set2 in Saccharomyces cerevisiae is linked to transcriptional elongation by RNA polymerase II. Mol. Cell. Biol. *23*, 4207–4218.

Krogan, N.J., Dover, J., Wood, A., Schneider, J., Heidt, J., Boateng, M.A., Dean, K., Ryan, O.W., Golshani, A., Johnston, M., et al. (2003b). The Paf1 complex is required for histone H3 methylation by COMPASS and Dot1p: linking transcriptional elongation to histone methylation. Mol. Cell *11*, 721–729.

Künzler, M., and Hurt, E. (2001). Targeting of Ran: variation on a common theme? J. Cell Sci. *114*, 3233–3241.

Kuras, L., and Struhl, K. (1999). Binding of TBP to promoters in vivo is stimulated by activators and requires Pol II holoenzyme. Nature *399*, 609–613.

La Spada, A.R., Fu, Y.H., Sopher, B.L., Libby, R.T., Wang, X., Li, L.Y., Einum, D.D., Huang, J., Possin, D.E., Smith, A.C., et al. (2001). Polyglutamine-expanded ataxin-7 antagonizes CRX function and induces cone-rod dystrophy in a mouse model of SCA7. Neuron *31*, 913–927.

Lam, Y.C., Bowman, A.B., Jafar-Nejad, P., Lim, J., Richman, R., Fryer, J.D., Hyun, E.D., Duvick, L.A., Orr, H.T., Botas, J., et al. (2006). ATAXIN-1 interacts with the repressor Capicua in its native complex to cause SCA1 neuropathology. Cell *127*, 1335–1347.

Lan, X., Koutelou, E., Schibler, A.C., Chen, Y.C., Grant, P.A., and Dent, S.Y.R. (2015). Poly(Q) Expansions in ATXN7 Affect Solubility but Not Activity of the SAGA Deubiquitinating Module. Mol. Cell. Biol. *35*, 1777–1787.

Lanctôt, C., Cheutin, T., Cremer, M., Cavalli, G., and Cremer, T. (2007). Dynamic genome architecture in the nuclear space: regulation of gene expression in three dimensions. Nat. Rev. Genet. *8*, 104–115.

Lang, G., Bonnet, J., Umlauf, D., Karmodiya, K., Koffler, J., Stierle, M., Devys, D., and Tora, L. (2011). The tightly controlled deubiquitination activity of the human SAGA complex differentially modifies distinct gene regulatory elements. Mol. Cell. Biol. *31*, 3734–3744.

Laribee, R.N., Krogan, N.J., Xiao, T., Shibata, Y., Hughes, T.R., Greenblatt, J.F., and Strahl, B.D. (2005). BUR kinase selectively regulates H3 K4 trimethylation and H2B ubiquitylation through recruitment of the PAF elongation complex. Curr. Biol. CB *15*, 1487–1493.

Lawrence, M., Daujat, S., and Schneider, R. (2016). Lateral Thinking: How Histone Modifications Regulate Gene Expression. Trends Genet. TIG *32*, 42–56.

Le, S., Davis, C., Konopka, J.B., and Sternglanz, R. (1997). Two new S-phase-specific genes from Saccharomyces cerevisiae. Yeast Chichester Engl. *13*, 1029–1042.

Lee, J.-S., Shukla, A., Schneider, J., Swanson, S.K., Washburn, M.P., Florens, L., Bhaumik, S.R., and Shilatifard, A. (2007). Histone crosstalk between H2B monoubiquitination and H3 methylation mediated by COMPASS. Cell *131*, 1084–1096.

Lee, K.K., Florens, L., Swanson, S.K., Washburn, M.P., and Workman, J.L. (2005). The deubiquitylation activity of Ubp8 is dependent upon Sgf11 and its association with the SAGA complex. Mol. Cell. Biol. *25*, 1173–1182.

Lee, K.K., Swanson, S.K., Florens, L., Washburn, M.P., and Workman, J.L. (2009). Yeast Sgf73/Ataxin-7 serves to anchor the deubiquitination module into both SAGA and Slik(SALSA) HAT complexes. Epigenetics Chromatin *2*, 2.

Lee, K.K., Sardiu, M.E., Swanson, S.K., Gilmore, J.M., Torok, M., Grant, P.A., Florens, L., Workman, J.L., and Washburn, M.P. (2011). Combinatorial

depletion analysis to assemble the network architecture of the SAGA and ADA chromatin remodeling complexes. Mol. Syst. Biol. *7*, 503.

van Leeuwen, F., Gafken, P.R., and Gottschling, D.E. (2002). Dot1p modulates silencing in yeast by methylation of the nucleosome core. Cell *109*, 745–756.

Lei, E.P., Krebber, H., and Silver, P.A. (2001). Messenger RNAs are recruited for nuclear export during transcription. Genes Dev. *15*, 1771–1782.

Lengronne, A., McIntyre, J., Katou, Y., Kanoh, Y., Hopfner, K.-P., Shirahige, K., and Uhlmann, F. (2006). Establishment of sister chromatid cohesion at the S. cerevisiae replication fork. Mol. Cell *23*, 787–799.

Li, B., Carey, M., and Workman, J.L. (2007). The role of chromatin during transcription. Cell *128*, 707–719.

Li, J., Moazed, D., and Gygi, S.P. (2002). Association of the histone methyltransferase Set2 with RNA polymerase II plays a role in transcription elongation. J. Biol. Chem. *277*, 49383–49388.

Liang, G., Klose, R.J., Gardner, K.E., and Zhang, Y. (2007). Yeast Jhd2p is a histone H3 Lys4 trimethyl demethylase. Nat. Struct. Mol. Biol. *14*, 243–245.

Lim, S., Kwak, J., Kim, M., and Lee, D. (2013). Separation of a functional deubiquitylating module from the SAGA complex by the proteasome regulatory particle. Nat. Commun. *4*, 2641.

Lindblad, K., Savontaus, M.L., Stevanin, G., Holmberg, M., Digre, K., Zander, C., Ehrsson, H., David, G., Benomar, A., Nikoskelainen, E., et al. (1996). An expanded CAG repeat sequence in spinocerebellar ataxia type 7. Genome Res. *6*, 965–971.

Ling, S.H.M., and Song, H. (2010). Mechanistic insights into mRNA export through structures of Dbp5. RNA Biol. *7*, 23–27.

Longtine, M.S., McKenzie, A., Demarini, D.J., Shah, N.G., Wach, A., Brachat, A., Philippsen, P., and Pringle, J.R. (1998). Additional modules for versatile and economical PCR-based gene deletion and modification in Saccharomyces cerevisiae. Yeast Chichester Engl. *14*, 953–961.

Luger, K., Mäder, A.W., Richmond, R.K., Sargent, D.F., and Richmond, T.J. (1997). Crystal structure of the nucleosome core particle at 2.8 A resolution. Nature *389*, 251–260.

Luthra, R., Kerr, S.C., Harreman, M.T., Apponi, L.H., Fasken, M.B., Ramineni, S., Chaurasia, S., Valentini, S.R., and Corbett, A.H. (2007). Actively Transcribed GAL Genes Can Be Physically Linked to the Nuclear Pore by the SAGA Chromatin Modifying Complex. J. Biol. Chem. *282*, 3042–3049.

MacKellar, A.L., and Greenleaf, A.L. (2011). Cotranscriptional association of mRNA export factor Yra1 with C-terminal domain of RNA polymerase II. J. Biol. Chem. *286*, 36385–36395.

Martinez-Pastor, B., Cosentino, C., and Mostoslavsky, R. (2013). A tale of metabolites: the crosstalk between chromatin and energy metabolism. Cancer Discov. *3*, 497–501.

Mattiroli, F., D'Arcy, S., and Luger, K. (2015). The right place at the right time: chaperoning core histone variants. EMBO Rep. *16*, 1454–1466.

McCormick, M.A., Mason, A.G., Guyenet, S.J., Dang, W., Garza, R.M., Ting, M.K., Moller, R.M., Berger, S.L., Kaeberlein, M., Pillus, L., et al. (2014). The SAGA histone deubiquitinase module controls yeast replicative lifespan via Sir2 interaction. Cell Rep. *8*, 477–486.

McCullough, S.D., and Grant, P.A. (2010). Histone acetylation, acetyltransferases, and ataxia--alteration of histone acetylation and chromatin dynamics is implicated in the pathogenesis of polyglutamine-expansion disorders. Adv. Protein Chem. Struct. Biol. *79*, 165–203.

McCullough, S.D., Xu, X., Dent, S.Y.R., Bekiranov, S., Roeder, R.G., and Grant, P.A. (2012). Reelin is a target of polyglutamine expanded ataxin-7 in

human spinocerebellar ataxia type 7 (SCA7) astrocytes. Proc. Natl. Acad. Sci. U. S. A. *109*, 21319–21324.

McMahon, S.J., Pray-Grant, M.G., Schieltz, D., Yates, J.R., and Grant, P.A. (2005). Polyglutamine-expanded spinocerebellar ataxia-7 protein disrupts normal SAGA and SLIK histone acetyltransferase activity. Proc. Natl. Acad. Sci. U. S. A. *102*, 8478–8482.

Meaburn, K.J., and Misteli, T. (2007). Cell biology: chromosome territories. Nature *445*, 379–781.

Miller, T., Krogan, N.J., Dover, J., Erdjument-Bromage, H., Tempst, P., Johnston, M., Greenblatt, J.F., and Shilatifard, A. (2001). COMPASS: a complex of proteins associated with a trithorax-related SET domain protein. Proc. Natl. Acad. Sci. U. S. A. *98*, 12902–12907.

Misteli, T. (2004). Spatial Positioning. Cell *119*, 153–156.

Mizzen, C.A., Yang, X.J., Kokubo, T., Brownell, J.E., Bannister, A.J., Owen-Hughes, T., Workman, J., Wang, L., Berger, S.L., Kouzarides, T., et al. (1996). The TAF(II)250 subunit of TFIID has histone acetyltransferase activity. Cell *87*, 1261–1270.

Mohan, R.D., Abmayr, S.M., and Workman, J.L. (2014). Pulling complexes out of complex diseases: Spinocerebellar Ataxia 7. Rare Dis. Austin Tex *2*, e28859.

Morgan, M.T., Haj-Yahya, M., Ringel, A.E., Bandi, P., Brik, A., and Wolberger, C. (2016). Structural basis for histone H2B deubiquitination by the SAGA DUB module. Science *351*, 725–728.

Mortimer, R.K. (2000). Evolution and variation of the yeast (Saccharomyces) genome. Genome Res. *10*, 403–409.

Mortimer, R.K., and Johnston, J.R. (1986). Genealogy of principal strains of the yeast genetic stock center. Genetics *113*, 35–43.

Mousson, F., Ochsenbein, F., and Mann, C. (2007). The histone chaperone Asf1 at the crossroads of chromatin and DNA checkpoint pathways. Chromosoma *116*, 79–93.

Munakata, T., Adachi, N., Yokoyama, N., Kuzuhara, T., and Horikoshi, M. (2000). A human homologue of yeast anti-silencing factor has histone chaperone activity. Genes Cells Devoted Mol. Cell. Mech. *5*, 221–233.

Ng, H.H., Feng, Q., Wang, H., Erdjument-Bromage, H., Tempst, P., Zhang, Y., and Struhl, K. (2002). Lysine methylation within the globular domain of histone H3 by Dot1 is important for telomeric silencing and Sir protein association. Genes Dev. *16*, 1518–1527.

Ng, H.H., Robert, F., Young, R.A., and Struhl, K. (2003). Targeted recruitment of Set1 histone methylase by elongating Pol II provides a localized mark and memory of recent transcriptional activity. Mol. Cell *11*, 709–719.

Nguyen, A.T., and Zhang, Y. (2011). The diverse functions of Dot1 and H3K79 methylation. Genes Dev. *25*, 1345–1358.

Oki, M., and Nishimoto, T. (1998). A protein required for nuclear-protein import, Mog1p, directly interacts with GTP-Gsp1p, the Saccharomyces cerevisiae ran homologue. Proc. Natl. Acad. Sci. U. S. A. *95*, 15388–15393.

Oki, M., Ma, L., Wang, Y., Hatanaka, A., Miyazato, C., Tatebayashi, K., Nishitani, H., Uchida, H., and Nishimoto, T. (2007). Identification of novel suppressors for Mog1 implies its involvement in RNA metabolism, lipid metabolism and signal transduction. Gene *400*, 114–121.

Orr, H.T., and Zoghbi, H.Y. (2007). Trinucleotide repeat disorders. Annu. Rev. Neurosci. *30*, 575–621.

Osley, M.A. (2006). Regulation of histone H2A and H2B ubiquitylation. Brief. Funct. Genomic. Proteomic. *5*, 179–189.

Otterstedt, K., Larsson, C., Bill, R.M., Ståhlberg, A., Boles, E., Hohmann, S., and Gustafsson, L. (2004). Switching the mode of metabolism in the yeast Saccharomyces cerevisiae. EMBO Rep. *5*, 532–537.

Palhan, V.B., Chen, S., Peng, G.-H., Tjernberg, A., Gamper, A.M., Fan, Y., Chait, B.T., La Spada, A.R., and Roeder, R.G. (2005). Polyglutamine-expanded ataxin-7 inhibits STAGA histone acetyltransferase activity to produce retinal degeneration. Proc. Natl. Acad. Sci. U. S. A. *102*, 8472–8477.

Palomino-Schätzlein, M., Molina-Navarro, M.M., Tormos-Pérez, M., Rodríguez-Navarro, S., and Pineda-Lucena, A. (2013). Optimised protocols for the metabolic profiling of S. cerevisiae by 1H-NMR and HRMAS spectroscopy. Anal. Bioanal. Chem. *405*, 8431–8441.

Pamblanco, M., Oliete-Calvo, P., García-Oliver, E., Luz Valero, M., Sanchez del Pino, M.M., and Rodríguez-Navarro, S. (2014). Unveiling novel interactions of histone chaperone Asf1 linked to TREX-2 factors Sus1 and Thp1. Nucl. Austin Tex *5*, 247–259.

Pascual-García, P., and Rodríguez-Navarro, S. (2009a). A tale of coupling, Sus1 function in transcription and mRNA export. RNA Biol. *6*, 141–144.

Pascual-García, P., and Rodríguez-Navarro, S. (2009b). A tale of coupling, Sus1 function in transcription and mRNA export. RNA Biol. *6*, 141–144.

Pascual-García, P., Govind, C.K., Queralt, E., Cuenca-Bono, B., Llopis, A., Chavez, S., Hinnebusch, A.G., and Rodríguez-Navarro, S. (2008). Sus1 is recruited to coding regions and functions during transcription elongation in association with SAGA and TREX2. Genes Dev. *22*, 2811–2822.

Pavri, R., Zhu, B., Li, G., Trojer, P., Mandal, S., Shilatifard, A., and Reinberg, D. (2006). Histone H2B monoubiquitination functions cooperatively with FACT to regulate elongation by RNA polymerase II. Cell *125*, 703–717.

Pérez-Ortín, J.E., Alepuz, P.M., and Moreno, J. (2007). Genomics and gene transcription kinetics in yeast. Trends Genet. TIG *23*, 250–257.

Pérez-Ortín, J.E., Medina, D.A., Chávez, S., and Moreno, J. (2013). What do you mean by transcription rate?: the conceptual difference between nascent transcription rate and mRNA synthesis rate is essential for the proper understanding of transcriptomic analyses. BioEssays News Rev. Mol. Cell. Dev. Biol. *35*, 1056–1062.

Peterson, C.L., and Laniel, M.-A. (2004). Histones and histone modifications. Curr. Biol. CB *14*, R546-551.

Plafker, K., and Macara, I.G. (2000). Facilitated Nucleocytoplasmic Shuttling of the Ran Binding Protein RanBP1. Mol. Cell. Biol. *20*, 3510–3521.

Pokholok, D.K., Harbison, C.T., Levine, S., Cole, M., Hannett, N.M., Lee, T.I., Bell, G.W., Walker, K., Rolfe, P.A., Herbolsheimer, E., et al. (2005). Genome-wide map of nucleosome acetylation and methylation in yeast. Cell *122*, 517–527.

Pray-Grant, M.G., Schieltz, D., McMahon, S.J., Wood, J.M., Kennedy, E.L., Cook, R.G., Workman, J.L., Yates, J.R., and Grant, P.A. (2002). The novel SLIK histone acetyltransferase complex functions in the yeast retrograde response pathway. Mol. Cell. Biol. *22*, 8774–8786.

Puig, O., Caspary, F., Rigaut, G., Rutz, B., Bouveret, E., Bragado-Nilsson, E., Wilm, M., and Séraphin, B. (2001). The tandem affinity purification (TAP) method: a general procedure of protein complex purification. Methods San Diego Calif *24*, 218–229.

Raices, M., and D'Angelo, M.A. (2017). Nuclear pore complexes and regulation of gene expression. Curr. Opin. Cell Biol. *46*, 26–32.

Ramakrishnan, S., Pokhrel, S., Palani, S., Pflueger, C., Parnell, T.J., Cairns, B.R., Bhaskara, S., and Chandrasekharan, M.B. (2016). Counteracting H3K4 methylation modulators Set1 and Jhd2 co-regulate chromatin dynamics and gene transcription. Nat. Commun. *7*, 11949.

Ramey, C.J., Howar, S., Adkins, M., Linger, J., Spicer, J., and Tyler, J.K. (2004). Activation of the DNA damage checkpoint in yeast lacking the

histone chaperone anti-silencing function 1. Mol. Cell. Biol. *24*, 10313–10327.

Rando, O.J., and Winston, F. (2012). Chromatin and Transcription in Yeast. Genetics *190*, 351–387.

Rao, B., Shibata, Y., Strahl, B.D., and Lieb, J.D. (2005). Dimethylation of histone H3 at lysine 36 demarcates regulatory and nonregulatory chromatin genome-wide. Mol. Cell. Biol. *25*, 9447–9459.

Recht, J., Tsubota, T., Tanny, J.C., Diaz, R.L., Berger, J.M., Zhang, X., Garcia, B.A., Shabanowitz, J., Burlingame, A.L., Hunt, D.F., et al. (2006). Histone chaperone Asf1 is required for histone H3 lysine 56 acetylation, a modification associated with S phase in mitosis and meiosis. Proc. Natl. Acad. Sci. U. S. A. *103*, 6988–6993.

Reed, R., and Cheng, H. (2005). TREX, SR proteins and export of mRNA. Curr. Opin. Cell Biol. *17*, 269–273.

Robzyk, K., Recht, J., and Osley, M.A. (2000). Rad6-dependent ubiquitination of histone H2B in yeast. Science *287*, 501–504.

Rodrigues, F., Ludovico, P., and Leão, C. (2006). Sugar Metabolism in Yeasts: an Overview of Aerobic and Anaerobic Glucose Catabolism. In Biodiversity and Ecophysiology of Yeasts, D.G. Péter, and P.C. Rosa, eds. (Springer Berlin Heidelberg), pp. 101–121.

Rodríguez-Navarro, S. (2009). Insights into SAGA function during gene expression. EMBO Rep. *10*, 843–850.

Rodríguez-Navarro, S., and Hurt, E. (2011). Linking gene regulation to mRNA production and export. Curr. Opin. Cell Biol. *23*, 302–309.

Rodríguez-Navarro, S., Fischer, T., Luo, M.-J., Antúnez, O., Brettschneider, S., Lechner, J., Pérez-Ortín, J.E., Reed, R., and Hurt, E. (2004). Sus1, a functional component of the SAGA histone acetylase complex and the nuclear pore-associated mRNA export machinery. Cell *116*, 75–86.

Rougemaille, M., Dieppois, G., Kisseleva-Romanova, E., Gudipati, R.K., Lemoine, S., Blugeon, C., Boulay, J., Jensen, T.H., Stutz, F., Devaux, F., et al. (2008). THO/Sub2p functions to coordinate 3'-end processing with gene-nuclear pore association. Cell *135*, 308–321.

Saguez, C., Schmid, M., Olesen, J.R., Ghazy, M.A.E.-H., Qu, X., Poulsen, M.B., Nasser, T., Moore, C., and Jensen, T.H. (2008). Nuclear mRNA surveillance in THO/sub2 mutants is triggered by inefficient polyadenylation. Mol. Cell *31*, 91–103.

Samara, N.L., Datta, A.B., Berndsen, C.E., Zhang, X., Yao, T., Cohen, R.E., and Wolberger, C. (2010). STRUCTURAL INSIGHTS INTO THE ASSEMBLY AND FUNCTION OF THE SAGA DEUBIQUITINATING MODULE. Science *328*, 1025–1029.

Samara, N.L., Ringel, A.E., and Wolberger, C. (2012). A role for intersubunit interactions in maintaining SAGA deubiquitinating module structure and activity. Struct. Lond. Engl. 1993 *20*, 1414–1424.

Saunders, A., Core, L.J., and Lis, J.T. (2006). Breaking barriers to transcription elongation. Nat. Rev. Mol. Cell Biol. *7*, 557–567.

Schmitt, C., von Kobbe, C., Bachi, A., Panté, N., Rodrigues, J.P., Boscheron, C., Rigaut, G., Wilm, M., Séraphin, B., Carmo-Fonseca, M., et al. (1999). Dbp5, a DEAD-box protein required for mRNA export, is recruited to the cytoplasmic fibrils of nuclear pore complex via a conserved interaction with CAN/Nup159p. EMBO J. *18*, 4332–4347.

Schneider, J., Wood, A., Lee, J.-S., Schuster, R., Dueker, J., Maguire, C., Swanson, S.K., Florens, L., Washburn, M.P., and Shilatifard, A. (2005). Molecular regulation of histone H3 trimethylation by COMPASS and the regulation of gene expression. Mol. Cell *19*, 849–856.

Schneider, J., Bajwa, P., Johnson, F.C., Bhaumik, S.R., and Shilatifard, A. (2006). Rtt109 is required for proper H3K56 acetylation: a chromatin mark associated with the elongating RNA polymerase II. J. Biol. Chem. *281*, 37270–37274.

Schneider, M., Hellerschmied, D., Schubert, T., Amlacher, S., Vinayachandran, V., Reja, R., Pugh, B.F., Clausen, T., and Köhler, A. (2015). The Nuclear Pore-Associated TREX-2 Complex Employs Mediator to Regulate Gene Expression. Cell *162*, 1016–1028.

Schulze, J.M., Hentrich, T., Nakanishi, S., Gupta, A., Emberly, E., Shilatifard, A., and Kobor, M.S. (2011). Splitting the task: Ubp8 and Ubp10 deubiquitinate different cellular pools of H2BK123. Genes Dev. *25*, 2242–2247.

Schwabish, M.A., and Struhl, K. (2006). Asf1 mediates histone eviction and deposition during elongation by RNA polymerase II. Mol. Cell *22*, 415–422.

Schwartz, T.U. (2016). The Structure Inventory of the Nuclear Pore Complex. J. Mol. Biol. *428*, 1986–2000.

Segref, A., Sharma, K., Doye, V., Hellwig, A., Huber, J., Lührmann, R., and Hurt, E. (1997). Mex67p, a novel factor for nuclear mRNA export, binds to both poly(A)+ RNA and nuclear pores. EMBO J. *16*, 3256–3271.

Setiaputra, D., Ross, J.D., Lu, S., Cheng, D.T., Dong, M.-Q., and Yip, C.K. (2015). Conformational Flexibility and Subunit Arrangement of the Modular Yeast Spt-Ada-Gcn5 Acetyltransferase Complex. J. Biol. Chem. *290*, 10057–10070.

Shahbazian, M.D., Zhang, K., and Grunstein, M. (2005a). Histone H2B ubiquitylation controls processive methylation but not monomethylation by Dot1 and Set1. Mol. Cell *19*, 271–277.

Shahbazian, M.D., Zhang, K., and Grunstein, M. (2005b). Histone H2B ubiquitylation controls processive methylation but not monomethylation by Dot1 and Set1. Mol. Cell *19*, 271–277.

Shandilya, J., and Roberts, S.G.E. (2012). The transcription cycle in eukaryotes: from productive initiation to RNA polymerase II recycling. Biochim. Biophys. Acta *1819*, 391–400.

Shi, Y., Lan, F., Matson, C., Mulligan, P., Whetstine, J.R., Cole, P.A., Casero, R.A., and Shi, Y. (2004). Histone demethylation mediated by the nuclear amine oxidase homolog LSD1. Cell *119*, 941–953.

Shilatifard, A. (2006). Chromatin modifications by methylation and ubiquitination: implications in the regulation of gene expression. Annu. Rev. Biochem. *75*, 243–269.

Shilatifard, A. (2012). The COMPASS Family of Histone H3K4 Methylases: Mechanisms of Regulation in Development and Disease Pathogenesis. Annu. Rev. Biochem. *81*, 65–95.

Shogren-Knaak, M., Ishii, H., Sun, J.-M., Pazin, M.J., Davie, J.R., and Peterson, C.L. (2006). Histone H4-K16 acetylation controls chromatin structure and protein interactions. Science *311*, 844–847.

Shukla, A., Stanojevic, N., Duan, Z., Sen, P., and Bhaumik, S.R. (2006). Ubp8p, a histone deubiquitinase whose association with SAGA is mediated by Sgf11p, differentially regulates lysine 4 methylation of histone H3 in vivo. Mol. Cell. Biol. *26*, 3339–3352.

Smale, S.T., and Kadonaga, J.T. (2003). The RNA polymerase II core promoter. Annu. Rev. Biochem. *72*, 449–479.

Song, Y.-H., and Ahn, S.H. (2010). A Bre1-associated protein, large 1 (Lge1), promotes H2B ubiquitylation during the early stages of transcription elongation. J. Biol. Chem. *285*, 2361–2367.

Spingola, M., Grate, L., Haussler, D., and Ares, M. (1999). Genome-wide bioinformatic and molecular analysis of introns in Saccharomyces cerevisiae. RNA *5*, 221–234.

Steggerda, S.M., and Paschal, B.M. (2000). The mammalian Mog1 protein is a guanine nucleotide release factor for Ran. J. Biol. Chem. *275*, 23175–23180.

Steggerda, S.M., Black, B.E., and Paschal, B.M. (2000). Monoclonal antibodies to NTF2 inhibit nuclear protein import by preventing nuclear translocation of the GTPase Ran. Mol. Biol. Cell *11*, 703–719.

Sterner, D.E., and Berger, S.L. (2000). Acetylation of Histones and Transcription-Related Factors. Microbiol. Mol. Biol. Rev. *64*, 435–459.

Sterner, D.E., Belotserkovskaya, R., and Berger, S.L. (2002). SALSA, a variant of yeast SAGA, contains truncated Spt7, which correlates with activated transcription. Proc. Natl. Acad. Sci. U. S. A. *99*, 11622–11627.

Sträßer, K., and Hurt, E. (2000). Yra1p, a conserved nuclear RNA-binding protein, interacts directly with Mex67p and is required for mRNA export. EMBO J. *19*, 410–420.

Strässer, K., and Hurt, E. (2001). Splicing factor Sub2p is required for nuclear mRNA export through its interaction with Yra1p. Nature *413*, 648–652.

Strässer, K., Masuda, S., Mason, P., Pfannstiel, J., Oppizzi, M., Rodriguez-Navarro, S., Rondón, A.G., Aguilera, A., Struhl, K., Reed, R., et al. (2002). TREX is a conserved complex coupling transcription with messenger RNA export. Nature *417*, 304–308.

Sun, Z.-W., and Allis, C.D. (2002). Ubiquitination of histone H2B regulates H3 methylation and gene silencing in yeast. Nature *418*, 104–108.

Sutton, A., Bucaria, J., Osley, M.A., and Sternglanz, R. (2001a). Yeast ASF1 protein is required for cell cycle regulation of histone gene transcription. Genetics *158*, 587–596.

Sutton, A., Bucaria, J., Osley, M.A., and Sternglanz, R. (2001b). Yeast ASF1 protein is required for cell cycle regulation of histone gene transcription. Genetics *158*, 587–596.

Taddei, A., Van Houwe, G., Hediger, F., Kalck, V., Cubizolles, F., Schober, H., and Gasser, S.M. (2006). Nuclear pore association confers optimal expression levels for an inducible yeast gene. Nature *441*, 774–778.

Tatebayashi, K., Tani, T., and Ikeda, H. (2001). Fission yeast Mog1p homologue, which interacts with the small GTPase Ran, is required for mitosis-to-interphase transition and poly(A)(+) RNA metabolism. Genetics *157*, 1513–1522.

Texari, L., Dieppois, G., Vinciguerra, P., Contreras, M.P., Groner, A., Letourneau, A., and Stutz, F. (2013). The nuclear pore regulates GAL1 gene transcription by controlling the localization of the SUMO protease Ulp1. Mol. Cell *51*, 807–818.

Thomas, M.C., and Chiang, C.-M. (2006). The general transcription machinery and general cofactors. Crit. Rev. Biochem. Mol. Biol. *41*, 105–178.

Tian, X.-L., Yong, S.L., Wan, X., Wu, L., Chung, M.K., Tchou, P.J., Rosenbaum, D.S., Van Wagoner, D.R., Kirsch, G.E., and Wang, Q. (2004). Mechanisms by which SCN5A mutation N1325S causes cardiac arrhythmias and sudden death in vivo. Cardiovasc. Res. *61*, 256–267.

Tous, C., and Aguilera, A. (2007). Impairment of transcription elongation by R-loops in vitro. Biochem. Biophys. Res. Commun. *360*, 428–432.

Van Oss, S.B., Shirra, M.K., Bataille, A.R., Wier, A.D., Yen, K., Vinayachandran, V., Byeon, I.-J.L., Cucinotta, C.E., Héroux, A., Jeon, J., et al. (2016). The Histone Modification Domain of Paf1 Complex Subunit Rtf1 Directly Stimulates H2B Ubiquitylation through an Interaction with Rad6. Mol. Cell *64*, 815–825.

Venkatesh, S., and Workman, J.L. (2015). Histone exchange, chromatin structure and the regulation of transcription. Nat. Rev. Mol. Cell Biol. *16*, 178–189.

Vermeulen, M., Eberl, H.C., Matarese, F., Marks, H., Denissov, S., Butter, F., Lee, K.K., Olsen, J.V., Hyman, A.A., Stunnenberg, H.G., et al. (2010). Quantitative interaction proteomics and genome-wide profiling of epigenetic histone marks and their readers. Cell *142*, 967–980.

Vitaliano-Prunier, A., Menant, A., Hobeika, M., Géli, V., Gwizdek, C., and Dargemont, C. (2008). Ubiquitylation of the COMPASS component Swd2 links H2B ubiquitylation to H3K4 trimethylation. Nat. Cell Biol. *10*, 1365–1371.

Vitaliano-Prunier, A., Babour, A., Hérissant, L., Apponi, L., Margaritis, T., Holstege, F.C.P., Corbett, A.H., Gwizdek, C., and Dargemont, C. (2012). H2B ubiquitylation controls the formation of export-competent mRNP. Mol. Cell *45*, 132–139.

Vlaming, H., van Welsem, T., de Graaf, E.L., Ontoso, D., Altelaar, A.F.M., San-Segundo, P.A., Heck, A.J.R., and van Leeuwen, F. (2014). Flexibility in crosstalk between H2B ubiquitination and H3 methylation in vivo. EMBO Rep. *15*, 1077–1084.

Wach, A., Brachat, A., Pöhlmann, R., and Philippsen, P. (1994). New heterologous modules for classical or PCR-based gene disruptions in Saccharomyces cerevisiae. Yeast Chichester Engl. *10*, 1793–1808.

Warfield, L., Ranish, J.A., and Hahn, S. (2004). Positive and negative functions of the SAGA complex mediated through interaction of Spt8 with TBP and the N-terminal domain of TFIIA. Genes Dev. *18*, 1022–1034.

Weake, V.M., and Workman, J.L. (2008). Histone ubiquitination: triggering gene activity. Mol. Cell *29*, 653–663.

Weake, V.M., and Workman, J.L. (2010). Inducible gene expression: diverse regulatory mechanisms. Nat. Rev. Genet. *11*, 426–437.

Weake, V.M., and Workman, J.L. (2012). SAGA function in tissue-specific gene expression. Trends Cell Biol. *22*, 177–184.

Wood, A., Schneider, J., Dover, J., Johnston, M., and Shilatifard, A. (2003a). The Paf1 complex is essential for histone monoubiquitination by the Rad6-Bre1 complex, which signals for histone methylation by COMPASS and Dot1p. J. Biol. Chem. *278*, 34739–34742.

Wood, A., Krogan, N.J., Dover, J., Schneider, J., Heidt, J., Boateng, M.A., Dean, K., Golshani, A., Zhang, Y., Greenblatt, J.F., et al. (2003b). Bre1, an E3 ubiquitin ligase required for recruitment and substrate selection of Rad6 at a promoter. Mol. Cell *11*, 267–274.

Wood, A., Schneider, J., Dover, J., Johnston, M., and Shilatifard, A. (2005). The Bur1/Bur2 complex is required for histone H2B monoubiquitination by Rad6/Bre1 and histone methylation by COMPASS. Mol. Cell *20*, 589–599.

Wu, L., Yong, S.L., Fan, C., Ni, Y., Yoo, S., Zhang, T., Zhang, X., Obejero-Paz, C.A., Rho, H.-J., Ke, T., et al. (2008). Identification of a New Co-factor, MOG1, Required for the Full Function of Cardiac Sodium Channel Nav1.5. J. Biol. Chem. *283*, 6968–6978.

Wyce, A., Xiao, T., Whelan, K.A., Kosman, C., Walter, W., Eick, D., Hughes, T.R., Krogan, N.J., Strahl, B.D., and Berger, S.L. (2007). H2B ubiquitylation acts as a barrier to Ctk1 nucleosomal recruitment prior to removal by Ubp8 within a SAGA-related complex. Mol. Cell *27*, 275–288.

Xiao, T., Hall, H., Kizer, K.O., Shibata, Y., Hall, M.C., Borchers, C.H., and Strahl, B.D. (2003). Phosphorylation of RNA polymerase II CTD regulates H3 methylation in yeast. Genes Dev. *17*, 654–663.

Xiao, T., Kao, C.-F., Krogan, N.J., Sun, Z.-W., Greenblatt, J.F., Osley, M.A., and Strahl, B.D. (2005). Histone H2B ubiquitylation is associated with elongating RNA polymerase II. Mol. Cell. Biol. *25*, 637–651.

Yan, M., and Wolberger, C. (2015). Uncovering the role of Sgf73 in maintaining SAGA Deubiquitinating Module Structure and Activity. J. Mol. Biol. *427*, 1765–1778.

Yang, H., Liu, S., He, W.-T., Zhao, J., Jiang, L.-L., and Hu, H.-Y. (2015). Aggregation of Polyglutamine-expanded Ataxin 7 Protein Specifically Sequesters Ubiquitin-specific Protease 22 and Deteriorates Its Deubiquitinating Function in the Spt-Ada-Gcn5-Acetyltransferase (SAGA) Complex. J. Biol. Chem. *290*, 21996–22004.

Yang, K., Gong, P., Gokhale, P., and Zhuang, Z. (2014). Chemical protein polyubiquitination reveals the role of a noncanonical polyubiquitin chain in DNA damage tolerance. ACS Chem. Biol. *9*, 1685–1691.

Yong, S.L., Ni, Y., Zhang, T., Tester, D.J., Ackerman, M.J., and Wang, Q.K. (2007). Characterization of the cardiac sodium channel SCN5A mutation, N1325S, in single murine ventricular myocytes. Biochem. Biophys. Res. Commun. *352*, 378–383.

Yoo, S.Y., Pennesi, M.E., Weeber, E.J., Xu, B., Atkinson, R., Chen, S., Armstrong, D.L., Wu, S.M., Sweatt, J.D., and Zoghbi, H.Y. (2003). SCA7 knockin mice model human SCA7 and reveal gradual accumulation of mutant ataxin-7 in neurons and abnormalities in short-term plasticity. Neuron *37*, 383–401.

Yvert, G., Lindenberg, K.S., Picaud, S., Landwehrmeyer, G.B., Sahel, J.A., and Mandel, J.L. (2000). Expanded polyglutamines induce neurodegeneration and trans-neuronal alterations in cerebellum and retina of SCA7 transgenic mice. Hum. Mol. Genet. *9*, 2491–2506.

Zhang, X., Pfeiffer, H.K., Thorne, A.W., and McMahon, S.B. (2008a). USP22, an hSAGA subunit and potential cancer stem cell marker, reverses the polycomb-catalyzed ubiquitylation of histone H2A. Cell Cycle Georget. Tex *7*, 1522–1524.

Zhang, X.-Y., Varthi, M., Sykes, S.M., Phillips, C., Warzecha, C., Zhu, W., Wyce, A., Thorne, A.W., Berger, S.L., and McMahon, S.B. (2008b). The putative cancer stem cell marker USP22 is a subunit of the human SAGA complex required for activated transcription and cell-cycle progression. Mol. Cell *29*, 102–111.

Zhao, Y., Lang, G., Ito, S., Bonnet, J., Metzger, E., Sawatsubashi, S., Suzuki, E., Le Guezennec, X., Stunnenberg, H.G., Krasnov, A., et al. (2008). A TFTC/STAGA module mediates histone H2A and H2B deubiquitination, coactivates nuclear receptors, and counteracts heterochromatin silencing. Mol. Cell *29*, 92–101.

Zhou, J., Wang, L., Zuo, M., Wang, X., Ahmed, A.S.I., Chen, Q., and Wang, Q.K. (2016). Cardiac sodium channel regulator MOG1 regulates cardiac morphogenesis and rhythm. Sci. Rep. *6*, 21538.

Doctoral Thesis:

- Exploring mechanisms of trinucleotide expansion and studying the normal function of the ataxin-7 yeat ortholog Sgf73. Mason, Amanda Gayle. University of California, San Diego. Proquest Dissertations Publishing, 2014. 3615172.
- Papel de Sus1 y proteínas relacionadas en el proceso de expresión génica. Encarna García Oliver. Universidad de Valencia, 2013.